Effect of Recycled Bauxite Grog Addition on Andalusite-Containing Refractory Castables for Tundish Applications

Prepared by

Sizwe Lloyd Msibi (1511027)

Supervised by

Dr. Elias Matinde

A dissertation submitted to the Faculty of Engineering and the Built Environment, University of the Witwatersrand, Johannesburg, in fulfilment of the requirements for the degree of Master of Science in Engineering.

18 December 2018

Table of Contents

DECLARATION

I, Sizwe Msibi, herewith declare that my dissertation on the "*Effect of Recycled Bauxite Grog Addition on Andalusite-Containing Refractory Castables for Tundish Applications*" dissertation report is solely my own work and all sources used have been acknowledged by means of references.

18/12/2018

Signature **Date**

Mr S.L. Msibi

ABSTRACT

Recycling of reclaimed refractory material (herein referred to as grog) has gained attention in recent years, particularly on the in-process recycling of reclaimed refractory grog for use in non-critical applications. Virgin refractory materials can be substituted with reclaimed material in different quantities without compromising the quality of the refractory products. In this study, the effects of reclaimed bauxite material on andalusite-containing refractory castables for tundish applications were investigated.

The recycled bauxite or grog was formulated in different proportions to replace virgin andalusite in castables. Standard tests were conducted to evaluate the physico-chemical and thermochemical properties of the formulated products as well as using the tundish slag to simulate the actual conditions of operation. The results show that some of the physical properties such as flow behaviour and cold crushing strength of the formulated castables were comparable to the values obtained from the reference castable. However, high-temperature properties such as static corrosion tests at 1400˚C and hot modulus of rupture at 1500˚C indicated that there is an upper constraint to the amount of substituted virgin raw materials.

The study established that substituting fresh andalusite castable raw material with 20 – 30% grog offers the best compromise between cost and quality of the grog-fresh formulation designs. This implies that up to 30% grog may be considered for recycling without compromising the quality of the reference castable, thus achieving optimal impact in terms of reducing bauxite refractory waste and improving the environmental footprint.

ACKNOWLEDGEMENTS

First and foremost, I would like to express my sincere gratitude to my wife Pamela Msibi and my entire family for the support and patience during the past three years of my study.

Heartfelt appreciation goes to Awie Potgieter and the Scaw Metals management team, particularly the rolled products division for all the support and resources provided during this journey, which has been the most incredible three years of my life. I assure you that I will use the skills and knowledge gained from this research to the utmost benefit of the company.

I would also like to express my appreciation to the refractory manufacturers who collaborated in developing the grog-fresh based castable formulations for the tundish application, and also providing laboratory facilities for all the testwork required for the study.

And finally, I would like to thank my research supervisor Dr Elias Matinde for his invaluable guidance and support in constructing this manuscript. Thank you for the countless intellectual discussions and providing the inspiration to complete my research. Your pragmatic guidance has not gone unnoticed.

LIST OF FIGURES

LIST OF TABLES

CHAPTER 1 INTRODUCTION

1.1 Background

Virtually everything used in modern society depends directly or indirectly on the manufacturing processes conducted at high-temperatures (Carniglia and Barna 1992). Refractory materials, or simply refractories, are indispensable in such high-temperature processes, and are widely used to provide thermal insulation and containment of molten phases in various furnaces. Refractory materials can be described as robust materials which can withstand mechanical stress and strain, thermal stress and strain, corrosion / erosion from solids, liquids and gases, gas diffusion, and mechanical abrasion at various temperatures (Schacht 2004). This non-destructive or robust nature of refractory materials by heat and chemical attack make it possible for manufacturing processes to alter the natural state of metals, ceramics, fuels and other compounds (Carniglia and Barna 1992; Hloben 2000).

Various types of refractories are used in the lining of furnaces for smelting, refining and conveying operations (Hanagiri et al. 2008; Hancock and Cannon 2000). When the degree of damage to the refractory lining of the furnace is such that continuous operation cannot be ensured thus risking a breakout, the refractory lining is removed and discarded (Hanagiri et al. 2008). When discarded, the non-destructive nature of refractories poses environmental challenges since these materials do not degrade easily. These environmental challenges are further exacerbated by a combination of significant increases in the cost of landfill disposal and stringent environmental regulations.

Ndlovu et al. (2017) stated that the robust nature of refractory materials present opportunities as well, particularly for the recyclability within the process producing them and reusability in other industrial markets. Spent refractory materials have been reused in conventional monolithic or unshaped products for many years and regarded as fit for purpose grades in substitution of virgin refractory raw materials. In the recent years, there has been an increasing demand to recycle these spent refractory materials in order to improve the environmental footprint as well as incorporating the reclaimed refractories into a variety of refractory finished products to ensure price stability and long-term supply (Bradley and Hutton 2014).

The recycling of refractory materials is currently being promoted through the emerging paradigm of a circular economy model (Lottermoser. 2011; World Steel Association. 2015; Ndlovu et al. 2017). In a circular economy, society is tasked with reducing the burden on nature by ensuring that resources remain in use for as long as possible to ensure sustainability (World Steel Association. 2015). Lottermoser (2011) stated that the issues of land degradation, resource depletion and waste recycling are regarded as some of critical global challenges for present and future generations. As such a sustainable future for the human race must include the effective reuse and recycling of waste streams.

In line with the global models of resource efficiency and circular economy (Ndlovu et al. 2017), the recycling of spent refractories results not only in cost savings by reducing the reliance on virgin raw materials, but also in improved raw material conservation and the reduction of imports (Bradley and Hutton 2014; World Steel Association. 2015). In addition, a combination of significant increase in the cost of landfill disposal, and global restrictions on the export of key refractory raw materials, particularly from China, has resulted in a drive to incorporate reclaimed refractory materials into a variety of refractory finished products to ensure price stability and long-term supply (Bradley and Hutton 2014). Foundry operations in South Africa, for example, face similar cost and supply challenges, and as a result, there is need to consider the alternative recycling and reuse opportunities for the spent refractory materials in their operations. Scaw faces similar cost and supply challenges mentioned by Bradley and Hutton (2014), and as a result is considering alternative recycling and disposal methods for spent refractory materials. In general, the roof bricks used in foundry furnaces are classified as high-alumina bricks either as andalusite or bauxite-based roof bricks based on their alumina (Al_2O_3) content (Hloben 2000). Scaw uses bauxite-based roof bricks containing 82wt% (Al_2O_3) high-alumina which makes it ideal for recycling owing to its robustness and refractoriness as indicated by Harbison and Walker (2005).

In terms of operation, a ferrous foundry entails melting of metal-controlled composition and temperature, supplied at a rate sufficient to match the varying demands of a specific moulding line (Brown 2000). The melting process is usually conducted in electric arc furnaces or induction furnaces. Scaw Metals, henceforth referred to as Scaw, utilises EAFs to manufacture different castings and other downstream processes. The company is currently segmented into four key business units, namely, grinding media, rolled products, cast products, and wire rod products. Cast products and grinding media products use EAFs, commonly referred to as

foundry furnaces, to produce liquid steel for alloy cast steel products and grinding media balls. The rolled products business division also utilises the EAFs, ladle furnace for refining and continuous casting process to manufacture billets. The wire rod products utilise reheating furnaces for its operations. All EAFs at Scaw are relined with bauxite or high-alumina roof bricks and the hotface or working lining with magnesia-carbon bricks, except the rolled products division which uses water cooled panels and precast castable on the furnace roof. Bauxite is a generic term used to classify high-alumina according to Al_2O_3 content which is usually 80wt% with ± 2.5% tolerance (Harbison and Walker 2000). Foundry ladles are relined with andalusite bricks, whereas rolled products ladles are relined with doloma and magnesia-carbon bricks. The reheating furnace at the wire-rod products division is also relined with andalusite bricks. Andalusite is also a generic term used to categorise high-alumina according to Al_2O_3 content which is usually 60wt% with ± 2.5% tolerance (Harbison and Walker 2000).

The recycling of reclaimed refractory materials or simply "grog" has been driven mainly by the need to develop refractory products for low-temperature and non-critical applications in various industries (Mazzanti et al. 2010; Schutte 2010; Bradley and Hutton 2014). Schutte (2010) defined "grog" as reclaimed refractory materials that are recycled and reused in different proportions as raw materials for various refractory applications. In view of this, Schutte (2010) investigated the potential of recycling spent chamotte, andalusite and magnesia-spinel refractory materials for use as monolithic materials and proposed that new product formulations containing up to 80wt% reclaimed material can actually be used in non-critical and low-temperature applications. Furthermore, Mazzanti et al. (2010) proposed that spent alumina refractory materials can be reclaimed and used in producing medium-high-alumina-based castables with little or no compromise to the product quality.

Hanagiri et al. (2008) proposed that for any given furnace several different types of refractory materials are used in different parts of the furnace. These refractory materials usually contain different material compositions within a refractory vessel, as a result, these are sorted and categorised into either magnesia (MgO), alumina (Al_2O_3), carbon (C) containing or carbon free refractories (Hanagiri et al. 2008). Fanga et al. (1999) proposed that a typical refractory recycling programme should include sorting, crushing or grinding, screening and separation to prevent mixing of different refractory types all of which would make the beneficiation process more expensive, if not impossible.

Spent refractories, in this case bauxite roof bricks have been considered owing to their residual thickness and the general condition of the bricks which shows less contamination after use. The general good conditions of these bricks after use increases confidence in quality, consistency and availability to be considered for reclamation (Hutton et al. 2009). Harbison and Walker (2000) stated that the refractoriness of alumina-based refractories is a function of its alumina content. In this case, the bauxite grog with 80 wt% Al_2O_3 can be considered a better raw material for refractory applications, better than virgin andalusite which typically contains 60 wt% Al_2O_3. As a result, marginal compromise on the quality of the castable can be expected from using this reclaimed material (Hanagiri et al. 2008; Bradley and Hutton 2014).

The focus of the research is to investigates the feasibility of recycling spent bauxite refractory roof bricks, herein referred to as grog, originating from Scaw foundry furnaces. The broad objective is to formulate castables for reuse as safety linings in the tundish furnace of the rolled products division at Scaw. The safety lining is a thick precast castable installed in the tundish to prevent breakouts during casting of steel in case the working lining diminishes. The study entails developing formulations using the reclaimed bauxite roof bricks and adding them in different proportions with virgin andalusite raw material in a refractory castable that can be used to reline tundish safety lining. The recycling and reuse of the reclaimed bricks thus contributes and improving the company's environmental footprint.

1.2 Significance

The recycling process of refractory materials has been well documented in recent years (Bradley and Hutton 2014; Hanagiri et al. 2008). However, the focus to date has been mainly on developing refractory products for low-temperature and non-critical applications (Mazzanti et al. 2010; Bradley and Hutton 2014). Exemplary to this, Schutte (2010) focused on the recycling of chamotte, andalusite and magnesia spinel grog for use as raw materials for monolithic refractory materials for non-critical applications. Non-critical or semi-critical applications refer to refractory applications where the grog is used as gunning materials and is usually not in-direct contact with the corrosive medium (Bradley and Hutton 2014). The targeted application of reclaimed grog is the substitution of virgin raw material (andalusite) for the castable installed as a tundish safety lining used in the continuous casting process. The tundish safety lining is considered to be a semi-critical application, as temperatures can reach

1565°C when the thickness of the hot face or working lining diminishes owing to wear associated with slag-metal corrosion.

This study focuses on the recycling of spent alumina-based roof bricks reclaimed from Scaw EAFs. Scaw uses EAFs in the melting of solid scrap to produce crude steel. The EAFs are lined with bauxite-based refractory roof bricks which are considered for in-process reclamation and reuse. Scaw uses on average about 6 tonnes per roof, 15 roofs per month, thus translating to approximately 90 tonnes of refractory materials. This means that over a 1000 tonnes of used bauxite roof brick waste is generated and discarded annually. Inclusive of other high-alumina refractory waste, the total mass generated exceeds 2500 tonnes annually.

Usually, a new roof bricks is 270mm, and the residual thickness at the end of each campaign is 135 mm or more. This translates to only 50% consumption of the brick before the furnace roof is taken out of service and demolished (See Figure 1.1). Figure 1.1 shows the condition of the electric arc furnace (EAF) roof bricks before and after each campaign. After service, the condition of the roof is initially intact thus making it easier to sort and prepare the bricks for recycling. Usually, the roof is taken out of service due to excessive wear around the electrode area caused by thermal degradation.

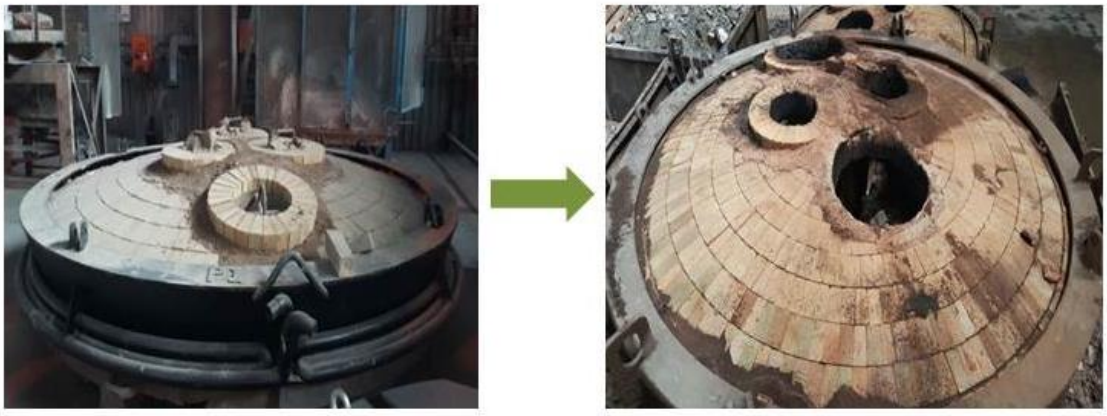

Figure 1.1: Condition of the EAF roof before (a) and after (b) campaign (Scaw Metals)

Figure 1.2 further shows that the initial periphery roof brick thickness is 270 mm. One can see that the residual thickness of a periphery brick after service is reduced by 50% or less of its

original size, thus more than 50% of the brick remain unused. This residual thickness of these roof bricks makes it economically viable for reclamation.

Figure 1.2: Comparison of residual thickness before and after campaign

The overlying challenge for Scaw is that over 2500 tonnes of alumina bricks and castable refractory rubble is generated on site annually and is taken to the dump site orlandfill, which has cost and environmental implications attached to it. The recovery, recycling and reuse of the spent bauxite roof bricks will improve Scaw's environmental footprint by reducing the amount of refractory material discarded as waste and dumping costs. Consequently, it is important that Scaw explore different options available to it to reduce the total cost of refractory materials used and waste generated.

This study developed insight into the salient aspects of recovering refractory waste from steelmaking processes. Physico-chemical characterisation of the spent bauxite roof bricks measured the level of penetration when interacting with process slag material, thus determining the optimum portion of the brick which can be recovered. In addition, the study also contributes to understanding the effects of reclaimed bauxite bricks on castable properties when added to fresh or virgin andalusite based castables. Testing formulated castable mixes assisted in determining the permissible amount of bauxite grog addition to an andalusite-based castable for semi-critical applications in steelmaking processes without adversely affecting the castable quality.

In this study, the effect of reclaimed bauxite grog on the quality of andalusite-containing refractory castables for tundish applications was investigated. The tundish safety lining was considered to be a semi-critical application, as temperatures in the tundish hardly exceed 1565°C even when the working lining is reduced by slag-metal corrosion. The working lining of the tundish, installed by wet gunning of monolithic refractory materials, has an average thickness between 40 and 50 mm (Figure 1.3). As a result, the formulated castable safety lining should be able to prevent penetration by liquid steel should the working lining diminish in order to prevent breakouts.

Figures 1.3(a) and 1.3(b) illustrate the freshly lined tundish castable and the configuration of the new working lining before slag attack, respectively. On the other hand, Figure 1.3(c) shows the condition of the reduced working lining before slag attack on the safety lining.

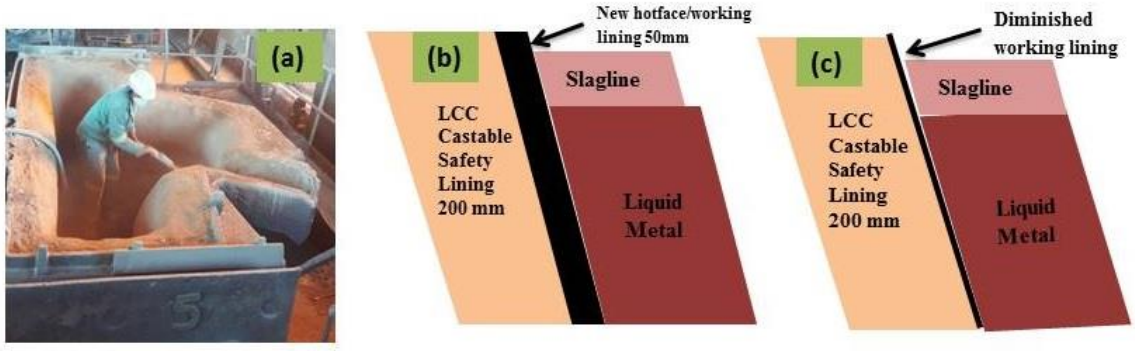

Figure 1.3: (a) freshly lined tundish and the tundish lining configuration with the (b) new and (c) used working lining

The different grog-fresh formulations were developed from the current tundish castable formulation for safety linings at Scaw. The safety lining used at Scaw is a low-cement alumina castable (LCC) based on virgin-andalusite aggregate as raw material (Parr et al. 1997). In this study, the LCC formulation logic remained unchanged for the grog-fresh proposed refractory formulations. In fact, Parr et al. (2003) mentioned that one of the first in-situ applications of low-cement castable (LCC) refractories within the steel plant were the tundish safety linings.

Despite the safety lining not being in direct contact with liquid slag or steel, the formulated product should be robust enough to prevent penetration by liquid slag or steel in order to prevent breakouts should the working lining disappear. This means that the physicochemical

and thermochemical behaviour of the grog-fresh andalusite-formulated products becomes an important parameter from a safety point of view. Therefore, the formulations were subjected to various refractory tests to assess performance and so evaluate the optimum formulation for the tundish application.

1.3 Research Objectives

The aim of the study is to assess the performance of different formulations and so determine the best formulation for the Scaw Metals application. In detail, the study entails the following:

a) The physico-chemical characterization of spent bauxite-based refractory bricks from Scaw's EAFs.
b) The formulation of alumina-castables based on grog-fresh andalusite mixing ratios.
c) Physico-chemical characterization of the formulated grog-fresh castables and so assessing performance to determine the optimum substitution level.
d) Cost-benefit and the estimation of the reduction of refractory cost for the different formulations.

CHAPTER TWO LITERATURE REVIEW

2.0. Introduction

This chapter introduces refractory materials and their applications; it focuses particularly on the ferrous foundry industry. The chapter introduces the different unit processes in a typical ferrous foundry and describes briefly the types of refractory material used in these unit processes. The operational parameters of a continuous casting tundish as the potential in-house application of recycled bauxite roof bricks, are discussed. The salient features of the current tundish castable formulation are considered in order to establish the use of grog as one of its raw-material component and resistance to corrosion thereof. Lastly, the chapter elaborates on the cost and environmental benefits of recycling refractory materials.

2.1 Refractory Materials

Hloben (2000) stated that refractory materials act as a heat buffer between the walls of the containing vessel and the hot substance, subsequently they act as an insulator by retaining the heat in the vessel when in operation. Schacht (2004) stated that refractory materials are indispensable in industries such as iron and steel making, petrochemical, glass and cement, and ferro-alloys.

Refractory materials are broadly classified into two categories, namely, shaped (bricks and cast shapes) and unshaped (monolithic) refractories (Schacht, 2004). Shaped refractories commonly refer to bricks or precast block of rectangular shapes or special shapes based on the design of a refractory vessel or furnace (Harbison and Walker 2005). Monolithic materials are refractory linings installed without joints by ramming, gunning or casting the lining material into place (Hancock and Cannon 2000). Hancock and Cannon (2000) proposed that monolithic refractories be divided further into six general types; these are castables, gunning, mortars, coatings, dry ramming and plastic mouldables. Routschka and Wuthnow (2008) emphasized that the iron and steel industry is the largest consumer of refractory products, specifically unshaped or monolithic refractory materials. Classes of refractories, products and their applications are shown in Table 2.1.

Table 2.1: Refractory classification and applications (Harbison and Walker 2005)

Refractory Type	Typical Refractory Products	Typical Applications
Basic refractories	Magnesites, magnesia-carbon (MgO-C), Magnesia-chrome	Steelmaking linings for electric arc furnace (EAF), Basic oxygen furnace (BOF), and Argon oxygen vacuum decarburisation (AOD).
High-alumina refractories	Most bricks with alumina Al_2O_3 composition higher that 47%. Andalusite-based and bauxite-based brick, alumina-carbon bricks, and alumina-chrome brick.	Rotary kilns, reheating furnaces, steel ladles, Incinerators, blast furnace stoves.
Fireclay refractories	Alumina products with Al_2O_3 content of 40 - 44%. Typical products include superduty fireclay bricks, high duty fireclay bricks, and low and medium fireclay bricks.	Glass tank lower checkers, boilers, stacks, charcoal furnaces, galvanizing pots, and cyclones.
Silica refractories	Superduty silica (SiO_2) brick, lightweight silica brick.	Glass tank furnaces, tunnel kiln crowns.
Special purpose refractories	Carbon and graphite, silicon carbide, zircon, zirconia, fused cast, and fused silica insulating brick.	Electrodes, blast furnace troughs, metering nozzles in continuous casting, coke oven doors, shroud tubes.
Mortar material	Divided into two classes: 1. air setting, mixture of high-fired, fireclay and high-alumina 2. heat setting mortars, high-alumina and basic mortars.	Mainly used for laying different types of bricks.
Monolithic refractories	These are joint-free linings usually used in place of bricks or pre-cast refractories. Ramming material, castables and gunning mixes fall into this category.	Foundry and steel making processes, and in many metallurgical operations; in rotary kilns.

2.2 Refractory Materials in the Steel Industry

2.2.1 An overview of the Steelmaking Process

Fruehan (1998) defined steelmaking as the refining or removal of unwanted elements or other impurities from hot metal produced in a blast furnace or the melting and refining of scrap and other forms of iron in a melting furnace, usually an electric arc furnace (EAF). Seetharaman (2014) stated that steel can be produced by using two types of raw material: hot metal or pig iron, and steel scrap. The refining of steel is carried out in two most prominent types of process, namely, the basic oxygen furnace (BOF) and electric arc furnace (EAF) (Seetharaman 2014).

In BOF steelmaking, about 75% of the iron comes as hot metal produced by a blast furnace process and the remaining 25% of the raw material is steel scrap (Seetharaman, 2014). In EAF steelmaking, either 100% scrap or a combination of scrap, direct-reduced iron (DRI) or sponge iron and pig iron, is utilised for steel production (Grobler and Minnitt 1999; Habashi 1997). The EAF route has become popular in the global steelmaking industry owing to the relatively lower investment capital costs and smaller scale when compared with the blast furnace route (Grobler and Minnitt, 1999; Habashi 1997). Fruehan (1998) emphasized that developments in electrical power and improvement in carbon electrodes coupled with relatively low-cost scrap contributed significantly to the growth of mini-mills or scrap-based EAF producers.

2.2.2 Electric Arc Furnace (EAF) Process

In a typical ferrous foundry, the EAF has a design similar to the one shown in Figure 2.1 and is charged with scrap as the main source of iron as well as other supplied raw materials. The energy needed to melt the solid charge is produced by electrical energy supplied via graphite electrodes, as well as the chemical energy from both oxygen and carbon injection (Fruehan, 1998). The furnace charge is heated to average bath temperatures of between 1630 and 1650°C before the liquid steel is tapped into the casting ladles for further treatment in the ladle furnace (Fruehan 1998).

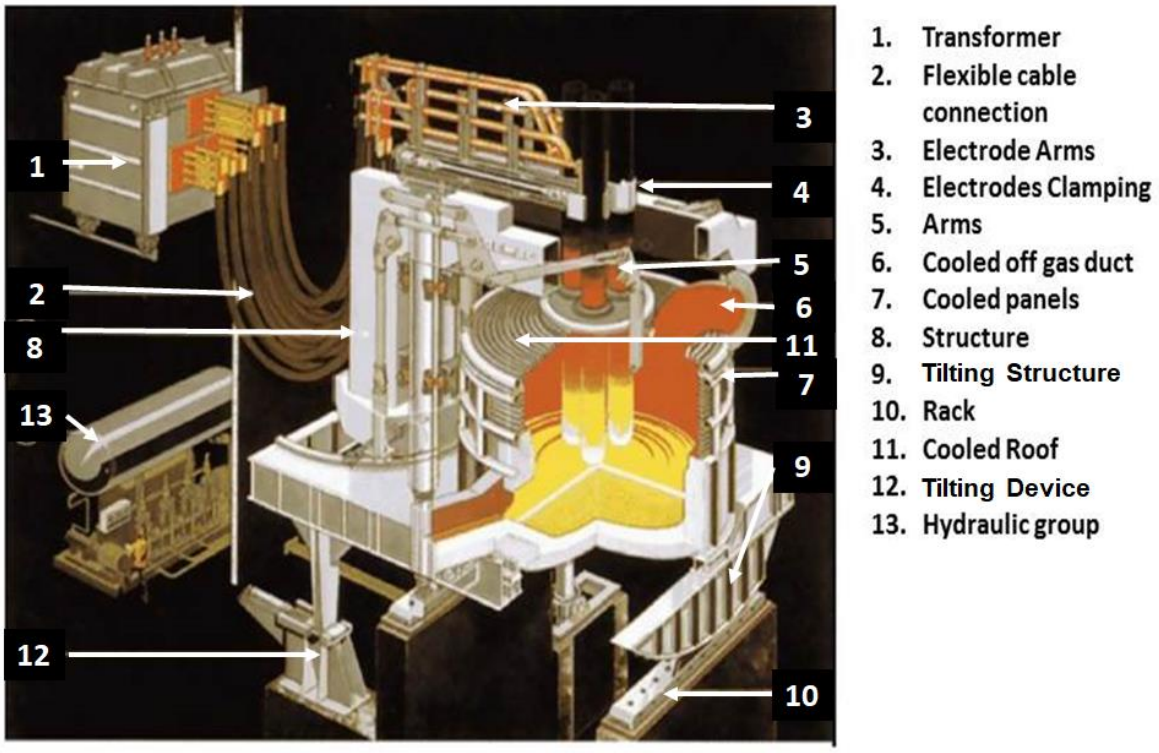

Figure 2.1: Electric arc furnace design (Seetharaman 2014)

The EAF utilizes different refractory materials in different zones of the furnace which consist of the hearth, slagline, upper side walls and taphole (Fruehan 1998). Fruehan (1998) noted that magnesite based-ramming is preferred in the hearth, magnesia-graphite bricks in the slagline and taphole, and water-cooled panels in the upper side wall and roof. The refractory materials are selected on the basis of resistance to oxidation and slag attack, and resilience under thermal shock (Hloben 2000). Refractories for an EAF roof are selected on the basis of resistance to thermal shock and high-temperature corrosion (Vert 2016). At Scaw, the EAF is lined with magnesia-carbon (MgO-C) bricks in the slagline, magnesite-based ramming material on the floor, and water-cooled panels for both the upper side-walls and roof.

2.2.3 Ladle Refining

In the ladle, the steel is treated for trimming of composition, deoxidation, desulfurization, and degassing using vacuum treatment (Seetharaman 2014). Seetharaman (2014) stated that the ladle furnace is used for further refining of steel and heating and temperature control of the steel before the steel is sent to the continuous casting machine with the required chemical specification. Figure 2.2 shows the schematic of a typical ladle used in the refining of steel.

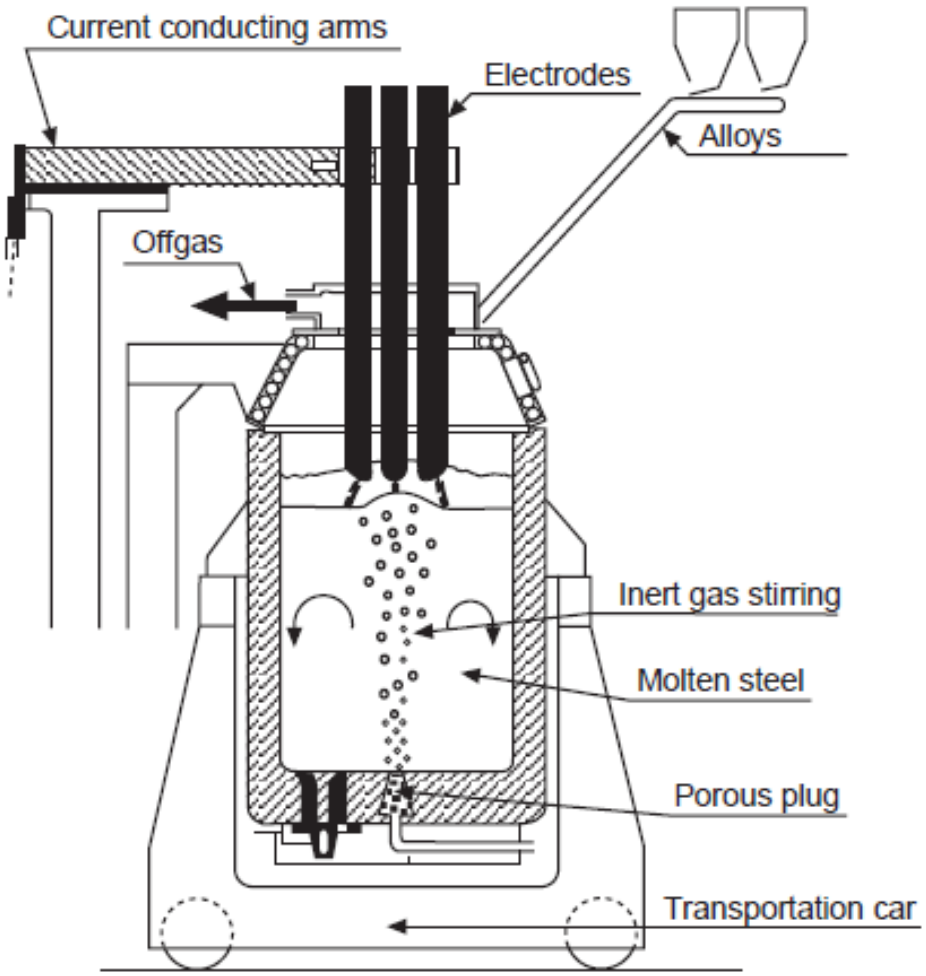

Figure 2.2: Schematic illustration of the ladle furnace (Seetharaman 2014)

Magnesia-carbon refractories are preferred in the ladle furnace slagline, whereas the barrel or lower sidewall and floor are usually lined either with doloma (CaO·MgO), alumina-magnesia-carbon or magnesia-carbon bricks (Fruehan 1998). In some cases, steel plants use the monolithic lining in the hotface (Hloben 2000). Hloben (2000) stated that safety or back up lining is usually built with high-alumina material, either in brick form or monolithic. At Scaw, the ladles are lined with magnesia-carbon brick in the slagline and dolomite bricks in the side-walls and floor. Safety lining in lined with andalusite-based high-alumina bricks.

2.3 Tundish and Continuous Casting Processes

One of the important functions of a tundish is to continuously deliver molten metal of desired composition, temperature and cleanliness from the ladle to one or several moulds at a desired flow rate (Sahai and Emi 2008). According to Sahai and Emi (2008) if proper care is not taken

during tundish operation, the improvements in metal quality brought about by various ladle refining operations may be totally negated during transfer of metal from the ladle to the tundish as a result of the metal interacting with air, tundish slag, and refractory materials. The tundish is a refractory-lined vessel consisting of inlet and outlet sections and is linked to the mould of a continuous casting machine (Sahai and Emi 2008).

The continuous casting process involves high-volume continuous production of solid metal sections with constant cross section from the liquid metal using the tundish ladle as a reservoir (Raja 2009). The casting process starts when the nozzle at the bottom of the ladle is opened and the steel flows at a controlled rate into the tundish and from the tundish through a submerged entry nozzle (SEN) into one mould or several moulds (Seetharaman 2014). The mould is water cooled to chill the steel, and the semi-solidified column of steel is further cooled by series of water sprays to produce blooms, billets or slabs (Hloben 2000). Figure 2.3 illustrates the continuous casting process where molten metal flows from the ladle into the tundish and subsequently to the mould and solidification happens in the strand.

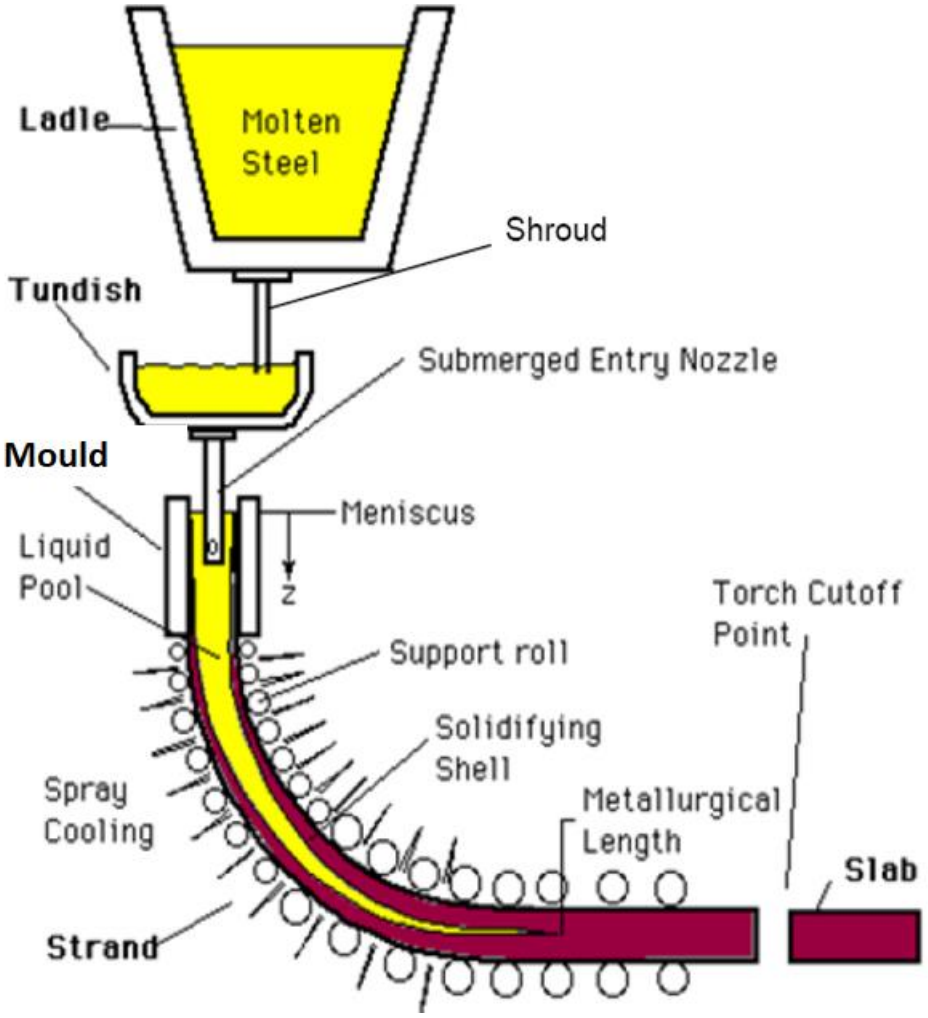

Figure 2.3: Schematic representation of the continuous casting process (de Kock 2005)

2.3.1 Refractory materials in tundish application

The common practice for lining tundish ladles is to employ a working lining backed by a safety lining, which consist of dense refractory materials 120 to 180 mm thick in the form of bricks, casting mixes or vibratables (Vert 2016; Hloben 2000). At Scaw, the continuous casting process utilises a tundish lining consisting of a 200 mm safety lining based on virgin andalusite castable for better lining life and economy. The working lining consist of between 40 and 50 mm olivine-based gunning material.

Sahai and Emi (2008) emphasized that some of the goals for the tundish are to minimize heat losses from the refined steel, deliver the melt evenly into the moulds, minimize the formation of inclusions, and maximise their removal. This implies that the tundish should provide adequate thermal insulation, and the refractory layer should not adversely react with molten steel and slag (Sahai and Emi 2008). Drofelnik et al. (2015) further stated that other functions

of the tundish include the entrapment of steel inclusions, the prevention of oxidation and minimal interaction with the working lining, thus reducing wear from slag-metal corrosion. In most cases, chemical reaction between the working lining and tundish slag is usually increased when the slag basicity from the ladle changed as a result of tundish covers or fluxes used (Sahai and Emi 2008; Bul'ko et al. 2014). According to Bul'ko et al. (2014) tundish powders act as both the cover and steel refiner and contribute to the degradation of the working lining in a tundish.

Interactions between the refined steel and refractory in the tundish are of fundamental importance in the steelmaking industry (Poirier 2015). The refractories used in the tundish have a significant influence on the steel cleanliness and inclusion control during steelmaking (Sahai and Emi 2008). As such, a good understanding of metal-slag-refractory interactions is necessary in order to have better control of process (Poirier 2015). Figure 2.4 show several types of refractory used in the continuous casting of steel.

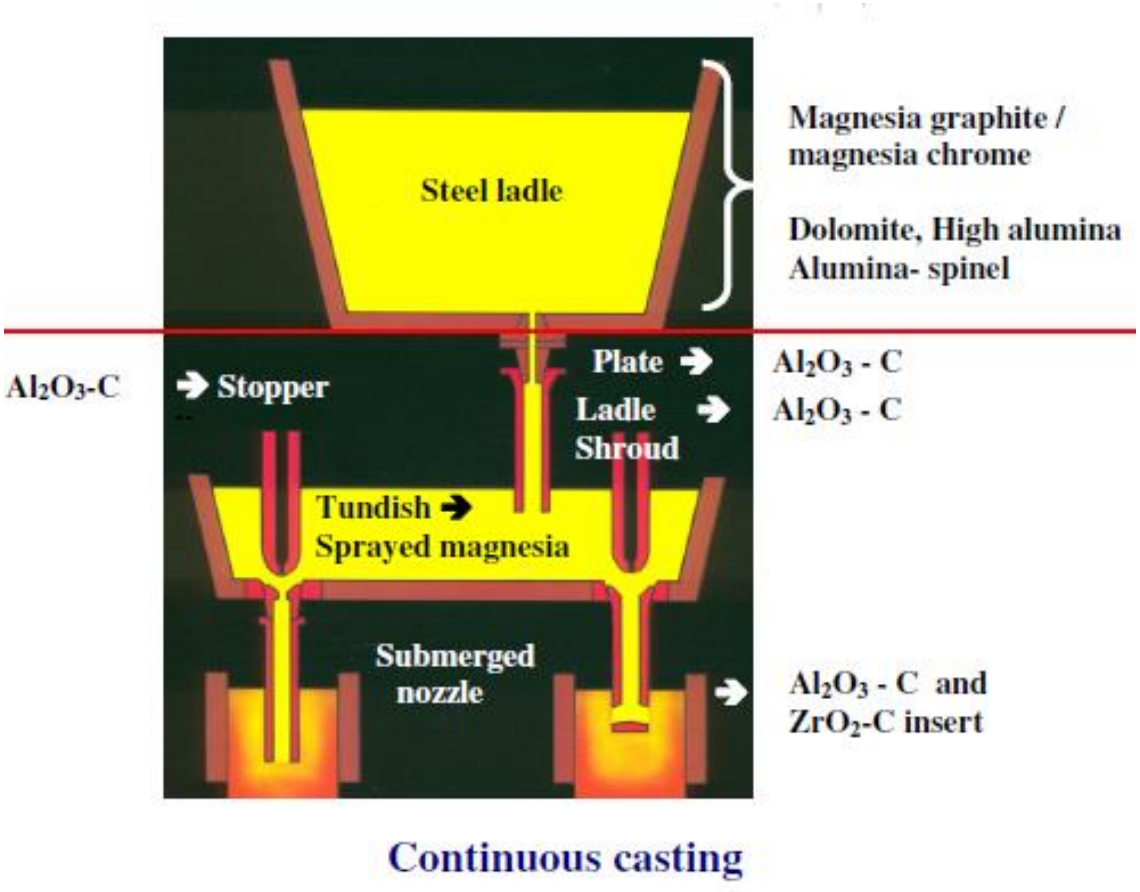

Figure 2.4: Main classes of refractory used in steel continuous casting (Poirier 2015)

From Figure 2.4, it is shown that ladle refractories are predominantly magnesia-based, dolomite and high-alumina-based. Pretorius (n.d) stated that in a steel ladle, slag requirements entail being compatible with the refractories used for the ladle lining in order to improve steel quality. For example, basic refractories such as magnesia-carbon are compatible with basic slags, which means those high in CaO content, thus causing the slag to be less aggressive towards the refractory lining (Schacht 2004, Pretorius n.d). According to Pretorius (n.d) slag fluidity (viscosity) is also an important factor, therefore slag should be fluid enough to refine the metal but not too fluid to cause accelerated wear on the refractory.

2.3.2 Refractory wear in tundish applications

The principal destructive wear mechanisms for tundish safety lining include slag corrosion, cracking and spalling of the lining (Parr et al. 2003). Spalling refers to thermal shock as result of heating and cooling of refractory material during service (Hancock and Cannon 2000). Refractory wear on the working lining can be attributed to a combination of ladle filler, ladle slag and tundish powders used (Bul'ko et al. 2014). Bul'ko et al. (2014) emphasized that to minimise wear on the working lining, due care is required in selecting comparable or suitable ladle fillers and tundish powders thus improving casting sequence and steel quality.
As indicated in section 2.3.1, the tundish lining usually consist of both the safety lining of between 120 and 180mm and the working lining of between 40 and 50 mm. The safety lining usually remains intact during casting, as such lasting for long time. However, the working lining experiences rapid degradation and as result is usually replaced after each casting sequence (Sahai and Emi 2008). A sequence refers to a number of ladles decanted in a single tundish continuously before the working lining is worn-out or before the process is interrupted. Parr et al. (2003) stated that the safety lining castable should possess the following properties to be suitable for steelmaking operations:

- Satisfactory placing properties (Flow)
- Mechanical Stability
- High resistance to thermal shock
- Volume stability and low creep
- High resistance to slag penetration and wear

From the wear point of view, the tundish safety lining experiences less wear when compared to the electric arc furnace and the ladle furnace, as it can be seen in the thermal, mechanical and chemical (TMC) analysis in Table 2.2. According to Vert (2016) TMC analysis is commonly used to identify process wear mechanisms for refractory-product suitability.

Table 2.2: Thermal, mechanical and chemical (TMC) analysis of the tundish safety lining based on the new proposed grog containing castable (Vert 2016).

Main Mechanism	Sub-Mechanism	Analysis
Thermal	Peak temperature	Working lining thickness ranges between 40 mm and 50 mm and exposed to peak temperatures of 1565°C, hence safety lining temperature will be less than that of the working lining which implies less corrosion wear.
	Thermal shock	Thermal cycling for a safety lining is a medium wear factor as long as the lining is allowed to air cool until it is time for the next spray.
Mechanical	Damage during Handling	Normally safety linings are not directly exposed for mechanical damage to occur, unless a scull (remaining solidified steel inside the tundish) is stuck and has to be removed by a demolition machine.
	Abrasion	Abrasion is only observed on the safety lining once the working lining is lost and the liquid steel is circulating in the tundish. This seldom happens.
Chemical (thermo-chemical)	Dissolution	Wear by dissolution is focused on the chemical compatibility of the slag with the brick. At Scaw slag is acidic in nature and the interaction is between the working lining and tundish slag, not the safety lining.
	Penetration	Penetration is caused by low viscosity metals and/or slags. This is not a major problem since Scaw employs a monolithic safety lining which is not directly in contact with tundish slag or steel.

At Scaw, the tundish working lining which is olivine-based material is exposed to temperatures ranging from 1510 to 1560°C. Therefore, it can be deduced that the tundish safety lining experiences lower temperatures than the working lining since it not in direct contact with liquid steel or slag. The refractory linings used in the electric arc and ladle furnaces are exposed to

more aggressive conditions than those in the tundish. This is because of higher operating temperatures, thus exacerbating corrosion attack on refractory linings. The EAF operating temperatures can be as high as 1680°C, and the slag attack is more aggressive owing to flux additions and the quality of scrap used in the process. This higher temperature also increases the thermal and chemical attack on the refractories (Sahai and Emi 2008). Ladle furnace operation can be as high as 1660°C, and fluxes are added during the process for desulphurisation and steel buffering to meet the right specification (Seetharaman 2014). However, the high-temperature conditions make the slag more aggressive toward ladle refractories (Vert 2016). In addition, the argon gas used to purge liquid steel to achieve homogenization composition has an adverse effect on the ladle refractory lining, thereby increasing the potential for erosion wear (Vert 2016).

Therefore, from the aforesaid, it is evident that the tundish is an ideal industrial application to evaluate the effect of alumina grog addition on fresh andalusite-based material.

2.4 Refractory Castables

Lee et al. (2001) described refractory castables as complex refractory formulations, requiring high quality, precision-sized aggregate, modifying fillers, binders and additives. According to them, refractory castables can be formulated into either dense or insulating refractories. Dense castables are prepared with different particle size distributions for installation by vibration or self-flowing (Myhre et al. 1998). Routschka and Wuthnow (2008) classified dense castables as refractories containing less than 45% porosity (i.e. **less than** 50% of the geometrical volume of the refractory consists of voids between particles). Contrary to dense castables, Lee et al. (2001) classified insulating castables as containing more than 45% porosity (i.e. **more than** 50% of the geometrical volume of the refractory consists of voids between particles).

Lee et al. (2001) and Parr et al. (1997) further classified refractory castables according to their lime (CaO) content (Table 2.3).

Table 2.3: Refractory castable classification based on CaO content (Lee et al. 2001)

Castable Classification	**CaO Content wt%**
Conventional Castable (CC)	CaO > 2.5%
Low-cement Castable (LCC)	1%< CaO < 2.5%
Ultra-Low-cement Castable (ULCC)	0.2% CaO < 1%
No Cement castable (NC)	CaO < 0.2%

Parr et al. (1997) emphasized that the reduction of CaO in castables by reduction of cement quantity reduces the formation of lower temperature phases such as anorthite and gehlenite in when evaluated in the CaO-Al_2O_3-SiO_2 ternary phase diagram. This in turn promotes the formation of mullite which greatly improves hot strength in refractory castables.

The lower CaO content in the castable results in LCCs and ULCCs are preferred in usage over CCs due to their ability to be in contact with liquid metal (Mangabhai and Glasser 2001). According to Lee et al. (2001), the main technical advantages of LCCs and ULCCs include their excellent physical properties, such as high density, low porosity, improved cold and hot strength and high abrasion and corrosion resistance. Lee et al. (2001) further stated that the use of fine fillers and admixtures allowed LCCs and ULCCs to improve particle packing hence reducing water demand and cement content in the castable as shown in Figure 2.5.

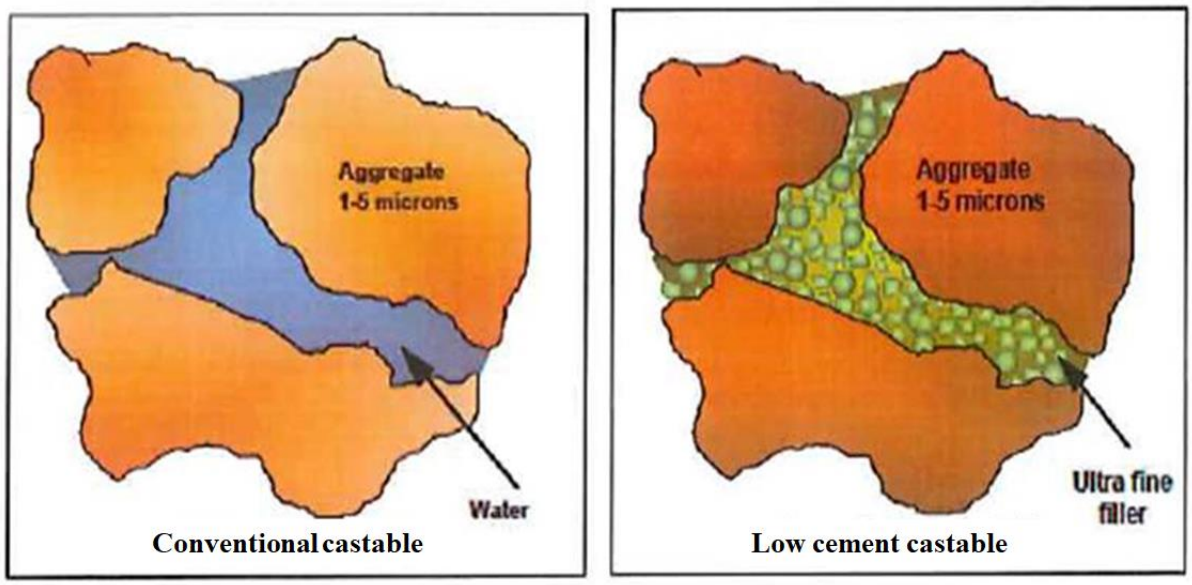

Figure 2.5: Reduced porosity and water demand for LCC when using fine fillers compared to conventional castables without fillers (Parr et al. 1997)

The benefits of incorporating these fillers and reduced cement include (Valdelièvre et al. 2002):

- Lower CaO in the castable which limit low-melting CAS_2 and C_2AS phases thus improving high-temperature mechanical properties
- Reduced water demand reduces porosity and increased density
- Corrosion and abrasion resistance are improved through a denser matrix structure
- Improved particle packing improves thermo-mechanical and corrosion resistance properties.

2.4.1 Formulation Design Fundamentals

Schnabel et al. (2014) and Liu et al. (2002) stated that a refractory castable contains both coarse aggregates particles coarser than 45μm and fine aggregates, which are commonly referred to as the matrix. The matrix makes up 25 to 35 % of the castable, whilst the aggregate portion constitutes between 65 to 75% of the total castable (Schnabel et al. 2014; Liu et al. 2002). The matrix component of a refractory castable is composed of different kinds of raw material such as calcined or reactive alumina, fume silica, calcium aluminate cement (CAC) and other additives which acts as either dispersants, accelerators or retarders (Liu et al. 2002). Whereas, the aggregate component consists of raw material such as reclaim refractory grog (or simply

grog), chamotte, andalusite, bauxite, brown fused alumina, andalusite, or a combination of these aggregates (Ghonaim et al. 2010; Hutton et al. 2009; Schnabel et al. 2014).

2.4.2 Refractory Matrix Components

2.4.2.1 Calcium Aluminate Cement (CAC)

Calcium aluminate cements (CACs) are the most important type of non-Portland or special cement (Mangabhai and Glasser 2001). Mangabhai and Glasser (2001) stated that CACs are predominantly used in refractory products owing to their resistance to severe chemical and abrasive environments. Liu et al. (2002) further summarised that CACs provide the following function in a refractory castable:

- Give the castable a proper curing and drying strength through the hydration of the cement phases
- Provide sufficient time for castable installation through addition of additives which regulate the castable setting time.
- Form a ceramic bond at high-temperatures by means of calcium hexaluminate $CaAl_{12}O_9$ formation.

CACs are classified according to purity and alumina (Al_2O_3) content (Lee et al. 2001). Hancock and Cannon (2000) proposed that typical high-alumina cements (HAC) contain between 50 and 80% Al_2O_3 and are manufactured by a high-temperature sintering process rather than a melting operation. On the other hand, 40% Al_2O_3 is regarded as a low-grade type of high-alumina and hence not considered (Table 2.4).

Table 2.4: Some typical calciumAlumina cements (Hancock and Cannon 2000)

Typical Alumina Cement Grades					
Al_2O_3	39	50	55	72	80
CaO	38	36	34	26	19
SiO_2	4,5	6,9	6	0,2	-
$FeO+Fe_2O_3$	16	2,3	1,5	0,2	0,3
TiO_2	1,8	1,9	2,5	-	-
Alkalies	0,25	0,3	-	-	1,5
Other Oxides	1	0,2	-	-	-

Wöhrmeyer et al. (2000) stated that the temperature resistance of the cement is dependent on the chemical composition; for example, a 50% HAC caters for temperature up to 1400°C, whilst 70% or equivalent up to 1800°C and 80% HAC up to 2000°C. In addition, Lee et al. (2001) stated that an important variable to note is that a 70% HAC range or equivalent is additive free whereas 80% HAC range or equivalent contains a mixture of additions such as plasticizers to ensure consistency and cement properties. The preferred calcium aluminate cement for low-cement castables (LCC) is typically a 70 % HAC or equivalent due to its tolerance for a wide scope of applications and higher flexibility in recipe designs (Liu et al. 2002; Valdelièvre et al. 2002).

Parr et al. (2004) emphasised that there is an intimate link between CAC hydration and castable properties, particularly placing properties, workability and hardening. Therefore, improvements in castable technology should consider this link and other interlinked system components such as fillers and additives (Valdelièvre et al. 2002). Fillers are sub-micron powders used in refractory castables to fill up voids between larger particles thus improving particle packing, flowability and reducing water demand (Myhre 1993; Samanta et al. 2012). Additives usually affect the setting time of refractory castables (Ressler 2009).

2.4.2.2 Refractory Fillers: Fume Silica (Microsilica)

Peng and Myhre (2008) classified low-cement castables (LCCs) into two major types: (1) products containing fume silica and (2) products with reactive alumina. Between the two categories, fume silica systems are more common. Fume silica, also known as microsilica, is an amorphous form of SiO_2 normally obtained by filtering and classifying the fumes produced during the carbothermic production of ferro-silicon and silicon in electric arc furnaces (Sandberg and Myhre 1994).

Sandberg and Myhre (1994) stated that fume silica consists of spheres which are the building units of primary agglomerates that improve particle-size packing which increases bulk density and workability of castables. Hancock and Cannon (2000) further stated that fume silica grades are available as densified and undensified grades. Densified grades contain loosely bonded secondary agglomerates which increase the bulk density and may prove difficult to disintegrate,

whereas undensified microsilica has relatively low density and is readily dispersed (Lee et al. 2001).

Carbon is an inherent impurity in fume silica and its presence, either as coke residue or as silicon carbide, greatly alters the fume silica colour (Sandberg and Myhre 1994). According to Wöhrmeyer et al. (2005), there is a strong correlation between the fume silica colour and its carbon content, fume silica with low-carbon content looks white whereas high-carbon containing fumes are black (Figure 2.6). An increase in carbon content of fume silica may result in initial flow decrease in castables, thus increasing water demand (Wöhrmeyer et al. 2005).

Figure 2.6: Different fume silica types based on colour and carbon content (Wöhrmeyer et al. 2005)

Parr et al. (2004) noted that the variable impurities in fume silica can interrupt the hydration reactions and lead to variable working and hardening times of low-cement castables (LCCs). They conducted a study of two fume silica types to illustrate their effect on the castable properties (Table 2.5). The study concluded that an increase in carbon content as an impurity reduces mechanical strength, whereas other impurities such as Na_2O, K_2O, MgO and SO_3 may result in reduced flow and rapid flow decay. Fume silica FS1 may yield better placing properties in terms of flow decay and setting time due to a more acidic pH and lower sulphate content (Parr et al. 2004; Wöhrmeyer et al. 2005).

Table 2.5: Analysis of two fume silica types (Parr et al. 2004)

Fume Silica Types			
		FS1	**FS2**
Specific Surface (BET)	m^2/g	20	17.6
C (free)	%	0.27	0.81
H_2O	%	0.78	1.98
SiO_2	**%**	**97.64**	**94.7**
Fe_2O_3	%	0.07	0.1
MgO	%	0.22	0.56
SO3	%	0.08	0.14
K2O	%	0.28	1.28
Na2O	%	0.09	0.13
pH	%	6.3	7.9

Depending on the type of fume silica used, rheology and hardening may vary over a wider range with the general trend showing that the higher the silica content, the higher the flow (Wöhrmeyer et al. 2005). In general, fume silica when used as a filler, has a positive effect on refractory castables by reducing the amount of cement and water required thus improving particle packing and reducing porosity (Myhre 1993; Sandberg and Myhre 1994).

2.4.2.3 Refractory Fillers: Calcined and Reactive Aluminas

All grades and types of calcined alumina are based on the leaching of bauxite with caustic soda at elevated temperature and pressure (Hancock and Cannon 2000). According to Hancock and Cannon (2000) the resulting aluminium hydroxide (hydrate) from the leaching process is then fired in a rotary kiln at 1300 to 1400˚C to produce calcined alumina. Lee et al. (2001) categorised calcined alumina according to its level of residual soda content. The first category includes normal calcined alumina with soda content between 0.18 and 0.55 wt% and 99 to 99.5% Al_2O_3, the second category has Al_2O_3 content of about 99.7wt% with less than 0.1wt% soda, and last category has Al_2O_3 of at least 99.9% (Lee et al. 2001). Schnabel et al. (2014) stated that calcined alumina contains agglomerates of individual alumina crystals when compared to reactive aluminas.

Unlike calcined alumina, reactive aluminas are ground down to primary or single crystal as shown in Figure 2.7. Reactive aluminas have relatively high surface-area fine crystals that exhibit higher densification and reaction rates which reduces water absorption thus improves particle packing (Lee et al. 2001; Schnabel et al. 2014).

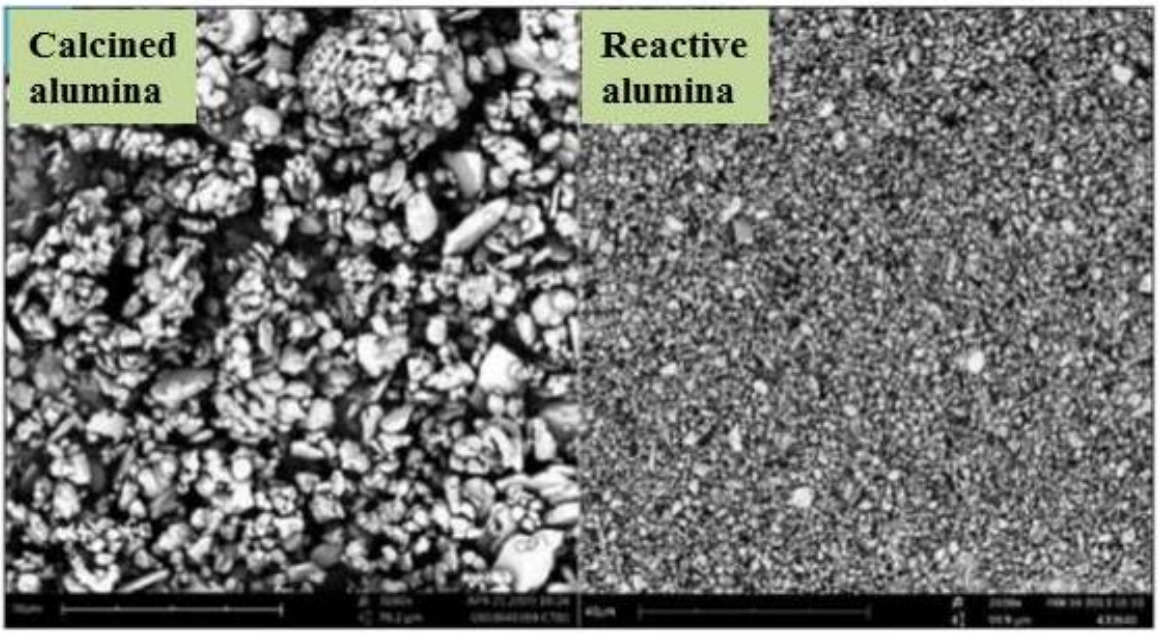

Figure 2.7: Scanning electron microscope images of calcined and reactive alumina (Schnabel et al. 2014)

In respect of particle size distribution (PSD), these aluminas fall into one of two categories namely mono-modal or multi-modal (Liu et al. 2002) as shown in Figure 2.8. In general, for refractory applications, different grades of calcined and reactive aluminas are used according to the requirements of reactivity, water absorption and cost.

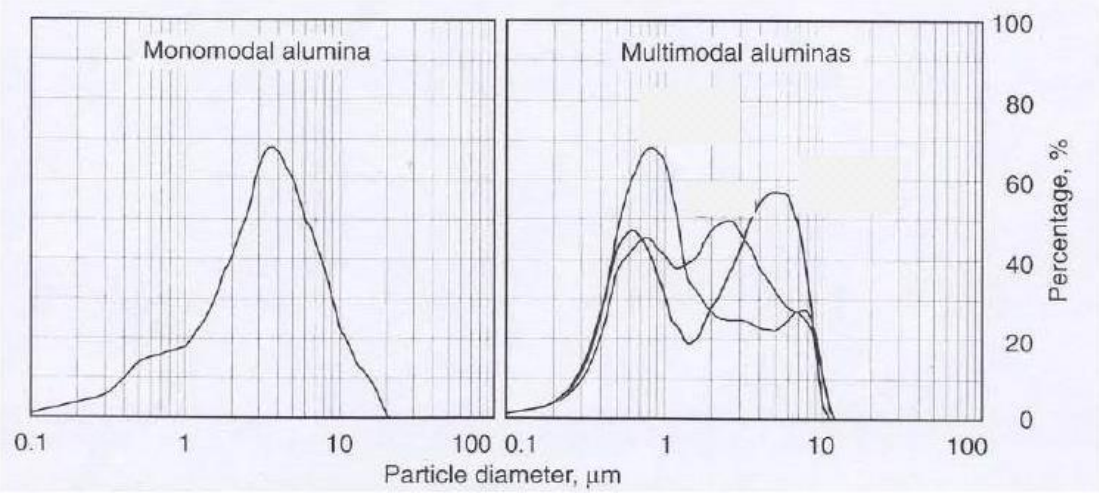

Figure 2.8: Comparison of mono-modal particle size distribution with various multi-modal aluminas (Buhr and Laurich 2000)

2.4.2.4 Additives or Admixture

Admixtures can be defined according to the ASTM C125 (2016) standard as materials other than water, aggregates, hydraulic cement and fibre reinforcement used as ingredients of concrete or mortar and added to the batch immediately before or during mixing. Chemical additives or admixtures can be used to modify the placing properties of refractories castables (Parr et al. 2004). Lee et al. (2001) proposed that refractory castables have three major admixtures; namely accelerators, retarders and plasticisers (water-reducing agents). Accelerators may speed up setting time thus influencing workability and early strength, whereas retarders tend to slow down the rate of hydration hence delaying setting time and early strength development (Bier and Parr 1996). On the other hand, plasticisers, also referred to as deflocculants or water-reducing agents, are absorbed on the cement grain surface thus increasing the zeta potential (degree of electrostatic repulsion between adjacent, similar charged particles) that causes good dispersion between particles (Bier and Parr 1996, Chabas et al. 2013).

Ressler (2009) conducted a study on the effect of deflocculating additives on the setting time of andalusite and bauxite-based castables. The study concluded that three phosphate additives were preferred as deflocculants in both andalusite and bauxite castable namely; sodium hexametaphosphate (SHMP), sodium tripolyphosphate (STPP) and sodium pyrophosphate (SPP).

Wöhrmeyer et al. (2006) conducted a similar study to determine the effect of deflocculants in the presence of calcium aluminate cements (CAC) with and without fume silica (Figure 2.9).

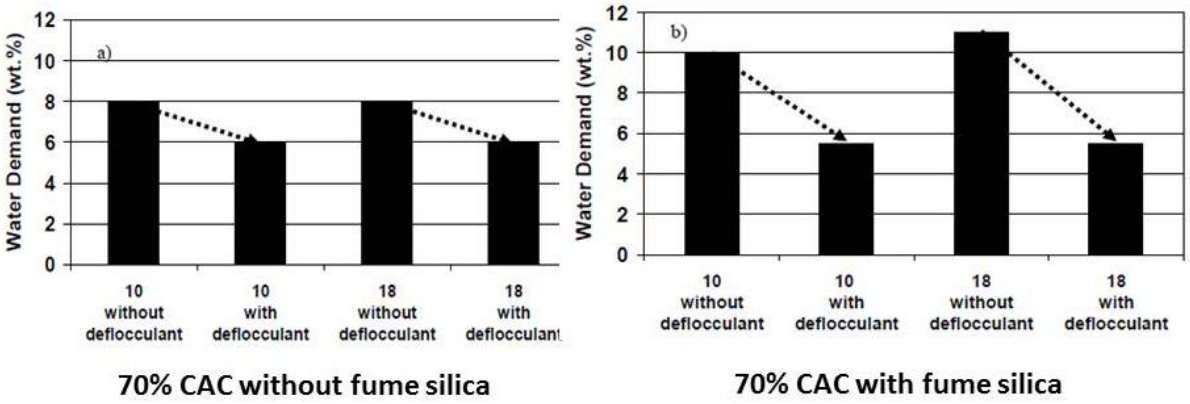

Figure 2.9: Effect of deflocculants on 70% CAC with and without fume silica (Wöhrmeyer et al. 2006)

The study concluded that the presence of fume silica with CAC tends to increase the water demand in castables when no deflocculants are added, however when deflocculants are added the effect of fume silica is negligible. The study also established that deflocculants are integral to providing good fluidity with less mixing water, thus emphasising the interdependency of fillers and additives that make up a refractory castable bonding system (Chabas et al. 2013; Cousin et al. 1998; Wöhrmeyer et al. 2006).

Therefore, it can be concluded that deflocculants have a significant impact on refractory castable strength, particularly in the presence of fume silica. Deflocculants ensure that fluidity is maintained at low amounts of mixing water which improves castable abrasion and corrosion resistance properties (Ressler 2009).

2.4.3 Refractory Aggregate Components

Refractory aggregate refers to particle size fractions above 45µm and plays an important role in the overall particle size distribution of the castable mix (Ghonaim et al. 2010). The chemical composition and physical characteristics of refractory aggregates are important as they ultimately affect the final properties of the castable, particularly thermal shock and corrosion resistance (Lee et al. 2001; Schnabel et al. 2014).

Practically any natural or synthetic refractory oxide that is normally used for refractories can be used as an aggregate in LCC and ULCC (Lee et al. 2001). General aggregate types include

alumina (Al_2O_3), magnesia (MgO) and zirconia (ZrO_2) (Ghonaim et al. 2010). Specifically, examples of aggregate materials used in castables for industrial applications are reclaim refractory grog (or simply grog), chamotte, andalusite, bauxite, fused alumina, tabular alumina, or a combination of these materials (Hutton et al. 2009; Schnabel et al. 2014).

Andalusite, bauxite and fused alumina are all regarded as high-alumina aggregate and are normally used in high-temperature applications (Lia et al. 2002; Peng and Myhre 2008). Chamotte-based aggregates are typically not regarded as high-alumina owing to limitations in service temperature which is usually 1400˚C (Schutte 2010).

2.4.3.1 High-alumina Aggregates

According to Harbison and Walker (2005), the term high-alumina refers to refractory materials with an alumina (Al_2O_3) content of 47% or higher. The most common classes of high-alumina are 50, 60, 70 and 80% Al_2O_3, with a tolerance of plus or minus 2.5% (Harbison and Walker 2005). They further proposed that other classes include 85% and 90% Al_2O_3 with a 2% tolerance, and lastly the 99% Al_2O_3 class which has minimum alumina content instead of a range. For the purpose of this study, only the 60% class (andalusite) and the 85% class (bauxite) will be considered as castable aggregates and discussed in more details. This because the raw material aggregate used in the virgin castable under study is andalusite and the recycled material consider for substituting it is bauxite-based.

2.4.3.2 Andalusite Aggregate (60 Alumina class)

Andalusite forms part of the trimorphous group with stoichiometry Al_2SiO_5. This group also consist of sillimanite and kyanite. These minerals yield a mixture of silica (SiO_2) glass phase and mullite ($3Al_2O_3 \cdot 2SiO_2$ or $Al_2O_3 \cdot SiO_2$) when heated in air in the temperatures range 1100-1480ºC (Equation 2.1) (Rebouillat and Rigaud 2002; Garbers-Craig 2008; Frulli 2016).

$$3Al_2O_3 \cdot SiO_2\,(andalusite) = 3Al_2O_3 \cdot 2SiO_2\,(mullite) + SiO_2\,(glass) \qquad [2.1]$$

The mullite phases are thermodynamically stable at high temperatures and possess good refractory properties such as low thermal expansion, low thermal conductivity, good chemical stability, and excellent thermomechanical stability, to refractory systems (Abou-Sekkina et al.

2011; Frulli 2016). Since andalusite transforms into mullite $Al_6Si_2O_{13}$ at relatively low temperatures with minor volume expansion, it has widely been used in both fired bricks and in unfired (unfired bricks, castables, plastic mixes) refractory materials for various applications (Frulli 2016; Rebouillat and Rigaud 2002). Harbison and Walker (2005) further stated that mullite is important in steelmaking refractory applications because of its melting point 1850°C, which is well above steelmaking temperatures (1600°C).

According to Botha (2010), the general chemical composition of andalusite is $Al_2O_3.SiO_2$ of which 62.9% is Al_2O_3 and 37.1% is SiO_2 as indicated by the red line A in Figure 2.10 on the alumina silica diagram.

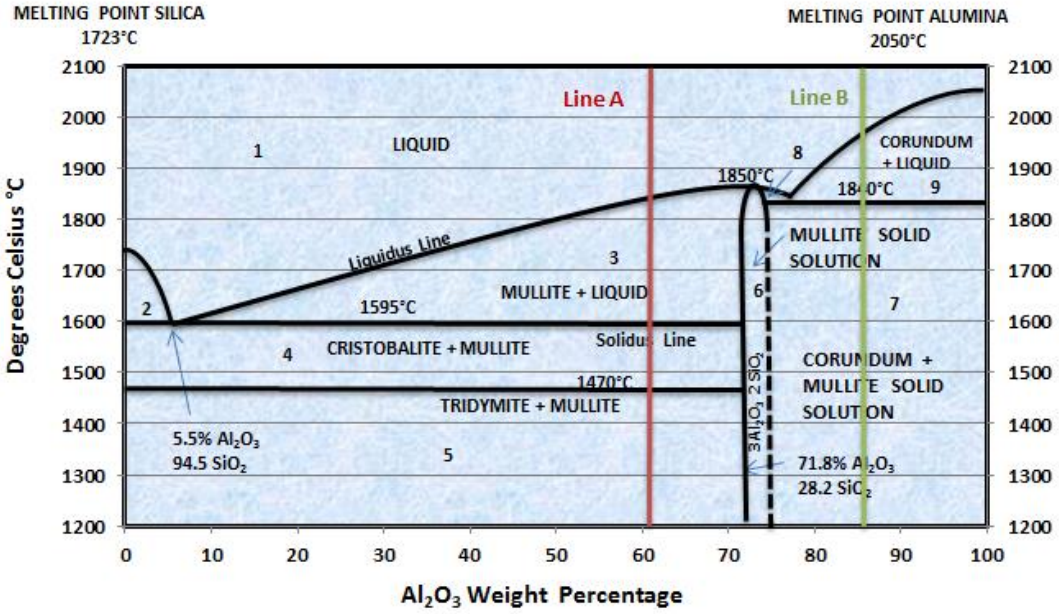

Figure 2.10: Alumina-Silica Phase Diagram (Harbison and Walker. 2005)

Harbison and Walker (2005) mentioned that for the andalusite composition line A, no liquid formation occurs upon heating until the eutectic point at 1595°C, and the first liquid to form will have the eutectic composition at that temperature. As such, andalusite is considered as suitable refractory raw material for refractory applications. The andalusite raw material used in this study has the following chemical composition:

Andalusite Aggregate Chemical Composition					
Al_2O_3	SiO_2	Fe_2O_3	TiO_2	MgO+CaO	$K_2O+N_2O_3$
59.4	39	0.85	0.15	0.2	0.4

2.4.3.3 Bauxite Aggregate (85 Alumina class)

Bauxite is naturally occurring as a mixture of aluminium hydroxide minerals with various levels of impurities, mainly, iron oxides, silica, titania and alumina silicates (Hancock and Cannon 2000). Hloben (2000) stated that bauxite used to produce refractories must fulfil more stringent requirements with respect to impurity levels of iron oxide, silica and titania. Furthermore, refractory bauxite must be calcined and must contain a minimum of 85% Al_2O_3 (Ghonaim et al. 2010). The bauxite composition is indicated by the **green line B** on the alumina silica diagram Figure 2.10, where no liquid formation is expected to occur upon heating until the eutectic point at 1840°C, and the first liquid to form will have the eutectic composition at that temperature (Harbison and Walker 2005).

A typical chemical composition for refractory grade bauxite is min 86.5% Al_2O_3, max 7.5% SiO_2, max 2.5% Fe_2O_3 and max 3.5% TiO_2 (Harbison and Walker 2005). Pivinskii et al. (2015) stated that depending on the bauxite supplied from China, TiO_2 content in one case is approximately 2% and in another between 3.5 and 4%, the Fe_2O_3 content is predominantly in the range 1.3 and 1.8%. The bauxite raw material used in this study showed similar impurities and has the following chemical composition:

Bauxite Aggregate Chemical Composition					
Al_2O_3	SiO_2	Fe_2O_3	TiO_2	MgO+CaO	$K_2O+N_2O_3$
81.8	12.6	1.6	3.2	0.3	0.5

Harbison and Walker (2005) stated that both Fe_2O_3 and TiO_2 are present in bauxite material as impurities and most bauxite aggregates have higher porosity when compared to andalusite aggregates. According to Hancock and Cannon (2000) impurities such as Fe_2O_3 and TiO_2 influence both high-temperature strength properties of refractory bauxite.

Overbeek (1989) stated that the difference in porosity between andalusite and bauxite is a result of the difference crystal structures. Andalusite has a single crystal structure with no channels along which slag can easily penetrate and offers better slag resistance when compared to chamottes and bauxitic materials (Figure 2.11).

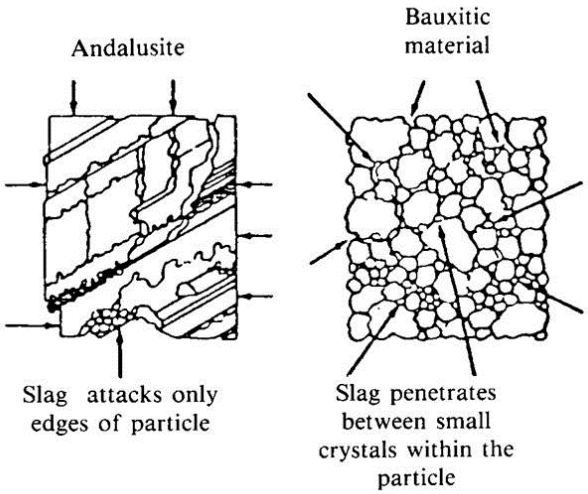

Figure 2.11: Illustration of effect of slag penetration on both andalusite and bauxite particles (Overbeek 1989)

In general, bauxite is classified according to the intended commercial application, such as abrasives, cement, chemical, metallurgical and refractory (Plunkert 2004). All the bauxite mined, approximately 85% is converted to alumina (Al_2O_3) for the production of aluminium metal, and an additional 10% is converted to various forms of specialty aluminas, with the remaining 5% mainly used for non-metallurgical applications.

For refractory applications, bauxite is selectively mined and processed before firing in a high-temperature kiln to remove the bonded water and produce a dense stable aggregate (Hancock and Cannon 2000). Frulli (2016) provided a qualitative description of the performance of bauxite, andalusite and mullite based on the properties commonly considered as critical in the modern refractory applications (Figure 2.12). The study stated resistance to corrosion and abrasion as being key properties to be considered depending on the refractory application. Spalling or thermal shock resistance were also considered to be key determining factors for tundish applications owing to the continuous cooling and heating of refractory material during operation (Frulli 2016; Parr et al. 2003).

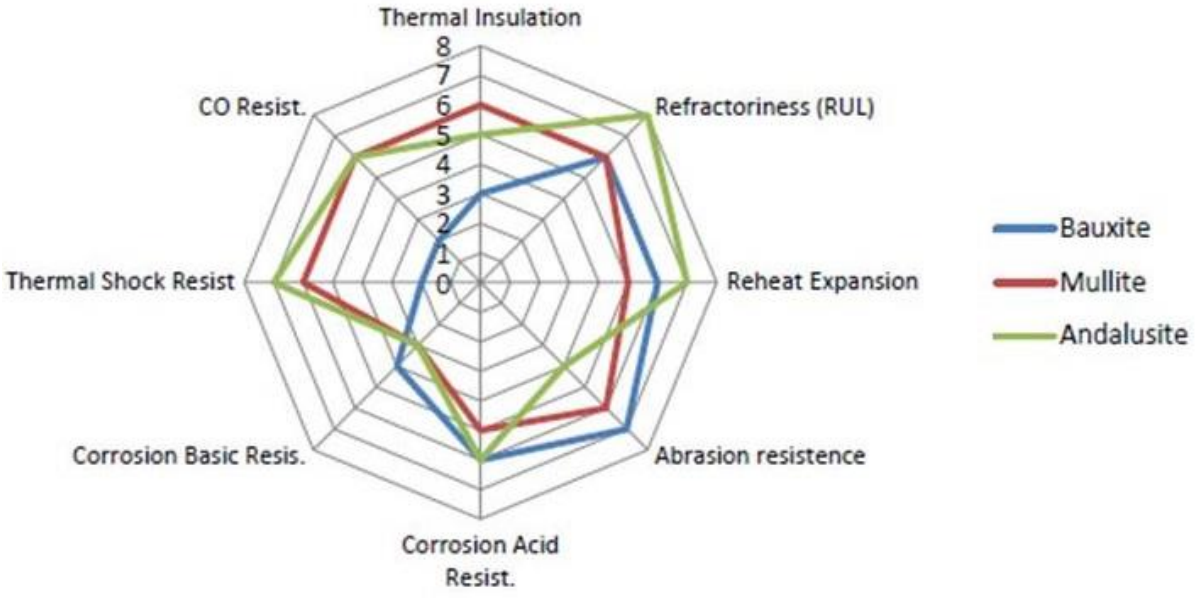

Figure 2.12: Qualitative description of the performance of three classes of refractories (1 being the lowest performance rating)

2.4.3.4 Reclaimed Refractory Grog (RRG or Grog)

The refractory industry has been experiencing continuous difficulty with the availability of raw materials and significant increase in costs, particularly from China (Hutton et al. 2009). The surge in raw material costs and availability necessitated the need to use more reclaim refractory materials which we previously dumped in landfill or crushed and used for general refractory purposes.

Ghonaim et al. (2010) and Hutton et al. (2009) described reclaimed refractory materials, also referred to as spent refractories or simply grog, as artificial aggregates usually obtained from the crushed spent or defective bricks for re-use in monolithic refractory materials.

Refractory manufacturers and end-users started substituting virgin raw material with grog over 20 years ago with the recycling philosophy well entrenched in different industries as a result of environmental drivers (Hutton et al. 2009). Hancock and Cannon (2000) and Schutte (2010) proposed that recycling of refractory materials ensure availability and consistency of grog material produced, whilst continuously monitoring performance in service.

Hutton et al. (2009) stated that such consistency and viability can be maintained through ensuring segregation of spent refractories and conducting the necessary testwork such as X-ray

diffractometry. Nevertheless, Almeida et al. (2016) proposed an integrated solution to recycling refractory waste which is aligned with operational requirements, thus determining the technical and financial viability as follows:

- Preliminary assessment which includes generation survey, demolition and segregation,
- Research and development
- Transport, handling and processing
- Application, implementation and validation

Hanagiri et al. (2008) further proposed the concept of 3Rs - reduce, reuse and recycle to conceptualise reducing and recycling spent refractories (see Table 2.6).

Table 2.6: Concept of 3Rs – Reducing, Reuse and Recycling spent refractories

Reduce	• Relaxation of operating conditions. • Continuous operation, operation at lower temperature. • Lifetime/campaign extension of refractories. • Lifetime extension of repairs. • Veneering, repair, shotcrete, gunning.
Re-use	• Slag conditioners, raw materials used in refining, refractory sand, road bed materials.
Recycle	• Reuse of slidegate plates, ladle shroud, spent brick, recycled products, landscape brick, and unshaped refractories.

Classification of reclaimed refractory grog

Bradley and Hutton (2014) proposed that reclaimed refractory materials be sorted into two categories, magnesia-based (MgO) and alumina-based (Al_2O_3) (see Table 2.7). Magnesia-based product can be further classified based on magnesia content and whether they contain carbon or not. For alumina-based products, classification is based on the alumina content, and whether the alumina source is chamotte, andalusite or bauxite based (Schutte 2010).

Table 2.7: Reclaimed refractory material classification (Bradley and Hutton 2014)

Classification of Reclaimed Refractory Grog	
Magnesia Based (MgO)	Alumina Based Al_2O_3
Magnesia Brick	Fired brick (35% Al_2O_3)
Magnesia Carbon	Mid Alumina (55% Al_2O_3)
Magnesia Carbon	Bauxite Brick (75% Al_2O_3)
Magnesia Chrome	Andalusite brick
Alumina Magnesia (Alumag)	Alumina Magnesia Carbon

Schutte (2010) further classified reclaimed refractory grog according to the operating temperature and the intended application which include production of monolithic refractory materials, slag conditioning, raw materials and fuel alternatives (see in Table 2. 8).

Table 2.8: Reclaimed refractory grog product type and application (Schutte 2010)

Typical products	Refractory grog type	Application area / industry
Refractory monolithic materials	Chamotte	Refractory applications up to 1600°C
	Andalusite	Refractory applications up to 1700°C
	Bauxite	Refractory applications up to 1700°C
	High alumina	Refractory applications up to 1750°C
	Silicon carbide	Refractory applications requiring high strength and abrasion resistance.
	Magnesia	Gunning, ramming, fettling and castables mainly for the steel industry.
	Magnesia-chrome	Gunning, ramming and castables for the steel, copper and platinum industries.
	Magnesia-spinel	Gunning, ramming and castable materials mainly for the steel industry.
	Magnesia-carbon	Gunning and castable materials for the steel industry
	Dolomite	Gunning and fettling material for the steel industry
Slag conditioning materials	Chamotte Andalusite	Source of alumina for the ferroalloy industry
	Magnesia Magnesia-spinel Magnesia-carbon	Slag conditioner for the steel industry to saturate steelmaking slag with respect to MgO to reducing refractory lining attack
	Magnesia-carbon	Foaming slag practice for electric arc furnaces in steel industry.
	Dolomite	Slag conditioner for the steel industry to increase slag basicity and to saturate slag with MgO.
Raw material and fuel replacement	Chamotte Andalusite	Source of alumina for the cement industry.
	Graphite/carbon	Recarburiser for steel and ferroalloy industries.
	Magnesia-carbon Magnesia-chrome	Furnace taphole and ladle well fillers.

The techniques used to remove the refractory lining after service is an important factor because many refractory vessels contain more than one type of refractory, and the reclamation process requires selective stripping of the lining to avoid contamination (Hancock and Cannon 2000).

Bradley and Hutton (2014) stated that it is possible to manufacture products based on 100% recycled refractory materials for lower alumina castables (<40 wt% Al_2O_3) used in non-critical applications. Other studies, particularly by Hutton et al. (2009), reported on the possibility of formulating compositions with between 40 and 70% reclaimed materials and still achieve comparable physical properties to existing standard grades. However, it should be noted that reclaimed materials may have lower densities and/or higher porosities than similar virgin materials, which may affect the water demand of the manufactured castable (Bradley and Hutton 2014; Hutton et al. 2009).

Hutton et al. (2009), in particular, conducted a study where low-cement castable mixed with grog was examined, and concluded that grog-based castables had a much higher water demand than standard castable without any detrimental effect on physical properties. Hanagiri et al. (2008) conducted a similar study in which different grog percentages were added in a refractory castable to determine the effect on water demand, apparent porosity and wear rate. The study concluded that water demand, apparent porosity and wear rate all increased with the increase in grog addition (see Figure 2.13).

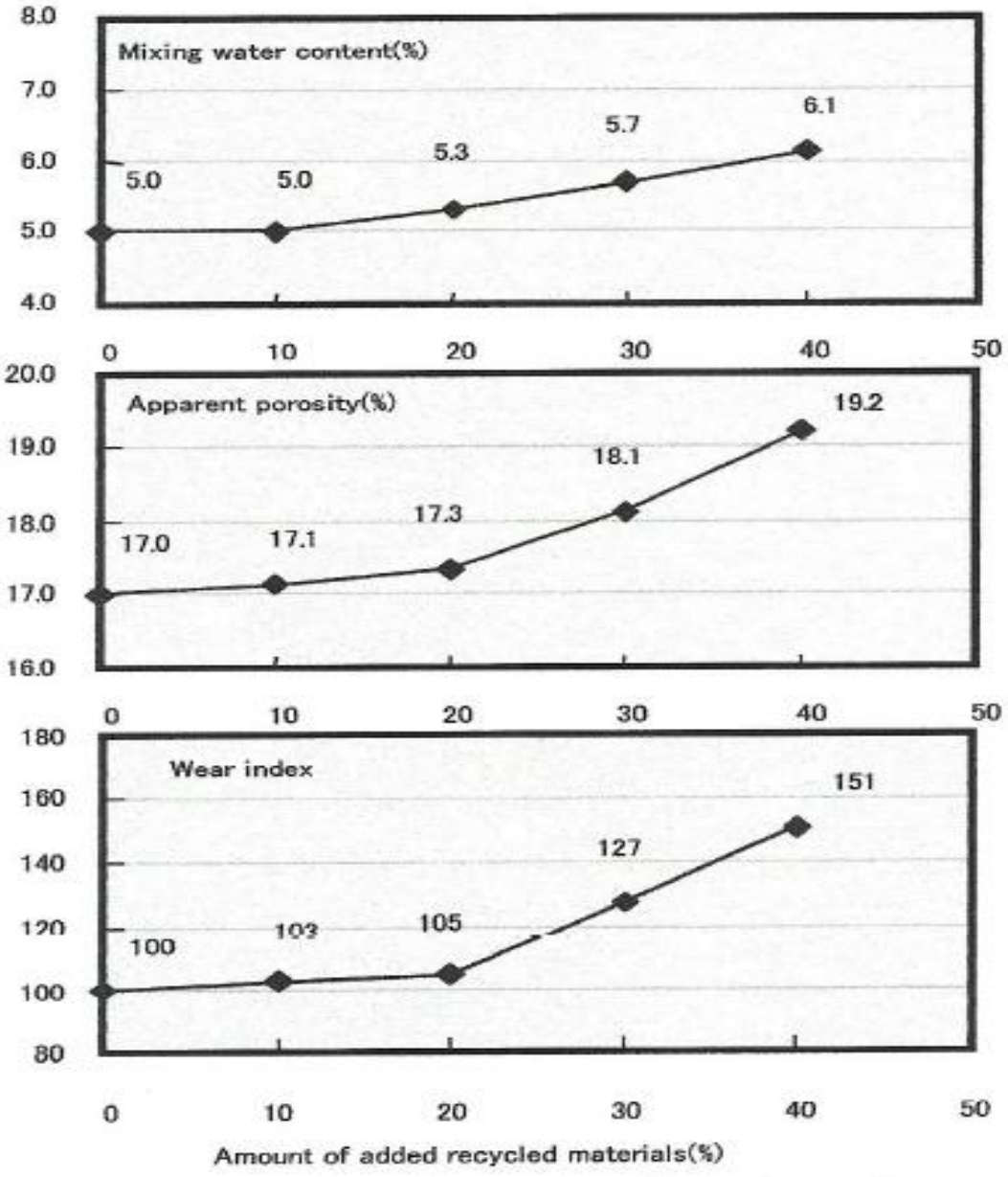

Figure 2.13: Influence of added recycled material on the castable properties (Hanagiri et al. 2008)

Inconsistencies in the physico-chemical properties is one of the major disadvantages of using grog (Hancock and Cannon 2000). According to Hancock and Cannon (2000), unlike virgin refractory materials, the properties of grog cannot be consistently maintained, and this can alter the properties of the final product. Schutte (2010) indicated that refractory monolithic manufacturers and users require consistent and high-quality grog to ensure that the products manufactured perform at least as well as its virgin-based counterparts. Schutte (2010) suggested that a good quality system should be implemented which includes site and refractory grog inspection to evaluate the condition of the grog and potential contamination. Although the consistency of refractory grog has improved over the years Hancock and Cannon (2000) and

Hutton et al. (2009) cautioned that the quality and source of grog is vital if final product consistency is to be maintained.

2.4.4 Particle Packing and Size Distribution in Castables

When the ingredients of LCC have been chosen, developing a refractory castable requires careful consideration of particle size distribution (PSD) to achieve maximum particle packing hence improving the overall properties of the castable product (Myhre, 2008). Particle packing simply refers to the efficiency of packaging particle to achieve maximum void reduction between particles; thus, more water is available to promote castable flow (Lee et al. 2001).

In recent years, Furnas and Andreasen's PSD models have been most commonly used for developing castables for either vibratable flow or self-flow (Peng and Myhre 2012). These packing models have been widely accepted for the design of refractory castable. The model is described as follows;

$$CPFT = \left[\frac{\mathrm{d}}{D}\right]^{q} \text{ x } 100 \qquad [2.2]$$

Where CPFT: (Cumulative particle finer than) against particle sizes for distribution coefficient

d: Particle Size

D: Maximum Particle Size

q: Distribution Coefficient (q-value)

Figure 2.14 shows a typical particle size distribution for a LCC suitable for installation by vibration (Myhre 1994). Myhre (1994) stated that this type of castable is characterised by very high strength and good flow when subjected to vibration, however it is relatively sensitive to incorrect water addition. Peng and Myhre (2012) further stated that the distribution coefficient for (q-value) play as huge role in determining whether the castable is suitable for vibration or self-flow.

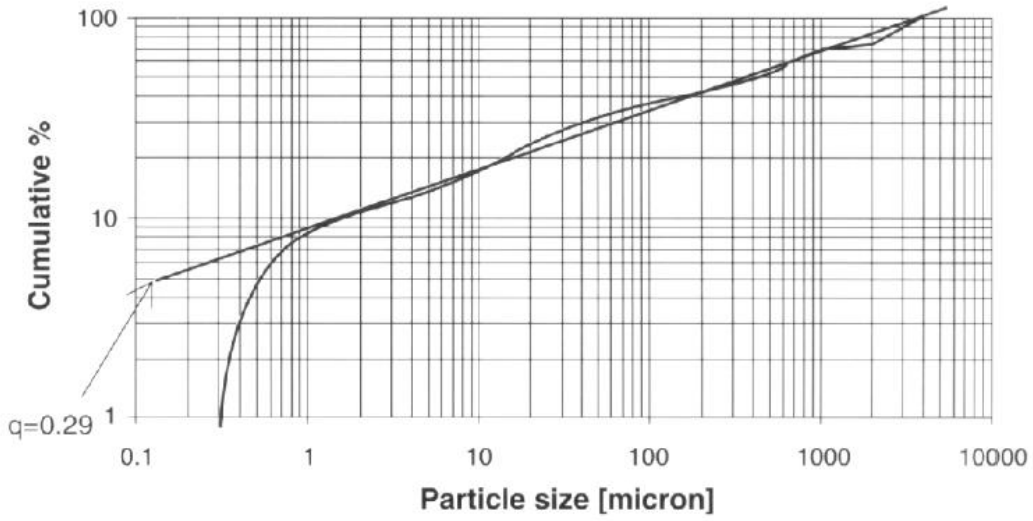

Figure 2.14: PSD for a high-alumina vibratable castable based on the Adreasen Model

Generally, the higher the q-value, lower the fines content; and the lower the q-value, the higher the fines in the system which makes it a self-flow castable (Myhre 1994). Fruhstorfer and Aneziris (2014) conducted a study to determine the influence of coarse particles on the porosity of refractory castables. The study concluded that the particle size distribution with a distribution coefficient (q) between 0.28 and 0.30 led to comparatively dense and stable castables with good flowability, hence commensurate with the Andreasen model for dense low-cement castables.

In the substitution of virgin material by recycled grog, Hanagiri et al. (2008) conducted a study to determine the effect of recycled materials on the properties of castables. The study concluded that the particle size of the recycled material added to the refractory castable is in the range of 5 to 20 mm, and in the case of wet gunning materials, the particle size ranges from 1 to 5 mm. Hanagiri et al. (2008) proposed that 20% of recycled material can be added to the virgin castable without compromising wear-resistance properties, water addition and apparent porosity (see illustration on Figure 2.15).

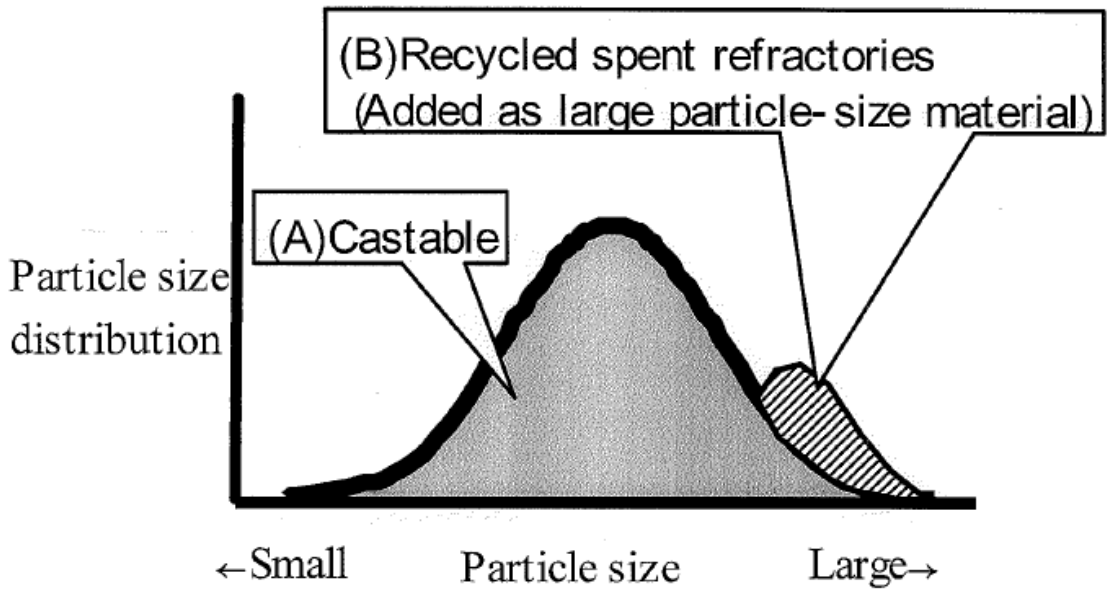

Figure 2.15: Addition of recycled material to a virgin castable (Hanagiri et al. 2008)

Schutte (2010) further stated that the general particle size grading specification for reclaimed refractory grog used as a refractory aggregate is 0-1 mm, 1-3 mm and 3-6 mm. The grog particle size suitable for replacement of virgin refractory raw materials is usually selected only for aggregate proportion of the castable. This is deliberately done to avoid significantly influencing the matrix components of the formulation which are integral in determining the final physico-chemical properties of the refractory material (Hanagiri et al. 2008; Schnabel et al. 2014). This is because the matrix components such as cement hydrates to form different phases, which upon heating further transforms to different phases which determine the final properties of a castable, whereas castable aggregates take part in latter chemical reactions at higher temperatures.

2.5 Corrosion wear of Refractory Castables

Hloben (2000) stated that the basic principle for a refractory material is high stability of its solid oxides at elevated temperatures. The stability of these solid oxides can be determined in oxidizing and reducing atmospheres by using an Ellingham diagram (see Figure 2.16).

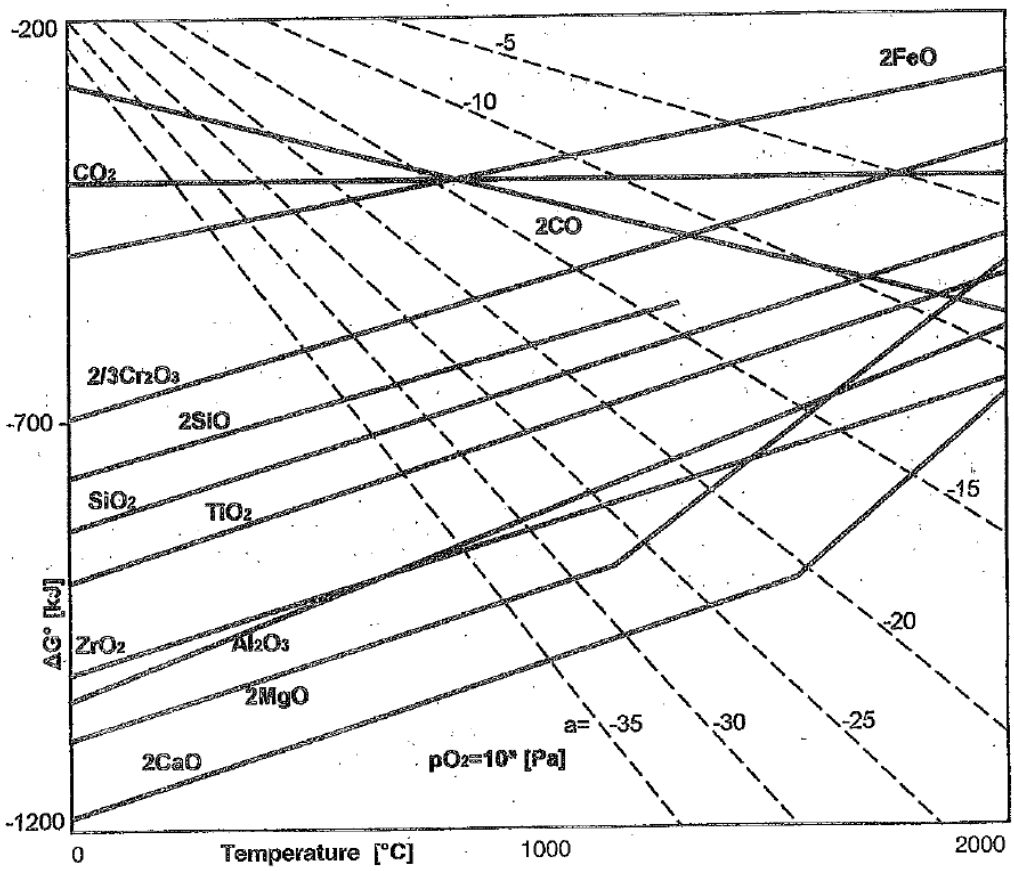

Figure 2.16: Ellingham diagram for refractory oxides (Gibbs free energy vs. temperature) (Hloben 2000)

The value of ΔG° for an oxidation reaction is a measure of chemical affinity of the metal for oxygen, and the more negative the value of ΔG° at any temperature, then the more stable the oxide. This implies that oxides such as CaO, MgO, and Al_2O_3 are more stable at the bottom of the graph with more negative ΔG° values than other oxides on the upper side of the graph (Hloben 2000). The stability of the compounds is also considered in respect to one another, a metal with a more stable oxide will tend to reduce the oxide of another metal where the oxide of the second metal is less stable than that of the first (Hloben 2000). Therefore, in refractory applications, it is important to consider solid oxides which are more stable such CaO, MgO, and Al_2O_3.

The fundamental principle of refractory-slag compatibility is to consider if both materials are either acidic or basic, since acid refractories tend to resist acid slags and similarly basic refractories tend to resist basic slags (Schacht 2004). For example, an acidic refractory material will contribute SiO_2 in a corrosion reaction, whereas a basic material will contribute CaO or MgO in a corrosion reaction. Depending on whether the two materials are in contact as

refractory-slag, this interaction can either speed up the corrosion reaction if there is no compatibility (e.g., acid-basic) or tend to resist the corrosion (e.g., acid-acid) (Schacht 2004). Therefore, if one uses a magnesia-carbon lining as refractory vessel, it is important that the slag be saturated with MgO for basic-basic compatibility, thus resisting corrosion. Kesseheim (2008) noted corrosion as the primary reason for the failure of many refractory linings. In view of this, Kesseheim (2008) stated five major steps in the steady state corrosion process;

- Wetting of the refractory by corrosion the melt
- Penetration of the refractory along pores and channels
- Reaction of corrosive melt with the refractory matrix and aggregate
- Formation of liquid phases which compromises the bonding strength of a refractory
- Washing away of the reacted refractory components by the dynamic melt

Lee and Zheng (2004) stated that the chemical attack on solid refractories by liquid slags can either be by permeation of liquid slag via open pores (penetration) or by reaction of slag with refractory phases (dissolution). In principle, corrosion reactions are viewed as an attempt by the system to achieve compatibility by progressing toward equilibrium (Schacht 2004). By way of illustration, Melcher et al. (2007) conducted cut tests to study corrosion mechanism of Alumina spinel castables by steelmaking slags at 1620°C. After testing, the samples were cooled down and cut in cross-sections before being examined by SEM and EDS (see Figure 2.17). The study illustrated that as the slag is under-saturated in Al_2O_3, a concentration gradient from the refractory surface into the slag develops, whilst, the diffusion of CaO from the slag into the refractory surface takes place. The study also showed that slag saturated in CaO and MgO is more aggressive towards Al_2O_3 castables.

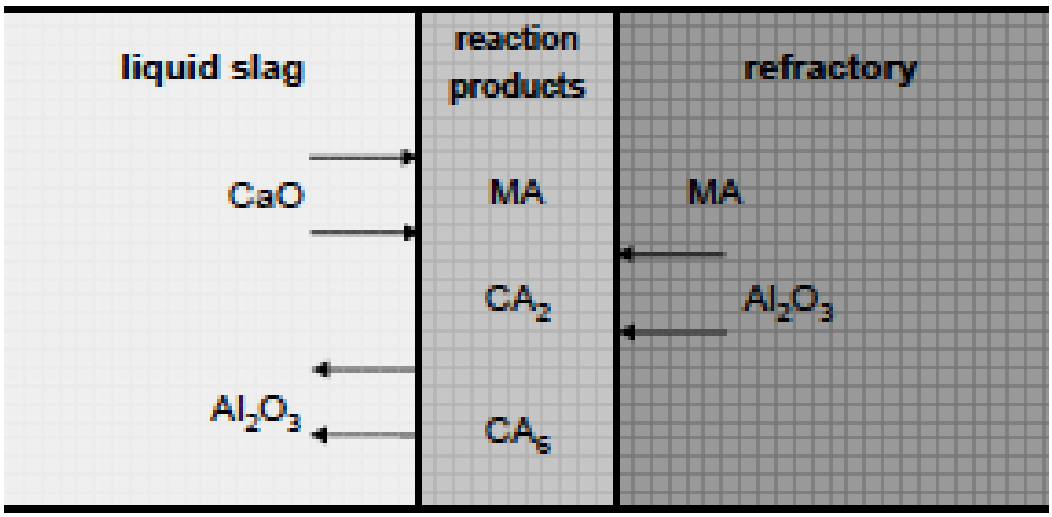

Figure 2.17: Schematic representation of the wear mechanism (Melcher et al. 2007)

Lee and Zheng (2004) noted that if the velocity of the slag is low, the dissolution rate of Al_2O_3 occurs indirectly with the intermediate step of calcium aluminate CA_2 and CA_6 formation. However, for aggressive slags, the intense movement of slag results in higher dissolution rate of Al_2O_3, and if the dissolution reaction rate is higher than the rate of formation of CA_2 and CA_6, direct dissolution of Al_2O_3 may also occur (Lee and Zheng 2004).

Schacht (2004) stated that both porosity and corrosion rate are salient aspects to be considered because most refractories contain voids or pores that affects the rate of corrosion. The temperature gradient also plays an important role in term of slag corrosion as illustrated by the three stages of corrosion:

- Stage 1 – Characterized by slag penetration with low-temperature gradient
- Stage 2 – Characterized by partial slag penetration as a function of temperature gradient
- Stage 3 – Characterized by full slag penetration as a function of temperature gradient.

Stage 1 corrosion, illustrated by Figure 2.18, shows that the refractory corrosion reaction occurs primarily at the immediate hotface and shows minor or no slag penetration. Schacht (2004) stated that in stage 1 corrosion, the hotface temperature primarily affects the rate of corrosion reaction, if this temperature is kept below the point where corrosion products become liquid, corrosion will be very slow or non-existent.

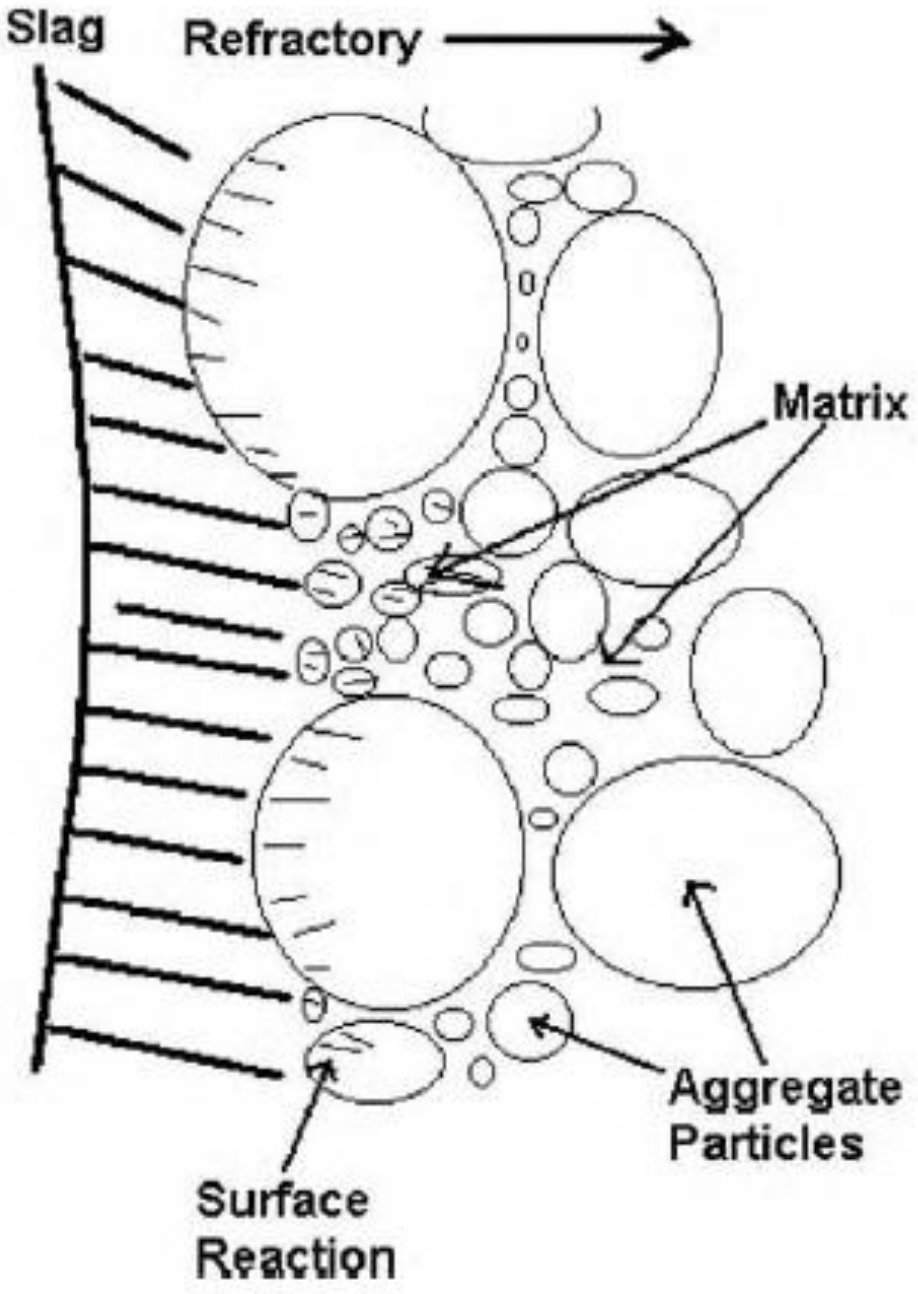

Figure 2.18: Stage 1 of slag attack (showing a bonded refractory) (Schacht 2004)

Stage 2 corrosion illustrated by Figure 2.19, is characterised by two phenomena, namely, the penetration of the refractory by slag and interruption of the hotface region (Schacht 2004). Stage 2 corrosion occurs after stage 1, but only if there is sufficient temperature gradient to allow penetration.

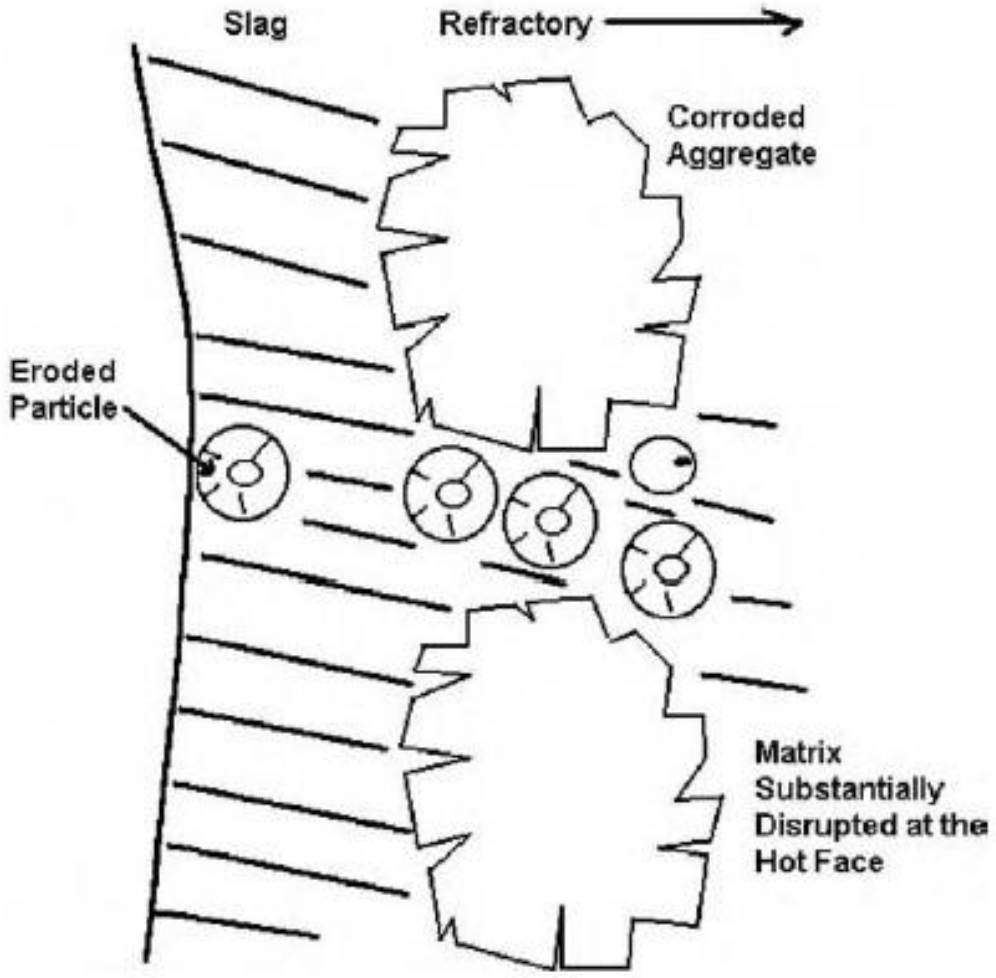

Figure 2.19: Stage 2 of corrosion process (Schacht 2004)

Stage 3 corrosion illustrated by Figure 2.20, shows deeper slag penetration and erosion, the slag appears to be the phase holding the refractory aggregate particles in place (Schacht 2004).

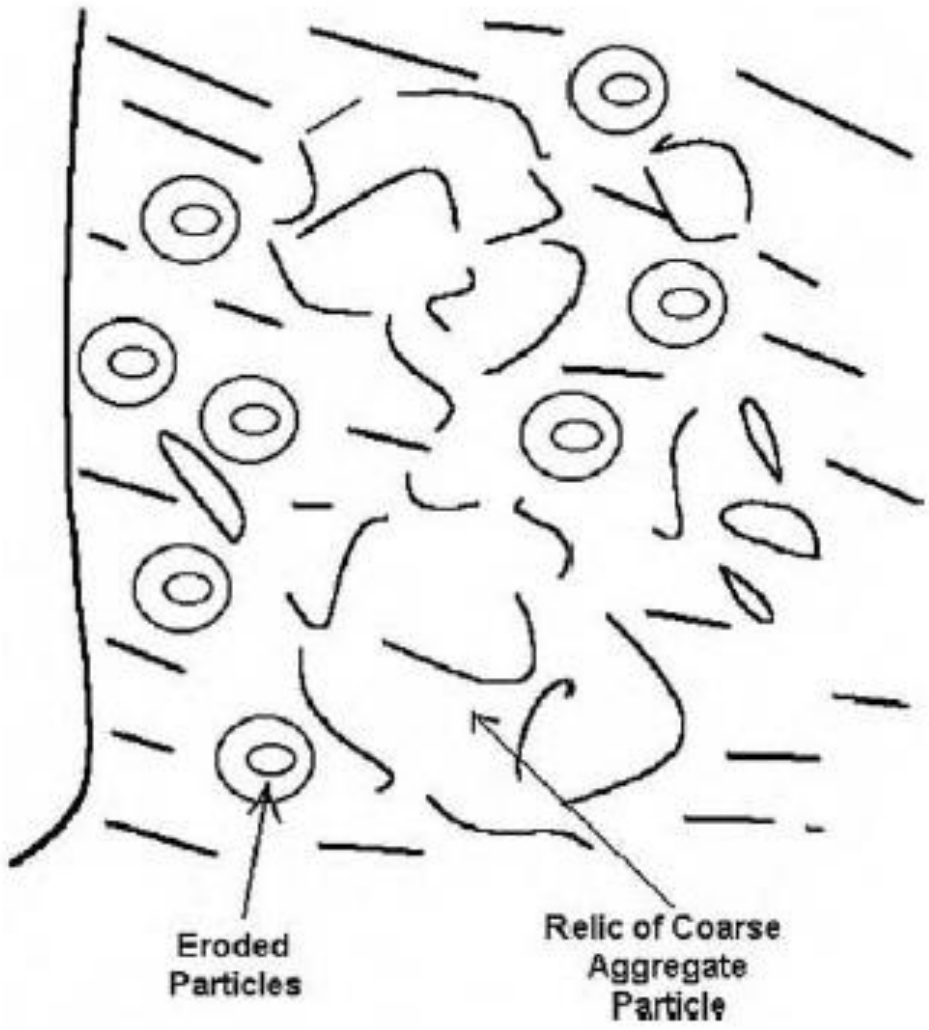

Figure 2.20: Stage 3 of corrosion process (Schacht 2004)

It is most likely that the tundish working lining ($MgSiO_2$) in contact with both metal and slag experiences any of these stages. Therefore, the safety lining castable targeted for substitution with grog should not be compromised in quality, in case the working reduces or experience stage 3 corrosion. the low-cement castable tundish safety lining castable at the foundry under study is not directly exposed to slag attack. Therefore, as precaution, it is important to simulate the condition of slag attack when the hotface/working lining reduces and the grog-fresh castable is prone to attack. Hloben (2000) and Vert (2016) noted the thermal gradient between the safety and working lining is lower than that between the slag and working lining, as a result, liquid phases are not expected to form between the safety and working lining. This indicates that there is no foreseeable interaction between the safety lining and slag if the working lining is not completely reduced.

Nevertheless, corrosion slag tests are important to simulate in-situ tundish slag/safety lining interactions should the working lining reduce to potentially catastrophic thickness levels (Lee and Zheng 2004; Schacht 2004).

The three corrosion test methods are commonly used to evaluate in-situ condition of slag-refractory interaction. These are static corrosion test, rotating spindle or finger test and rotary slag test. However, due to cost and availability of both the rotating spindle or finger test and rotary slag test, the static corrosion test was selected for this study.

2.5.1. Static corrosion test

The static corrosion test method involves filling up a cored-out refractory brick with slag and exposing it to high-temperature to promote slag-refractory interaction (Lee and Zheng 2004). The samples are prepared according to the DIN 51069 Blatt 2 standard test method which entails preparing mould cubes with a cylindrical section core drilled to specified dimensions, 50 mm diameter and 35 mm depth (see Figure 2.21). The cylindrical holes are then filled with equal amounts of slag and covered with a lid of the same refractory material.

Figure 2.21: Cup/Pot static test for slag-metal corrosion test method (Kesseheim 2008)

The sample is the heated up to refractory solidus temperature and soaked at that temperature for 12 hours to allow sufficient refractory-slag interaction. This dissolution process at the refractory-slag interface is governed by chemical reactions and diffusion of reacting species through the liquid (Lee and Zheng 2004). Once the firing is complete, the samples are then cut in the middle to evaluate corrosion pattern of each sample using the SEM-EDS analysis (Kesseheim 2008). This test reflects only the isothermal reaction and penetration between slag and the refractory (Lee and Zheng 2004).

2.6 Use of phase diagrams to study refractory corrosion

Zheng and Lee (2000) stated that understanding corrosion mechanisms and comparing corrosion resistance of refractories in various slags is important for evaluating their service life. According to them, phase diagrams provide useful information about the compatibility between refractory components and slag that can be used to interpret corrosion mechanism and predict corrosion behaviour.

Schacht (2004) conducted a corrosion study to evaluate 70% and 90% alumina-Silica bricks in a ferrous foundry with the slag containing CaO, SiO_2 and FeO and other oxides. The slags were assumed to be a binary mixture of CaO–SiO_2, whereas the brick components were presented by using the binary Al_2O_3-SiO_2 phase diagram (Harbison and Walker 2005; Zheng and Lee 2000). This allows the corrosion to be predicted using the ternary phase diagram CaO-Al_2O_3-SiO_2 (see Figure 2.22).

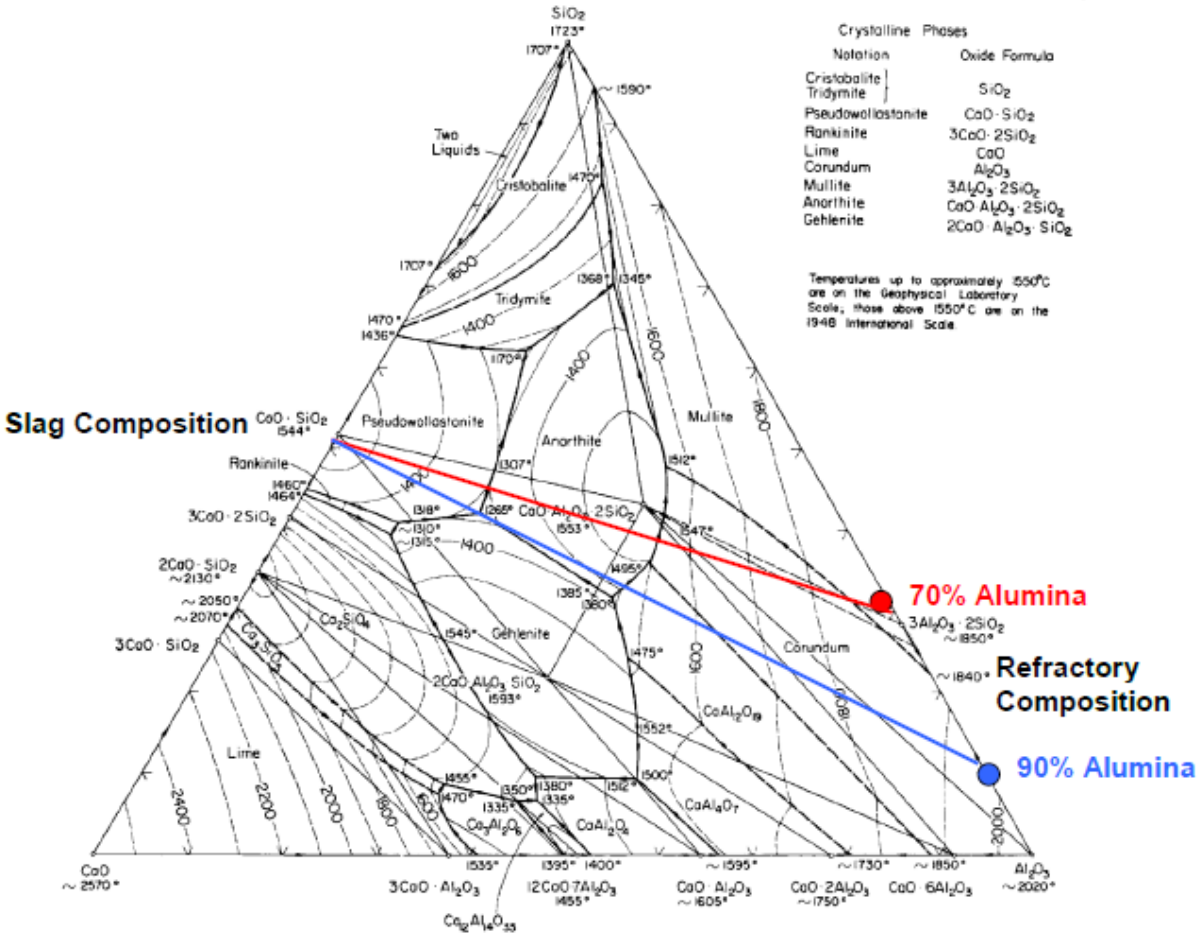

Figure 2.22: Interpretation of corrosion wear of Alumina Silica bricks in foundry slag (Schacht 2004)

Based on the ternary phase diagram CaO-Al_2O_3-SiO_2, Schacht (2004) summarized the corrosion interpretation of the 70% and 90% alumina silica bricks with the slag composition highlighting the following observations;

- Both lines between the bricks and the slag pass close to ternary eutectic at 1265°C, indicating the potential for liquid phases to form between the slag and the bricks. As a result, corrosion reactions are most likely to occur under these conditions.

- The CaO from the slag will react with the bricks forming low melting phase CAS_2 and C_2AS, thus dissolving mullite into slag and forming other corrosion products (Valdelièvre et al 2002). In the 70% Al_2O_3 brick, the mullite is stable until the local composition reaches approximately 20% CaO, while for the 90% brick, mullite disappears when the local composition reaches 8% CaO.
- The higher the CaO/SiO_2 ratio or slag basicity the quicker the initial reaction temperature between the slag and refractory with respect to formation of liquid phases and beginning of corrosion.

2.7 Cost Considerations and Refractory Waste Management Concept

In line with the emerging paradigm of the circular economy (Ndlovu et al. 2017), the recycling and reuse of reclaimed bauxite refractory materials for tundish applications provides significant cost savings. The practical benefits not only include the environmental and regulatory compliance, but also result in significant cost savings by reducing reliance on virgin andalusite raw materials. Bradley and Hutton (2014) stated that at least 20 % savings can be achieved by refractory recycling alone, apart from conveyance and landfill disposal costs.

As indicated in the preceding chapters, the one of the issues for Scaw is the 200 tons of alumina waste generated monthly. Currently, this waste is either sent to the landfill/dump site, or is randomly given to refractory producers at zero cost. From an environmental perspective and compliance to government legislations, this practice is not sustainable and may result in penalties in the near future. Consequently, the foundry has a pressing need to find alternative ways to handle these refractory wastes. The issue is exacerbated by the fact that Scaw does not recycle any of it refractory waste at present.

Figure 2.23(a) illustrates the recycling current practice at Scaw, whilst figure 2.23(b) shows proposed concept for recycling the bauxite alumina roof bricks. The proposed approach will result in reduced costs of landfill disposal and hence overall reduce the cost of ownership of the refractories.

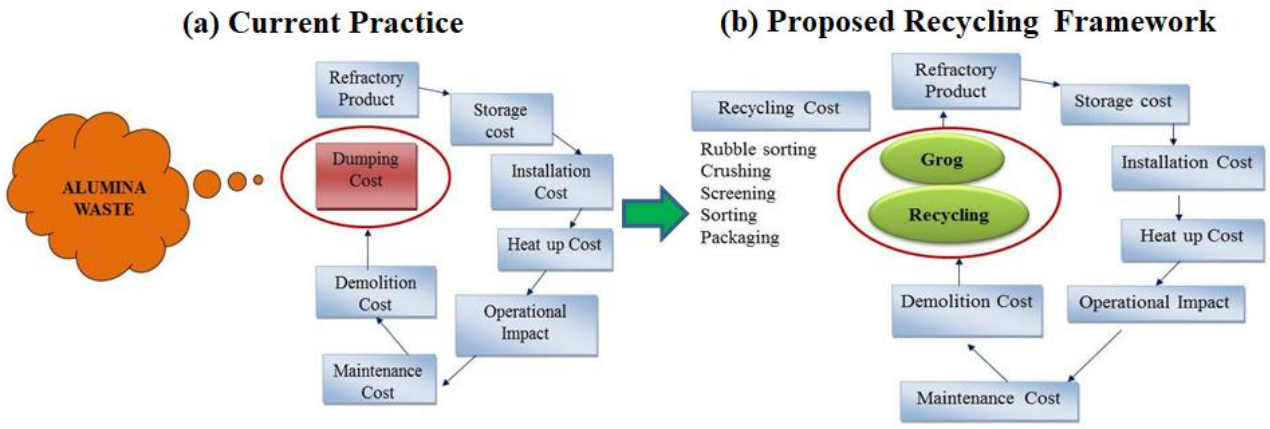

Figure 2.23: (a) Current operational practice (b) Proposed concept for the recycling of bauxite-alumina roof bricks.

In line with the integrated solution proposed by Almeida et al. (2016) for recycling refractories in steel operations. Scaw adopted a similar approach to implementing the integrated solution which entails quantifying total refractory usage annually and identifying different refractory materials suitable for recycling after demolition and segregation. This dissertation covers the second stage of the integrated solution which addresses research and development and assesses the technical and economic viability of the recycling project (Almeida et al. 2016). In this case, the spent roof bricks will be characterised and analysed to ascertain viability, suitable grog will be crushed and sieved into the different size fractions and integrated to the constituted castables to replace virgin andalusite raw material.

CHAPTER 3 METHOD

3.0 Introduction

The recycling of alumina-based refractory materials requires a fundamental knowledge of the thermophysical, thermochemical and thermomechanical behaviour of the alumina-based refractory materials. In addition, their degradation behaviour when contacted with molten slag, liquid steel, and corrosive and abrasive gases commonly found in steelmaking is particularly important from a safety perspective (Kumar et al. 2015; Sadiki et al. 2014). Therefore, standard tests are often conducted in order to determine the physico-chemical, thermomechanical and thermochemical behaviour of the refractory under simulated conditions of service.

This chapter covers the experimental procedure followed in recycling bauxite roof bricks for potential re-use in tundish applications at Scaw. The experimental procedure involved the following stages:

- Selection and characterization of spent roof bricks for recycling
- Formulation of castables from reclaimed alumina grog
- Standard quality tests on the formulated refractory castables
- High-temperature tests on the formulated refractory castables

3.1 Selection and characterization of spent roof bricks for recycling

As stated in Section 1.2, the remaining thickness of some of the roof bricks can be as high as 80% of the original size, and the wear profiles of these bricks are not uniform across the entire furnace roof. As such, three brick samples were randomly selected from the EAF roof at different sections of the roof as shown in Figure 3.1 a, b and c. The selected brick samples were then characterized by means of using scanning electron microscopy (SEM), energy dispersive spectrometry (EDS) and X-ray diffractometry (XRD) in order to determine their recyclability.

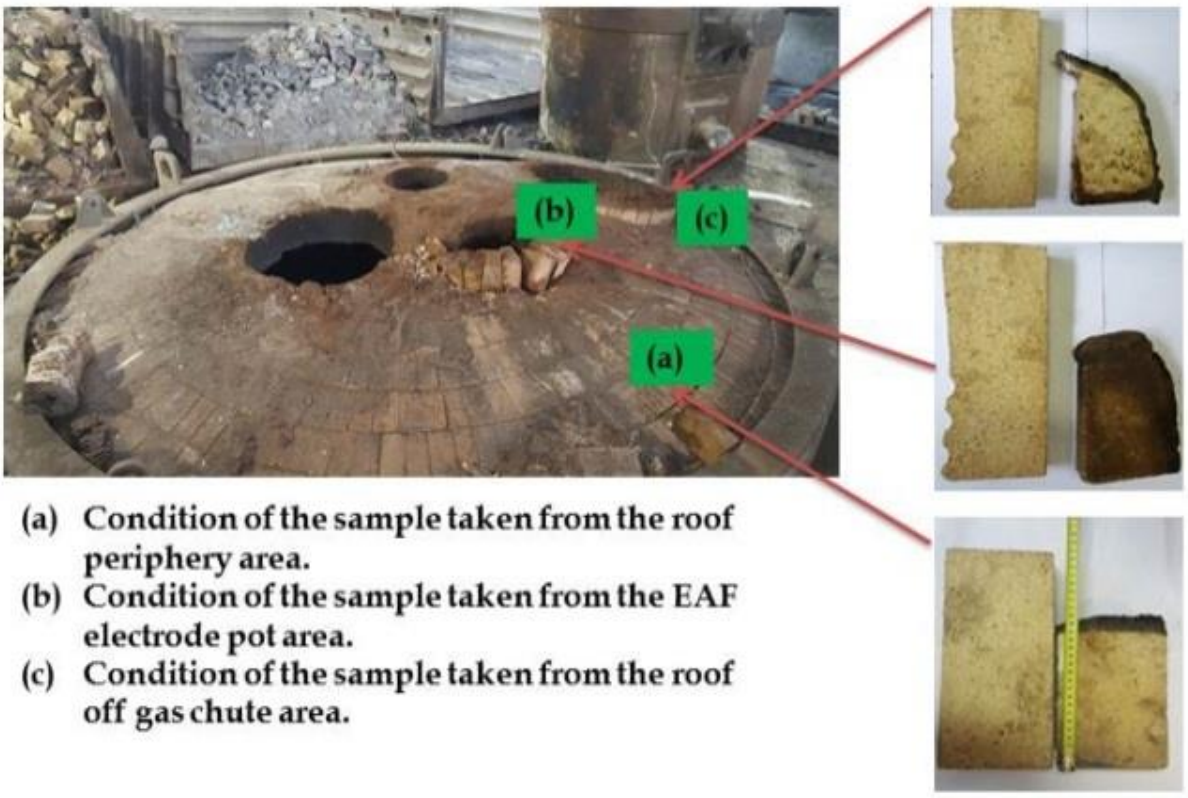

Figure 3.1: Conditions of the reclaimed refractory bricks after service/campaign

3.2 Formulation of castables from reclaimed grog

In general, the targeted particle sizes mostly considered for substitution in reclaimed refractory grog are the 0-1 mm, 1-3 mm and 3-5 mm aggregate fractions (Schutte, 2010). Similarly, in this study, only the 0-1 mm, 1-3 mm and 3-6 mm aggregate portions of the castable were considered for substitution. The recycled bauxite castables were then formulated in afore-mentioned proportions to replace virgin andalusite in castables for tundish applications. According to Fruhstorfer and Aneziris (2014), the central problem in designing unshaped refractory castables is the simultaneous optimization of the interrelated properties of stability, flowability and density. In this case, the optimization of particle size distribution, particularly that of the coarse aggregates, plays a key role in obtaining the desired final properties (Schutte. 2010; Fruhstorfer and Aneziris 2014). The matrix components, which include calcium aluminate cement binder, fillers and deflocculating additives remained unchanged to avoid affecting the flowability, workability, early strength and volume stability of the castable (Schnabel et al. 2014). The composition of the formulated products was then analysed by X-ray florescence (XRF) spectrometry.

For ease of referencing, the formulated samples were labelled as follows: (1) Virgin sample (VS) representing the current specifications of the virgin andalusite castable without grog addition; VS sample was thus regarded as the reference formulation; (2) Sample S1 contain 10% bauxite grog; and (3) Samples S2, Sample S3, Sample S4 contain 20%, 30%, and 40% bauxite grog respectively (see Table 3.1).

Table 3.1: Design formulations of the grog-fresh samples

Virgin Andalusite vs Bauxite Grog-Based Castable Formulations										
Description	**VS (kg)**	**0%G**	**S1(kg)**	**10%G**	**S2(kg)**	**20%G**	**S3(kg)**	**30%G**	**S4(kg)**	**40%G**
Binder Premix	1,1	8	1,1	8	1,1	8	1,1	8	1,1	8
calcined Alumina	0,3	2	0,3	2	0,3	2	0,3	2	0,3	2
Bauxite Grog 0-1 mm	**0**	**0**	**0,3**	**2**	**0,6**	**4**	**0,9**	**6**	**1,2**	**8**
Bauxite Grog 1-3 mm	**0**	**0**	**0,5**	**4**	**1,1**	**7**	**1,6**	**11**	**2,1**	**14**
Bauxite Grog 3-6 mm	**0**	**0**	**0,2**	**2**	**0,5**	**3**	**0,7**	**5**	**0,9**	**6**
Andalusite 200 µm	3	20	3	20	3	20	3	20	3	20
Andalusite 0-1 mm	3	20	2,7	18	2,4	16	2,1	14	1,8	12
Andalusite 1-3 mm	5,3	36	4,8	32	4,3	28	3,7	25	3,2	21
Andalusite 3-6 mm	2,3	15	2	14	1,8	12	1,6	11	1,4	9
Total	**15**	**100**	**15**	**100**	**15**	**100**	**15**	**100**	**15**	**100**

Formulated castable mixtures of 15 kg per sample were prepared for conducting different test methods of refractory classification. A binding premix consisting of calcium alumina cement, admixture, and microsilica were added in predetermined ratios and maintained at 8% of the total formulation. Calcined alumina content remained unchanged at 2%, similar to the reference formulation. The andalusite 200 µm finer size fraction also remained unchanged.

S1 contained 10% bauxite grog in each size fraction of 0-1 mm, 1-3 mm and 3-6 mm, 0.3 kg, 0.5kg and 0.2kg respectively. Similar to S1, each size fraction of 0-1 mm, 1-3 mm and 3-6 mm contained S2-20%, S3-30% and S4-40% bauxite grog respectively (see Table 3.1).

No other additives, in the form of an accelerator or retarder were added to formulations to modify the placing properties of the refractory castable in order to replicate the current reference formulation which does not contain additives. The standard particle size distribution for the reference castable was used as the basis for the different grog formulations (see Table

3.2). Furthermore, for validity, the particle size distribution was based on the typical standard formulations for low-cement castables as recommended by Ressler (2009).

Table 3.2: Standard sieve grouping for the reference castable

Sieve Grouping for the Reference Castable				
Sieve Group (mm)	**Min %**	**Low %**	**Upper %**	**Max %**
3.1 <	12	13	16	18
1-3.15	33	34	37	38
0.5-1	5	7	11	12
0.106- 0.500	8	10	11	12
<0.106	27	28	30	32

After the castable products were formulated, X-ray diffractometry was conducted to determine the prevailing phase compositions of the samples and phase diagrams were used to predict primary phases between the refractory and slag, and the interaction thereof. Furthermore, physical and high-temperature tests were conducted to determine the substitutability of virgin andalusite raw material in castables with grog material.

3.3 Standard quality tests on formulated refractory castables

Standard refractory tests were conducted to evaluate the physico-chemical, thermomechanical and thermochemical properties of the formulated products. The performance of the formulated castables were compared to the values obtained from the reference castable based on physical properties such as flow behaviour (ASTM C1446), open porosity (ASTM C20-00), bulk density (ASTM C357), and cold crushing strength (ASTM C133).

3.3.1 Flow test, water addition and setting time

The flow measurement of the formulated castables were recorded after mixing the castable with water for 3 minutes. This is because the tundish castable installation is installed by vibration, therefore no flow delay is expected. The parameters and procedure for measurements

were guided by ASTM C1446 and studies by Myhre (2008). The flow properties of the formulated castables were then compared to those of the reference castable.

Based on the procedure recommended by Hanagiri *et al.* (2008), the amount of water added to the formulated castables was monitored in order to determine the change in water content with the addition of bauxite grog. The amount of water added to the formulated castables was then compared with that of the reference castable which, according to standard practice, is in the range of 5 to 7%.

3.3.2 Apparent Porosity

Apparent porosity is the ratio of the volume of voids in a sample to the volume of the sample and expressed as a percentage (Hancock and Cannon, 2000; ASTM C830, 2000). Hutton et al. (2009) and Hanagiri et al (2008) stated that higher apparent porosities result in lower bulk density; as a result, the castable wear resistance may decline. In the present study, the apparent porosity test was conducted according to ASTM C830 (2000). The apparent porosity is calculated using Equation 3.1:

$$\% \text{ Apparent Porosity} = \frac{W-D}{W-S} \text{ x } 100 \qquad [3.1]$$

Where:
W= Saturated weight of the sample
D= Dry weight of the sample
S= Suspended weight of the sample

3.3.3 Bulk density (BD)

Bulk density is the measure of the ratio of the weight of the refractory material to the volume it occupies (Harbison and Walker 2005). Higher bulk densities are indicative of better particle size packing and reduced porosity thereby improving the wear resistance of refractory castables (Lee et al. 2001). The bulk density of formulated castables was conducted according to ASTM C830 (2000) and calculated using Equation 3.2:

$$\text{Bulk density} = \frac{D}{V} \quad [3.2]$$

Where:

D= Dry weight of the sample

V= Volume of the sample (W – S)

3.3.4 Cold crushing strength

The cold crushing strength (CCS) of a material is determined by placing a standard size sample between the plates of a press and increasing the load at a specified rate until failure occurs (Hancock and Cannon 2000). The CCS measures the mechanical strength at room temperature, and also serves to indicate susceptibility to damage from handling on site or during transportation of refractory materials (Hancock and Cannon 2000). According to Wöhrmeyer et al. (2006) CCS above 20MPa are considered acceptable for 60% alumina castable. The CCS test for the formulated products was conducted according to ASTM C133 (2003).

3.4 High-temperature tests on formulated refractory castables

The thermochemical and thermomechanical attributes of the formulated products were also evaluated based on high-temperature properties such as static corrosion tests and hot modulus of rupture. The hot modulus of rupture (HMOR) tests are critical in determining the strength of the refractory material at high-temperatures. Hancock and Cannon (2000) emphasized that the HMOR test method measures the strength of the bond in the refractory at high-temperatures, thereby indicating resistance to structural spalling, slag attack and abrasion. Other tests such as apparent porosity (ASTM C20-00) and permanent linear change (ASTM 865-02) were conducted to validate the efficacy of the formulated products and to determine the upper limit to the amount of substituted virgin raw materials.

3.4.1 Hot modulus of rupture (HMOR)

In this study, HMOR tests were conducted according to ASTM C583-15 (2015) to measure the hotstrength at 1500°C thereby approximating the actual tundish operating temperatures at 1565°C. HMOR is a three-point bending test that entails a 25 x 25 x 150 mm cross-section bar sample heated up at 5°C per min until a temperature of 1500°C is reached. The sample is then

soaked at this temperature for 12 hours before a bend test is performed until failure occurs. This procedure is then repeated 6 times to get an average figure for the different samples.

3.4.2 Permanent Linear Change (PLC)

Permanent linear change (PLC) test involves measuring dimensional changes of a refractory brick or castable from mould size to post-firing (Harbison and Walker 2005). PLC measures the structural stability of refractory material upon heating (Vert 2016). Hloben (2000) stated that unfired or monolithic materials exhibit different changes on reheating owing to mineralogical changes. Therefore, it is important that refractory materials neither exhibit excessive expansion nor shrinkage during reheating to maintain structural stability in-situ. In this study, the specimens were fired at 1500˚C for 12 hours and allowed to cool down to ambient temperature to determine linear dimensions and volume.

3.4.3 Static Corrosion Test

As indicated in Section 2.5.1, this test entails preparing mould cubes with a cylindrical section core-drilled to specified dimensions, 50 mm diameter and 35 mm depth according to the DIN 51069 Blatt 2. The cylindrical holes are then filled with equal amounts of slag and covered with a lid of the same refractory material. The samples are then heated up 1400°C and soaked at that temperature for 12 hours to allow sufficient refractory-slag interaction. This dissolution process at the refractory-slag interface is governed by chemical reactions and diffusion of reacting species through the liquid (Lee and Zheng 2004). Once the firing is complete, the samples are then cut in the middle to evaluate corrosion pattern of each sample using the SEM-EDS.

The volume corrosion test method was used to measure the dimensional deformation of the specimen from its original shape and the severity of slag penetration (Luz et al. 2011). The volume change, measured as % corrosion volume, was calculated according to Equation 3.3.

$$\%\ Corrosion\ Volume = \frac{V_f - V_i}{V_i} \times 100 \qquad [3.3]$$

Where: V_i is the initial volume and V_f is the final volume.

CHAPTER 4 RESULTS AND DISCUSSION

4.0. INTRODUCTION

In this chapter, four sets of results are presented and discussed. The first set of results focuses on the physico-chemical characterization of the spent bauxite-based refractory bricks to determine the ones that are more suitable for reclamation. Two test methods are utilised for this purpose, namely, the SEM-EDS and XRD.

The second set of results focuses on the formulation of the tundish lining castable based on grog-fresh andalusite mixing ratios, and the effect of in-situ tundish slag as received from the Scaw. The particle size distribution (PSD) of the design formulations and X-Ray Fluorescence (XRF) are results also discussed.

The third set of results covers standard refractory test methods based on two sets of temperature ranges, the lower temperature ranges between 110 and 1200°C, and the higher temperature ranges of 1400 and 1500°C. Lastly, the fourth set of results covers the cost and environmental benefits envisaged from the recycling of bauxite grog.

For ease of referencing and the discussion of results, the samples are labelled as follows:

Virgin/fresh sample (VS)	: Contains 0% bauxite grog
Sample (S1)	: Contains 10% bauxite grog
Sample (S2)	: Contains 20% bauxite grog
Sample (S3)	: Contains 30% bauxite grog
Sample (S4)	: Contains 40% bauxite grog

4.1 Physico-chemical characterization of the spent bauxite-based refractory bricks

The results from the characterization of the three brick samples collected in different area of the roof are presented in Figures 4.1(a), (b) and (c). The scanning electron microscope (SEM) image and the energy dispersive spectroscopy (EDS) compositions were divided into three zones, (1) the contaminated proportion of the brick- consisting of slag, entrained materials and/or dust from the melting process, (2) interface, and (3) unreacted proportion of the brick.

Characterization of Brick A: The brick claimed from the roof periphery had sufficient residual thickness at the end of campaign for reclamation (see Figure 4.1a).

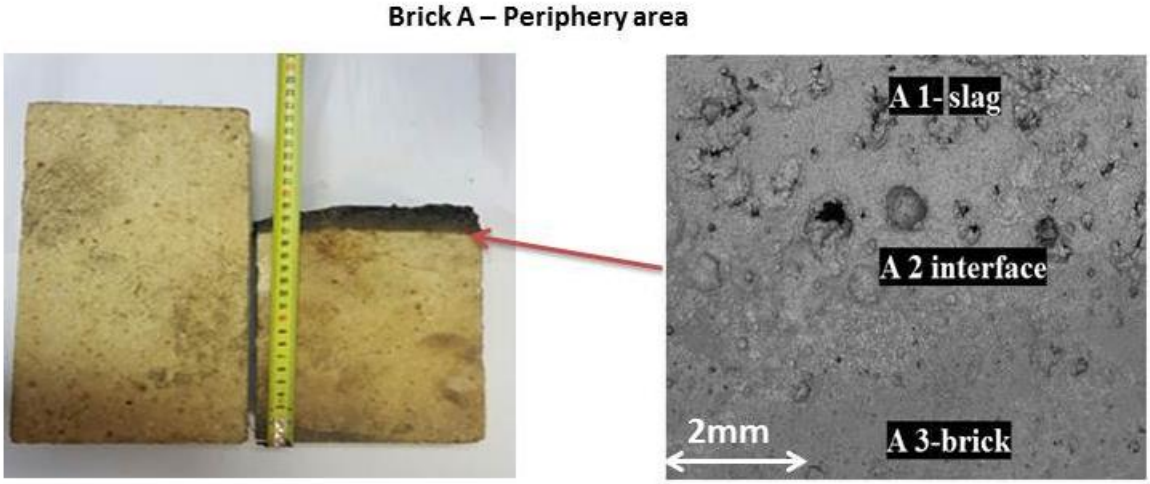

Composition area	Al_2O_3	SiO_2	CaO	MgO	FeO	MnO	TiO_2	ZnO	Na_2O	K_2O
A 1- slag	34	19	6.5	10	24	1.1	1.5	0.4	0.5	0.17
A 2 – Interface	48	26	9	3	10	0.5	2	0	0.5	0.2
A 3- Brick	74	17.5	0.7	0	1.7	0	5.3	0	0.2	0.2

Figure 4.1: (a) SEM-EDS analysis and image of brick A reclaimed from the peripheral area of the roof

The SEM image of brick A showed minimal interaction between the process material and refractory brick. Furthermore, brick A exhibited minimum signs of micro crack formation as a result of thermal shock or spalling. Hancock and Cannon (2000) defined thermal spalling as cracking of a refractory due to rapid changes in temperature. Hloben (2000) emphasized that spalling is a problem in refractories because most refractories are generally brittle and are used at elevated temperatures. Owing to high-temperature conditions, refractories are required to withstand the effects of rapid and frequent heating and cooling which can lead to cracking and failure of refractory materials. Spalling is further exacerbated when refractory materials are in contact with process slag, or the intrusion of foreign substances such as alkalies, zinc, lead and

other volatile metal compounds, which causes structural spalling of refractory materials (Buzin et al. 2015; Lee et al. 2001).

The composition areas of the brick A, B and C where measured 5 mm from the surface of the reacted or contaminated part of the used brick to the unreacted part. Brick A with a composition of 74% Al_2O_3 is close to the composition of the virgin brick which 81.8% Al_2O_3. There are no significant changes in the compositions of SiO_2, CaO and Fe_2O_3 which is indicative that the brick experienced stage 1 corrosion.

The EDS compositions of the three zones analysed show that the contaminated area A1 slag consist of predominantly FeO, SiO_2 and Al_2O_3 components with basicity CaO/SiO_2 of 0.34. Schacht (2014) noted that the lower basicity of 0.34 is indicative of corrosion reactions beginning at lower temperatures resulting in higher dissolution of Al_2O_3. However, in this case, the temperature gradient is lower as the roof bricks are not in direct contact with slag or liquid bath. This implies that erosion is the main wear mechanism affecting the roof bricks. The slag also has a substantial amount of FeO (24 wt%) which can be attributed to the type and quality of scrap used. If the scrap contains a lot of metallic fines these can find their way to the surface of the roof bricks. Guézennec et al. (2005) stated that metallic fines probably result from direct fly-off of solid particles during introduction of powder materials into the EAF and/or from a phenomenon of liquid droplets projection at the impact points of the arc or of the oxygen jet on the liquid bath. Schacht (2014) stated that the presence iron oxide (FeO) tends to reduce the liquidus temperature of the corrosion reaction products. Consequently, this lowers the liquidus temperature which promotes early formation of liquid phases which increases the wear rate on the hotface of the brick (Lee and Zhang 2004; Slag Atlas 1995).

Alkali compounds such as Na_2O and K_2O inherently fall under the volatile compounds in the electric arc furnace dust (Buzin et al. 2015; Sofilić et al. 2004). According to Buzin et al. (2015), similarly to FeO, the presence of Na_2O and K_2O in the EAF slag tends to lower the liquidus temperature hence contribution to accelerated wear of refractory materials. TiO_2 is a major impurity for bauxite bricks, together with alkalies can particularly be detrimental in bauxite bricks since they tend to react with SiO_2 to form low melting glass phases when the brick is fired or reach high-temperatures in service (Hancock and Cannon 2000; Harbison and Walker 2000).

Characterization of Brick B: The brick claimed from the electrode area was heavily contaminated by process materials and showed signs of crack formation (see Figure 4.1b).

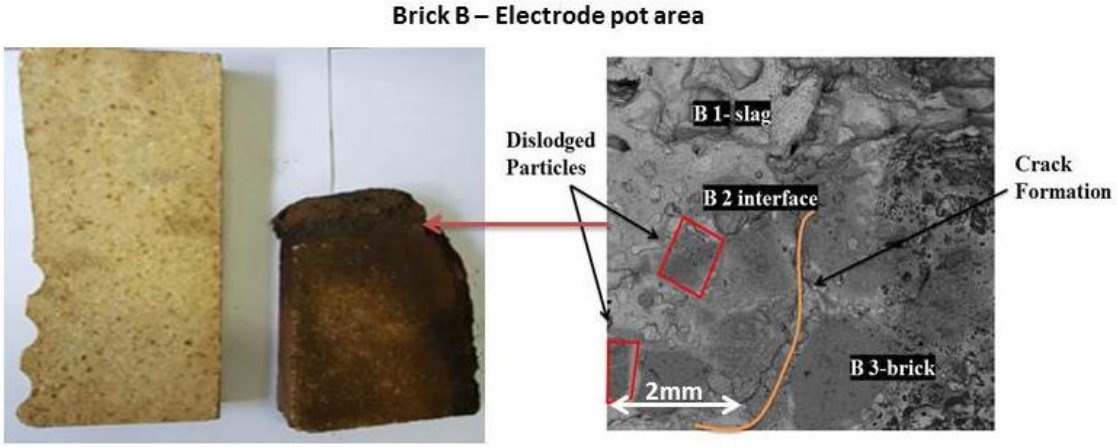

Composition area	Al_2O_3	SiO_2	CaO	MgO	FeO	MnO	TiO_2	NiO	ZnO	Na_2O	K_2O	CuO	Cr_2O_3
B 1- slag	30	17	0	0	27	0	0	8.3	0	0	0	0	17
B 2 – Interface	45	14	3.7	1	14	0.5	2	0	8.1	5	2	0.51	0.32
B 3- Brick	63	24.5	0.5	0	1.6	0	2.5		1.12	2.3	3	0	

Figure 4.1:(b) SEM-EDS analysis and image of brick B reclaimed from the electrode pot area of the roof

The SEM image of brick B shows that the process materials penetrated the refractory brick resulting in difficulty to locate the interface line when conducting SEM analysis. B3 with lower Al_2O_3 of 63% compared to the virgin bauxite brick 81.8% is indicative of higher contamination for the electrode area. The SEM image of brick B shows evidence of severe chemical attack by process materials. Brick B showed sign of thermal spalling and the contaminated portion could easily be removed by hand. This was expected because these bricks are in proximity to the EAF electrode which causes temperature variation during scrap melting. A study by Buzin et al. (2015) mentioned that presence of an arc from EAF which exhibit high-temperature and is placed in an environment exposed to gases, vaporization (and oxidation), of entrained materials results in severe chemical attack and thermal shock of refractory materials use for the roof. Therefore, it can be deduced that brick B experience stage 2 corrosion since the thermal gradient is not sufficient to exacerbate formation of liquid phases on the surface of the brick thereby accelerating corrosion.

The EDS results show that the process material contained slag components FeO, SiO_2 and Al_2O_3 with no presence of CaO to calculate the CaO /SiO_2 basicity and very high chromium

oxide levels in B1 17% Cr_2O_3. This high chromium oxide levels originates from the electric arc furnace charge scrap inputs which may have high chrome content. The presence of NiO in B1-slag, CuO and ZnO in the interface is indicative of the high level of contamination from the electrode pot area roof brick. Buzin et al. (2015) indicated that electric arc furnace dust contains metals such as Pb, Cd, r, Ni and Cu in varying levels which may form oxides when in contact with the refractory roof bricks.

Characterization of Brick C: The brick claimed from EAF off-gas chute was moderately intact and showed minor signs of cracks at the end of campaign and also the residual thickness was sufficient for reclamation (see Figure 4.1c).

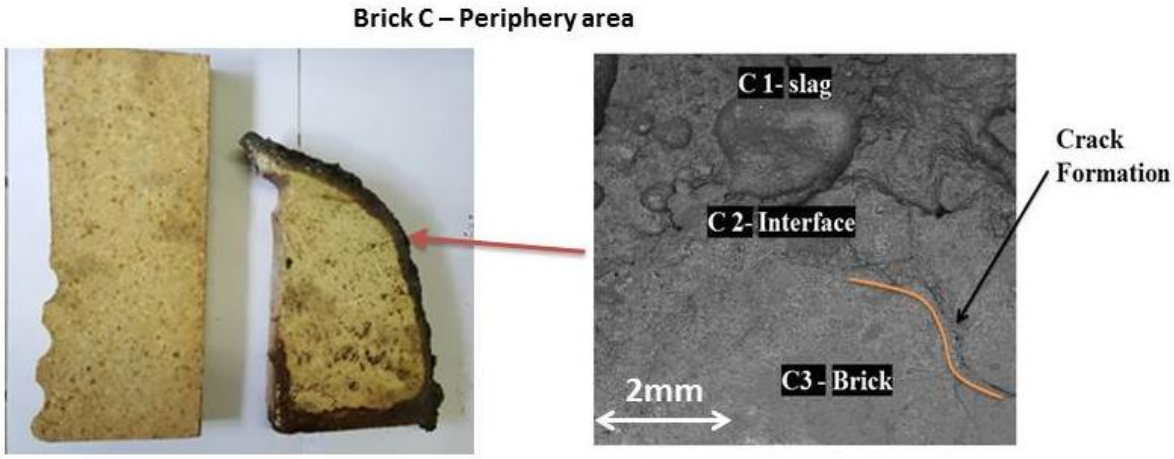

Composition area	Al_2O_3	SiO_2	CaO	MgO	FeO	MnO	TiO_2	ZnO	Na_2O	K_2O
C 1- slag	61	24	0	0	16	0	0	0	0	0
C 2 – Interface	57	29	3.1	1.3	5.7	0.5	2.6	0	0.9	0.7
C 3- Brick	63	28	1.4	0.6	3.2	0	2.7	0	0.4	0.4

Figure 4.1: (c) Scanning electron microscope (SEM) and energy dispersive spectroscopy (EDS) analysis of brick images from the off-gas chute area of the roof.

The SEM image of brick C shows that there was minimal slag-refractory interaction. The image also shows minor signs of microcrack formation (orange line) resulting from thermal shock, however it is less severe than in brick (b). The similar compositions of B3 and C3 with lower Al_2O_3 of 63% compared to the virgin bauxite brick 81.8% are indicative of higher contamination for the electrode and off-gas chute areas.

The major components of the refractory brick are SiO_2 and Al_2O_3 as shown by brick samples A, B, and C, and that of slag are FeO, SiO_2 and Al_2O_3. Therefore, the ternary phase diagram for FeO-SiO_2-Al_2O_3 can be used predict the interaction between slag and refractory brick (see Figure 4.2).

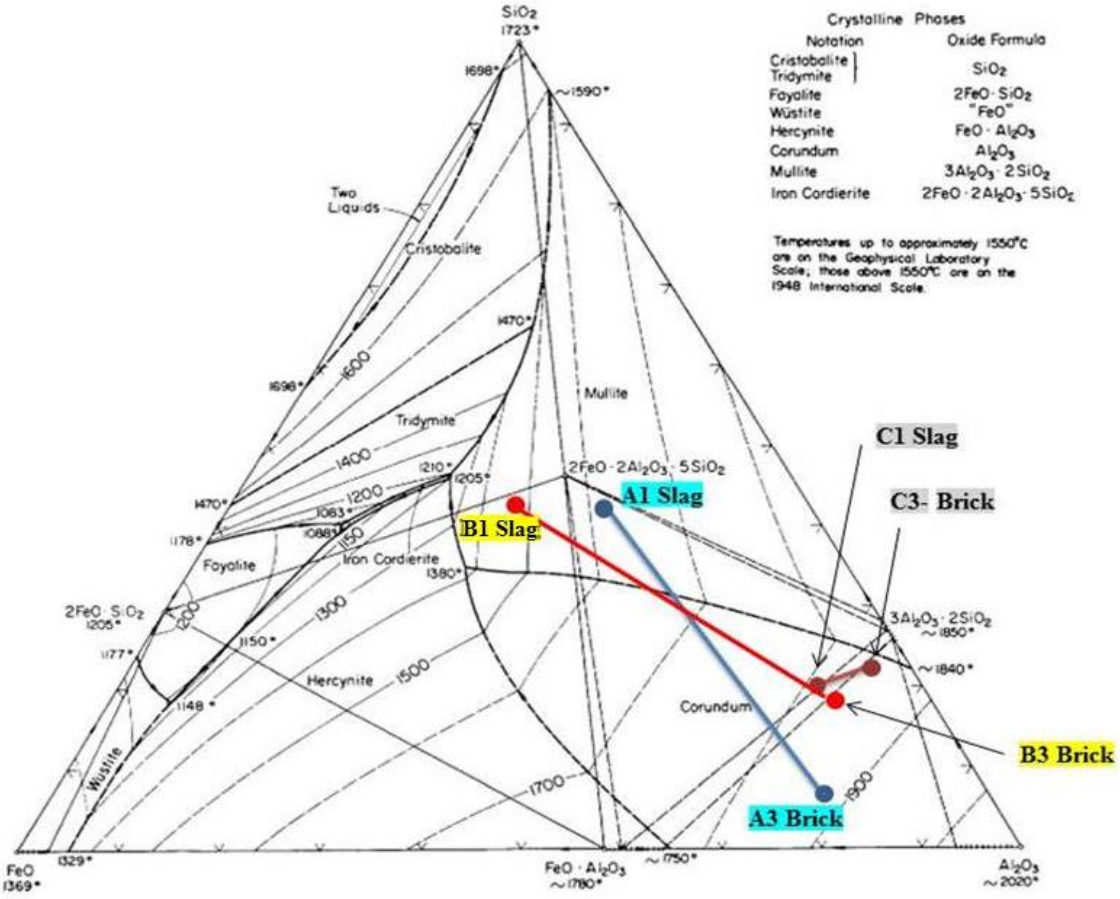

Figure 4.2: Ternary Diagram for FeO-SiO_2-Al_2O_3 System (Slag Atlas 1995)

Figure 4.2 shows that A1 fall within the alkemade or compatibility triangle iron cordierite-fayalite -hercynite which has a peritectic invariant point at 1205˚C and eutectic point at 1083˚C. A2 indicates the altered composition of A1 and A3 asserting the thermodynamic driving force for the slag to react with the brick until equilibrium is reached. A3 fall within the alkemade triangle corundum-mullite-hercynite, and hence it can be deduced that only solid phases are present in the brick when initially interacting with A1 slag.

On the other hand, it is shown that the composition point B1 slag is closest to the peritectic invariant point at 1205˚C and eutectic point at 1083˚C which is indicative of low melting point phases, thus further negating the reclamation potential for sample B.

Regarding brick C, both C1-slag and C3 brick fall within the alkamade triangle iron cordierite–mullite– hercynite and the red line joining the two points is too short to consider a temperature gradient (Figure 4.2). Furthermore, the variance in Al_2O_3 content and general composition for C1, C2 and C3 is trivial to consider any slag-refractory interaction.

Therefore, it can be deduced that less liquid phases will form in brick C, as a result less corrosion wear is expected, as such the residual thickness was adequate for reclamation at the end of campaign. However, although brick C showed less tendency of crack formation, it was rejected on the grounds of economic viability due to potentially low quantities of reclaimable portions at the end of each campaign. Only a few bricks are installed in the off-gas chute system of EAFs.

Nyirenda (1991) stated that the composition of EAF dust or entrained materials can be widely variable and may change not only from one day to another, but also from heat to heat of the same steel shop. Therefore, in this study, visual inspection of the general condition of reclaimable bricks was also used to select and discard less favourable ones for recycling based on levels of contamination and micro-cracking formation.

Nevertheless, the preliminary analyses showed that brick A was suitable for reclamation, intact, and showed minimum signs of thermal spalling and chemical attack from process materials. Brick B was rejected on the grounds of high contamination levels and micro-cracks, whereas brick C was rejected on the grounds of economic viability, which means that not enough quantities can be generated for recycling.

After rejecting the bricks B and C for recycling, XRD tests were conducted on brick A and the findings were compared to the virgin bauxite brick in order to further determine the suitability of the sample for reclamation. The XRD analyses confirmed that there was no significant difference in mineralogical phases between the virgin and reclaimed brick as indicated in Table 4.1. Based on the XRD results, brick A was considered suitable for reclamation and further tests were conducted based on this sample.

Table 4.1: XRD results for reclaimed and virgin bauxite bricks

Phases Present	Reclaimed Sample (a)	New Bauxite brick
Corundum	36	39
Mullite	41	33
Magnetite	0.2	0.25
Quartz	0.6	0.4
Iron	0.07	0.11
Amorphous	22	28

The findings in Table 4.1 can be correlated to refractory phases for the bauxite bricks (> 80 % Al_2O_3). According to Schacht (2004), corundum and mullite are the main refractory phases present in fired (1450-1550ºC) bauxite materials. The amorphous phases are usually associated with the presence of glassy silica and other indigenous impurities such as Na_2O, K_2O, Fe_2O_3, FeO and TiO_2 (Schacht 2004). However, the high content of these amorphous phases in the two samples is of substantial concern as they affect the liquidus temperatures of bauxite refractories (see Figure 4.3).

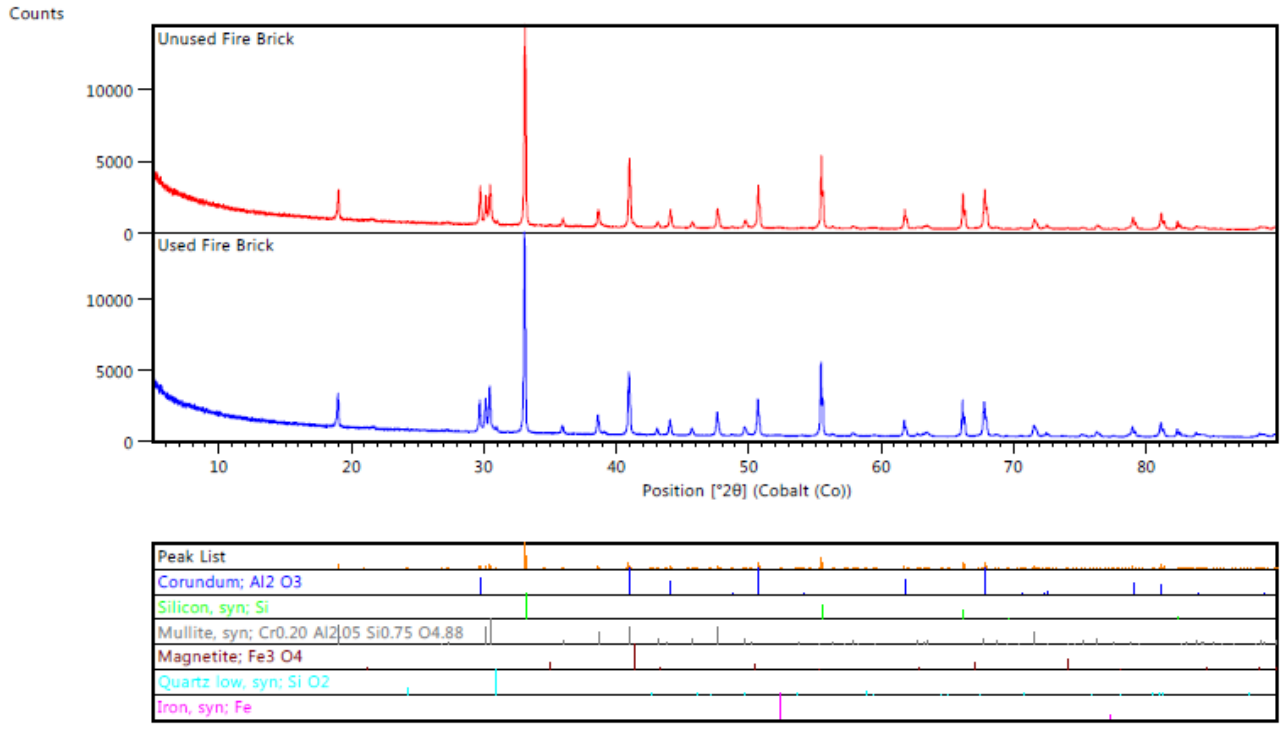

Figure 4.3: XRD patterns for reclaimed and virgin bauxite bricks

4.2 Formulation of the alumina castables

In general, the target particle sizes mostly considered for substitution in recycling grog are the coarser 1-3 mm and 3-5mm aggregate fractions (Schutte 2010). As such, for this study, only the courser aggregate portion of the castable, specifically the 0-1 mm, 1-3 mm and 3-6 mm fractions were substituted. The particle size distributions (PSDs) of the grog-fresh formulations were developed using the formulation logic and standard sieve grouping of the reference castable. The sieve analysis results show that there is no significant difference between the PSDs of the formulated grog-fresh castables vs. the reference castable (see Figure 4.4).

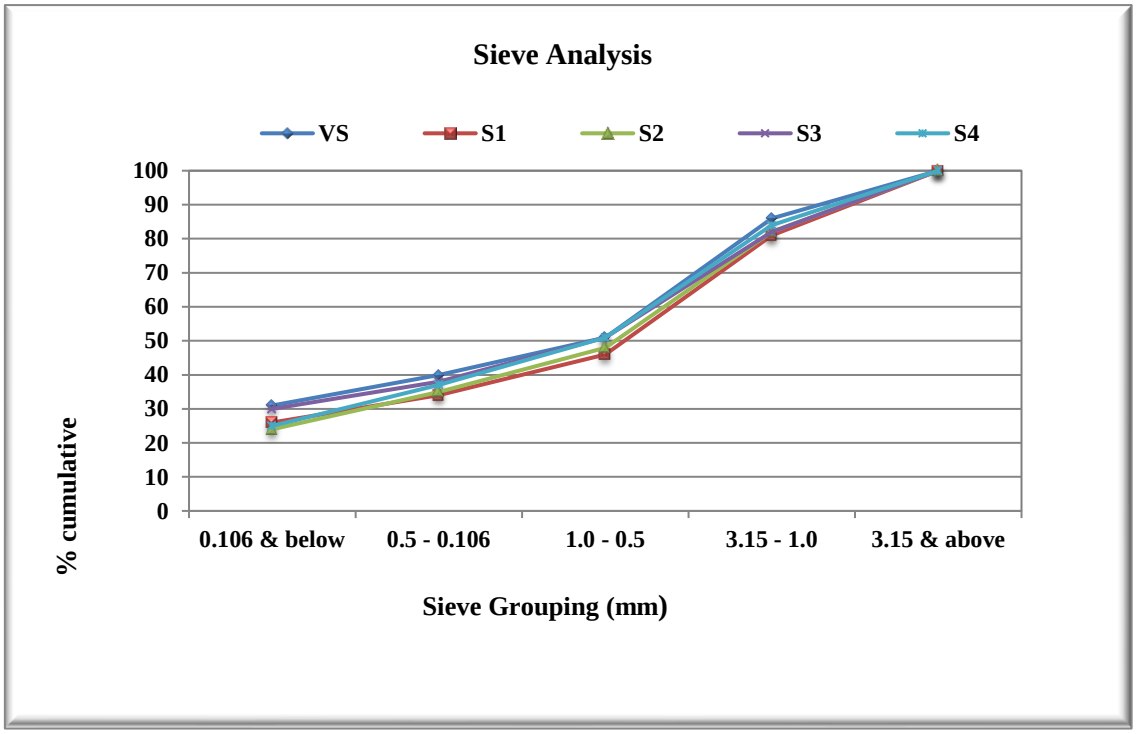

Figure 4.4: Sieve Analysis results for the formulated castables

Subsequently, after ensuring that PSD for the formulated castables is similar to that of the reference castable. The formulated castables were analysed using the X-ray florescence (XRF) to determine chemical composition (see Table 4.2). These results were then normalised to focus on three primary components Al_2O_3, CaO and SiO_2 for ease of predicting phase formations using the Al_2O_3-CaO-SiO_2 phase diagram. Other compounds such as MgO and TiO_2 were present, but in negligible amounts to be considered.

Table 4.2: X-ray florescence (XRF) results of formulated castables.

	VS	S1	S2	S3	S4
Al_20_3	61	63	65	69	70
SiO_2	37	34	32	28	27
CaO	1,6	1,5	1,7	1,6	1,8
Fe_2O_3	0,7	0,9	1,0	1,1	1,2

Table 4.2 shows that there is an increase in Al_2O_3 content with an increase of bauxite grog addition in the castable. This can be attributed to the aggregate grog having higher alumina content than the virgin sample (VS), 59% Al_2O_3 in andalusite versus 81.8% Al_2O_3 in bauxite

raw material. The CaO content of 1.5 to 1.8 in the formulated castables is congruent with the CaO tolerance for low-cement castables (LCCs) as classified by Lee et al. (2001) and Parr et al. (1997). It is also evident that Fe_2O_3 increases with the increase in grog addition. This increase can be attributed to bauxite grog aggregate which has Fe_2O_3 as an impurity, the actual bauxite grog contained 1.6% Fe_2O_3. Pivinskii et al. (2015) stated Fe_2O_3 present in bauxite is in the range of 1.3 to 1.8% and has an influence in high-temperature strength properties of refractory bauxite.

4.2.1 Physical properties of the formulated castables

The physical quality tests were conducted to evaluate the physicochemical, thermomechanical, and thermochemical properties of the formulated products. The performance of the formulated castables was compared to the reference castable based on physical properties such as flow behaviour (ASTM C1446), open porosity (ASTM C20-00), bulk density (ASTM C357), and cold crushing strength (ASTM C133).

Flow test: The installation method for the tundish safety lining requires that the flowability of the castable be acceptable after immediate mixing. In the present study, the flow measurements were taken after mixing for 3 minutes and vibrating for 30 seconds (Figure 4.5).

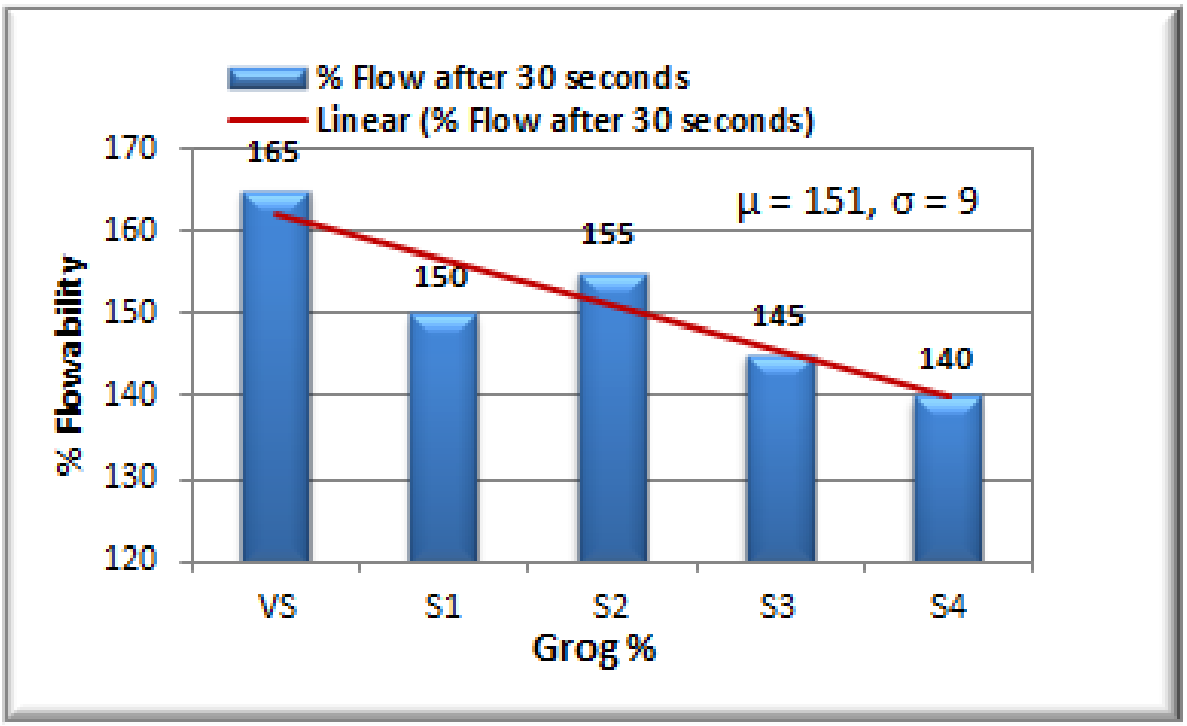

Figure 4.5: Flow Test Results for the formulated castables

The average (μ) % flow of 151 with the standard deviation (σ) of 9 was considered acceptable for all grog-fresh formulations as it was within tolerance of the reference castable flow specification which is between 60-180%. It is also evident that the flow properties of the castables decreased with an increase in the addition of grog. Hanagiri et al. (2008) noted that the loss of flow (flow decay) can be directly attributed to the addition of grog owing to other slag components which may be contained in the grog thus requiring additional water to achieve the same flow as virgin refractories. Flowability measurements of 80-180% are considered acceptable for castables installed by vibration in tundish applications (Myhre et al. 1998).

Setting time: Setting time or time to flow decay of refractory castable is strongly influenced by the temperature so that unless the castable is somehow retarded, installation may be problematic under hot climatic conditions. By way of example, a castable installed in ambient temperature condition reaching an average 35˚C, will experience rapid setting times of less than an hour depending on the environmental climate (Myhre 1998). Figure 4.6 shows results of thefrom setting time measurements of average (μ) 156 minutes and standard deviation (σ) of 29. In practice, the setting times of 3-9.93 hours are considered acceptable depending on the ambient temperature conditions (Parr et al. 2013, AGC Ceramics n.d.)

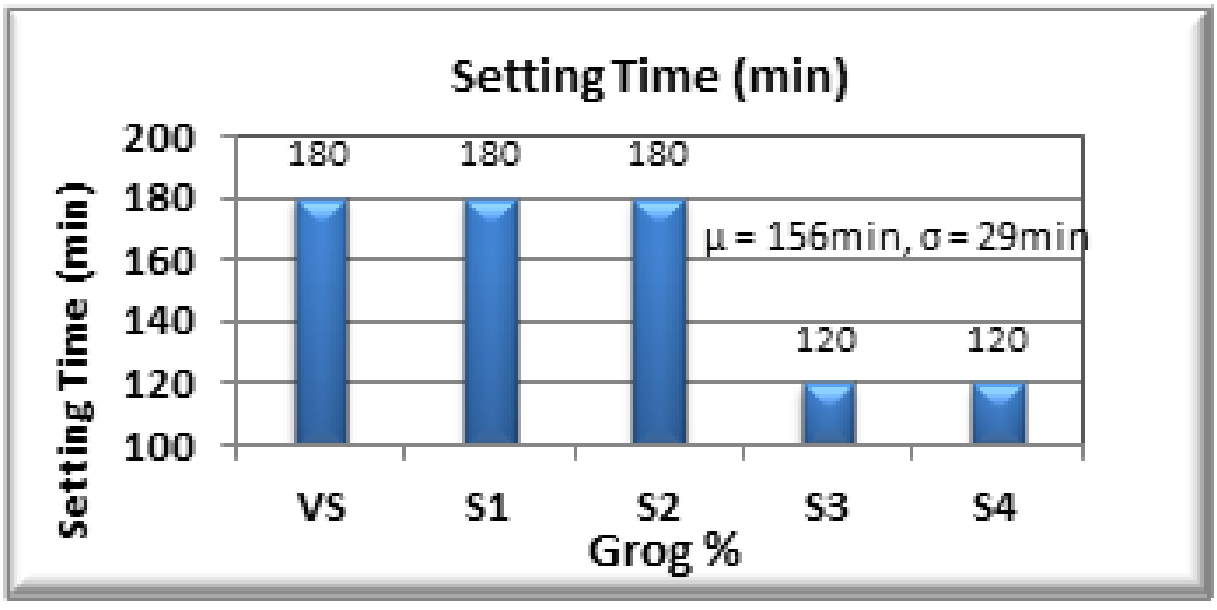

Figure 4.6: Setting time Measurements for the formulated castables

In this study, setting times for S1 and S2 was constant at 180 minutes but decreased to 120 minutes for S3 and S4. This is also in accordance with the reference castable setting time

specification of between 120-140 minutes. These setting times are neither considered too fast nor too slow (Ressler 2009; Myhre et al. 1998), and hence were acceptable for all formulations.

Water addition: Water addition to a castable has a direct effect on the final properties and castable specifications (Hanagiri et al. 2008; Zawrah and Khalil 2008). According to Zawrah and Khalil (2008), excess water can reduce the strength and increase the shrinkage of the castable, while too little water can result in voids and poor consolidation. Based on the propositions, the effect of water addition on formulated castables was investigated. Figure 4.7 water addition results showed a slight increase in the water requirement from 6 and 8% with an increase in the amount of grog.

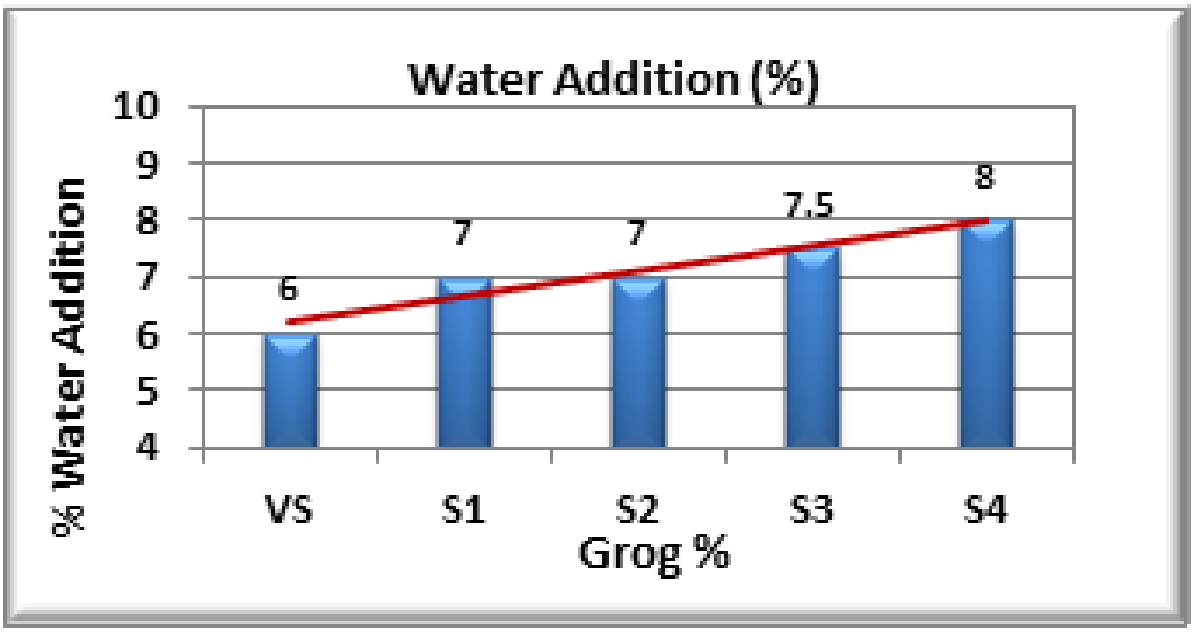

Figure 4.7: percentage water addition for the formulated castables

The water additions for S1 and S2 at 7% were within tolerance of the reference castable specification VS which is between 5 and 7%. S3 and S4 had slightly higher water demand at 7.5 and 8% respectively than VS. The study conducted by Hanagiri et al. (2008) indicated that an increase in the amount of grog slightly increased the water requirement for the castables. In other words, the amount of water that must be added to maintain the same fluidity of the castable increases as the addition rate of the recycled materials increases. The water additions for the formulated castables were thus considered acceptable as they were within the ranges proposed by Hanagiri et al. (2008), Hutton et al. (2009) and Bradley and Hutton (2014).

4.2.2 Open porosity, bulk density and cold crushing strength at 110 ˚C, 600 ˚C, 1000 ˚C and 1200˚C.

Apparent Porosity: Apparent porosity was calculated according to equation 3.1 and the study found that the apparent porosity slightly increased for the respective formulations at different temperatures compared to the reference formulation (see Figure 4.8).

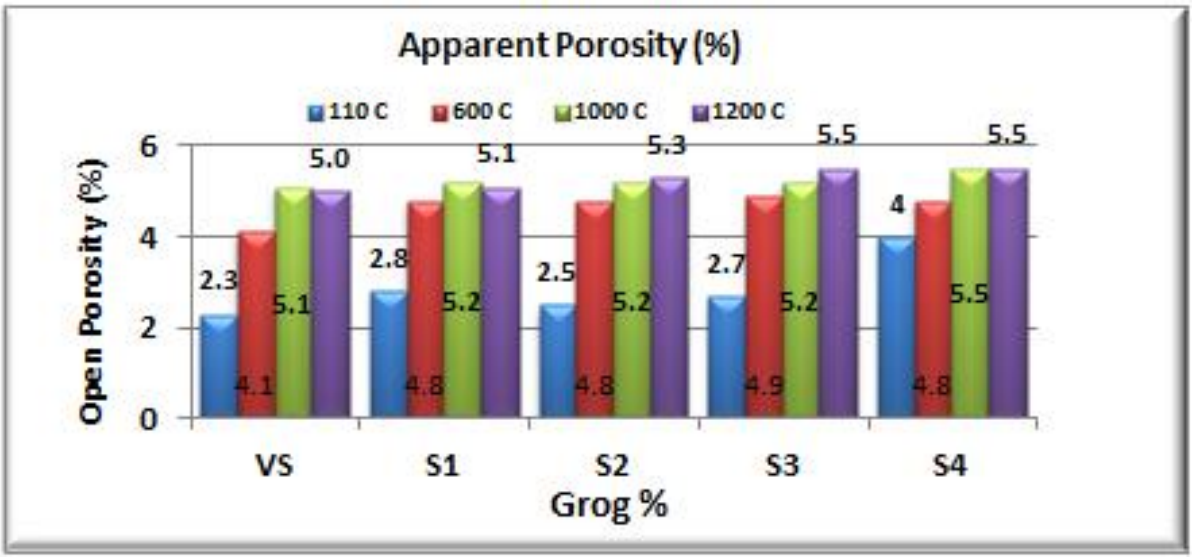

Figure 4.8: Apparent Porosity for the formulated castables

Although, there is no clear trend, apparent porosity also increased with the increase in the amount of grog added. For example, apparent porosity for S3 increased from 2.7% at 110˚C to 5.5% at 1200˚C, whereas apparent porosity for VS increased from 2.3% at 110˚C to 5.0% at 1200˚C. In general, low-cement castable LCCs usually possess apparent porosity values not higher than 10% (Lee et al. 2001), and as such, the porosity for the formulated castables was considered acceptable relative to the virgin castable specification. Zawrah and Khalil (2008) noted that higher water additions result in higher porosity, and as a result, the thermochemical wear resistance of the castable tends to decline. However, in this study, this trend is expected counterbalanced to a degree by using a better alumina raw material than the virgin castable.

Bulk density: Higher bulk density is indicative of good particle size packing and reduced porosity thus improves the wear resistance of refractory castables (Lee et al. 2001). In this study, bulk density tests were conducted according to the ASTM C 357 methods, and the results are shown in Figure 4.9.

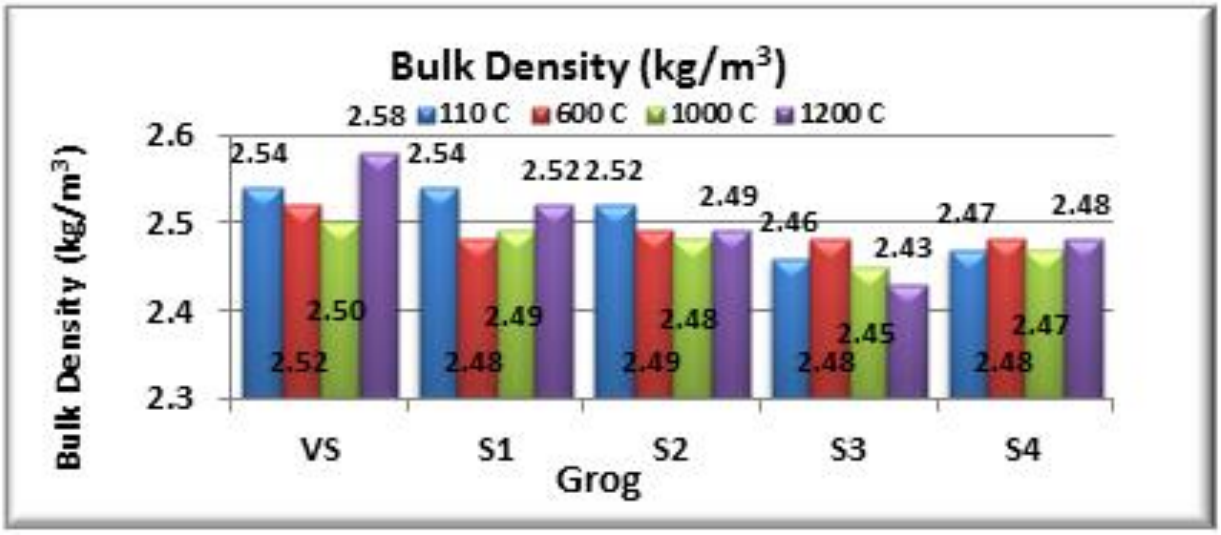

Figure 4.9: Bulk Density for the formulated castables

Generally, there was a slight decrease in bulk density with the increase in grog addition. Although there is no clear comparison trend in bulk density for the formulated castables at lower temperatures, the decrease in bulk density is apparent with the increase in grog at 1200˚C. The findings indicated that the lower bulk density is linked to the higher water requirements as a result of grog addition, thus affect apparent porosity. This trend was found to be supported by studies conducted by Hanagiri et al. (2008) and Hutton et al. (2009). Hutton et al. (2009) noted that reclaimed refractory materials tend to have lower bulk density and higher porosity values when compared to virgin materials, which in essence, tend to affect the water demand for the castable product. The bulk density properties significantly affect the performance of refractory castables (Hutton et al. 2009). Lee et al. (2001) proposed that the higher the bulk density, the higher the cold and hot strength, and hence the higher the abrasion and corrosion resistance. In this case, the decrease in the bulk density at 1200˚C with the increase in grog content of the formulated castables is most likely to affect such high-temperature properties in service.

Cold Crushing Strength (CCS): The CCS measures the mechanical strength at room temperature, and also serves to indicate susceptibility to damage from handling on site or during transportation of refractory materials (Hancock and Cannon 2000). CCS tests were conducted according to the ASTM C 133 (Figure 4.10).

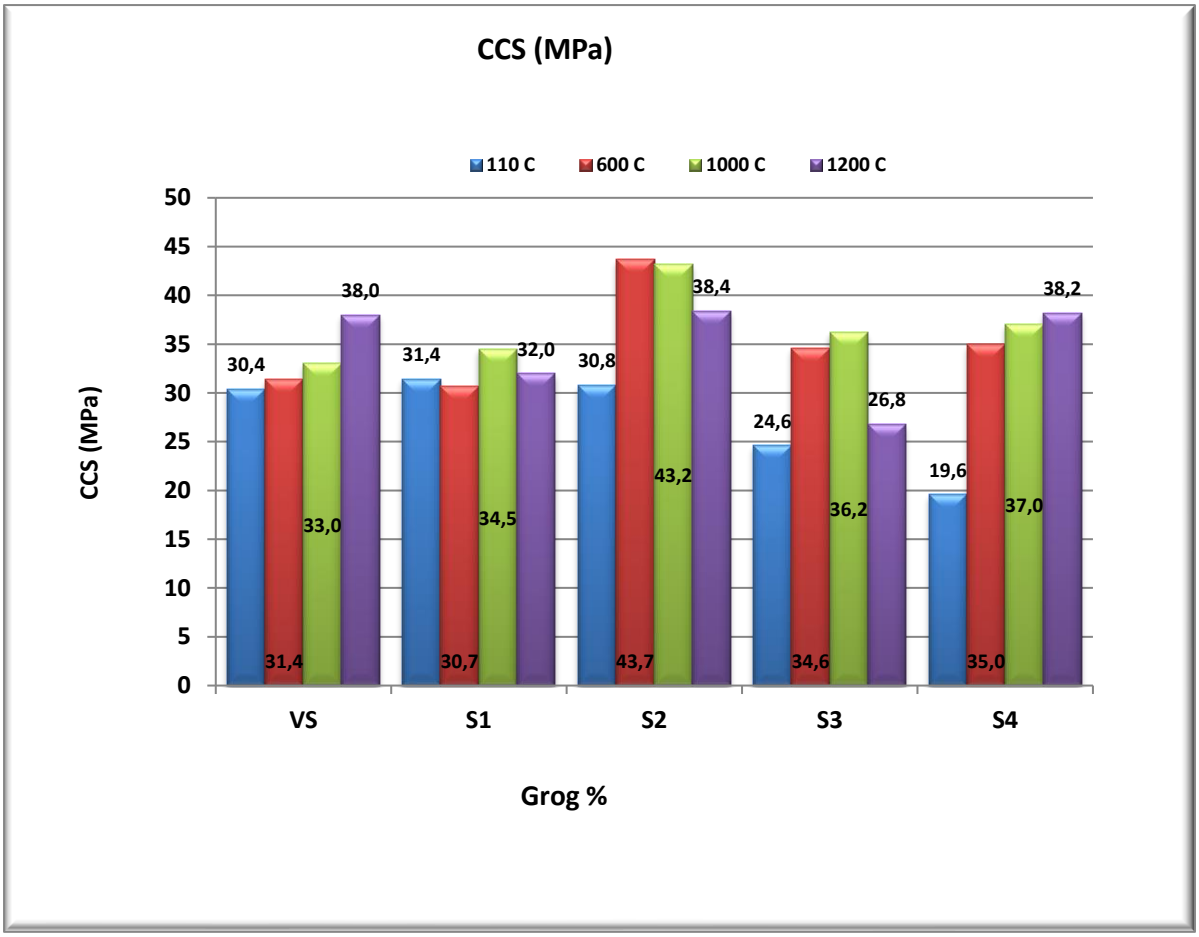

Figure 4.10: Cold Crushing Strength for formulated castables

Figure 4.10 shows that the results for the grog-fresh formulations are comparable to that of the virgin formulation VS. This indicates that the cold crushing properties of the formulated castables are within acceptable ranges. Wöhrmeyer et al. (2006) stated that CCS above 20 MPa are considered acceptable for 60% alumina castable.

4.2.3 Characterization of tundish slag

Table 4.3 shows the chemical composition of tundish slag used in the static corrosion tests. Although the basicity of the slag is 1.03, which make it acidic thus comparable with the formulated castables, an interaction between the slag and the safety lining can be expected should the working lining reduces to unacceptable levels. This is because the slag is not saturated in alumina and alumina is the major component in the formulated castables. To predict the predominant phases involved between the slag-refractory interaction at 1400°C, the Al_2O_3-SiO_2-CaO ternary phase diagram was used (see Figure 4.11).

Table 4.3: Chemical composition of tundish slag

Average tundish slag composition as received from Scaw operation				
Al_2O_3	SiO_2	CaO	MgO	Fe_2O_3
7	31	32	16	14

Using the SiO_2-CaO-Al_2O_3 phase diagram below, the following primary phases will exist at a 1400°C isorthem for the formulated castables:

VS – Cristobalite (SiO_2) + Mullite ($3Al_2O_3$-$2SiO_2$) + Liquid

S1 – Cristobalite + Mullite + Liquid

S2 - Cristobalite + Mullite + Liquid

S3 – Corundum (Al_2O_3) + Mullite + Anorthite (CaO- Al_2O_3-SiO_2)

S4 - Corundum + Mullite + Anorthite

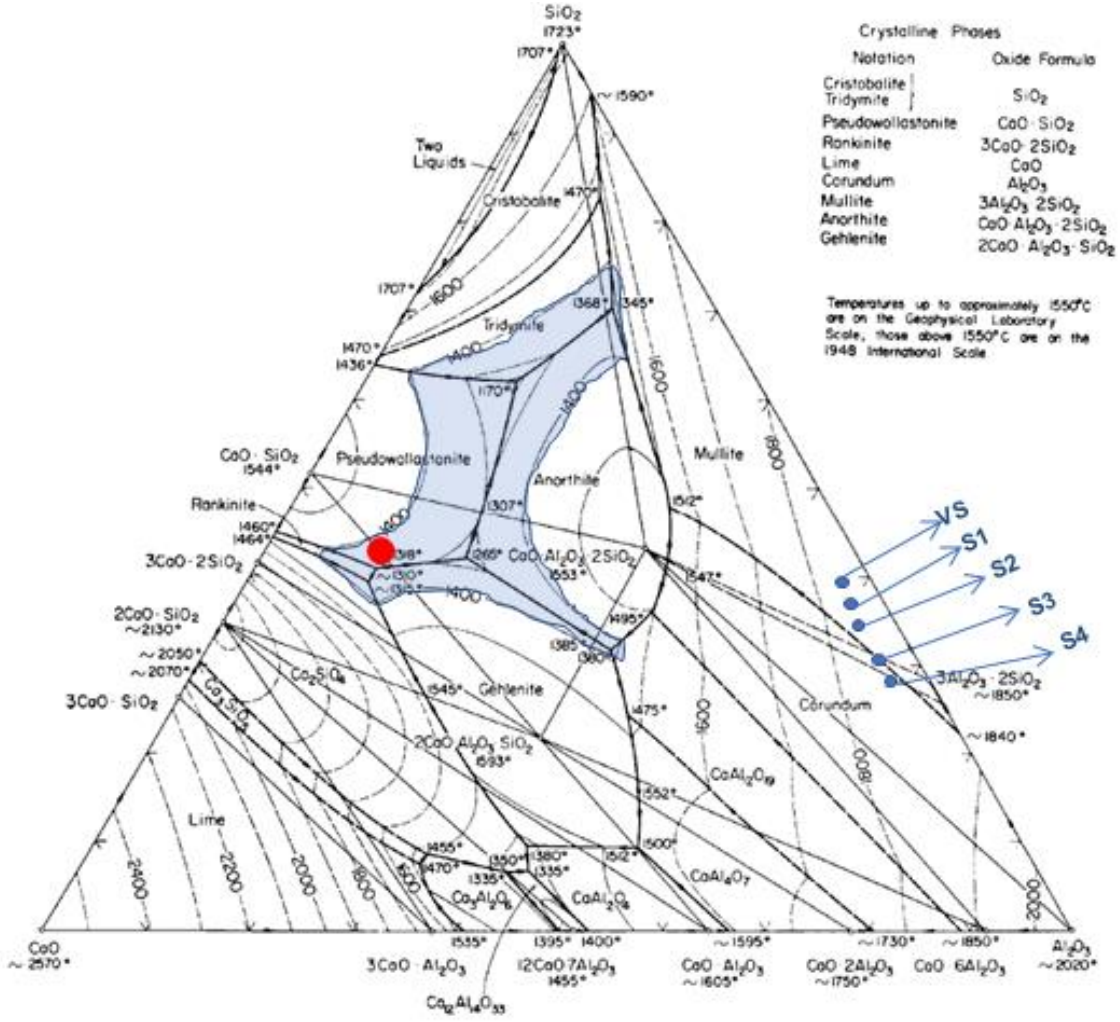

Figure 4.11: CaO-Al_2O_3-SiO_2 Ternary Phase Diagram (Slag atlas 1995)

Evaluating the Al_2O_3-SiO_2-CaO phase diagram, it is shown that the slag composition indicated by the red dot lies within the pseudowollastonite, rankinite and anorthite alkemade triangle with a eutectic composition at 1310°C. The castable compositions are given on the same ternary phase diagram in blue dots as VS, S1, S2, S3 and S4 in series showing an increase in Al_2O_3 content. From the diagram, it is shown that VS, S1 and S3 fall within the alkemade triangle cristobalite, anorthite and mullite. Whereas S3 and S4 fall within the alkemade triangle corundum, anorthite and mullite. It can be deduced that the interaction between the slag and castables will result in the dissolution of the different compounds present in the mix until equilibrium is reached between the slag and castables. From the diagram, it can be deduced that for VS, S1 and S2 some liquid will form at 1400˚ isorthem, whilst no liquid formation is expected to be formed for S3 and S4 at that temperature. Therefore, less corrosion wear is expected on castables as the Al_2O_3 content increases. In as much as the safety lining is not in direct contact with tundish slag, the corrosion tests at 1400°C were nevertheless conducted as a precautionary measure and to ascertain the aforementioned phase diagram predictions.

4.2.4 Static corrosion tests

Figure 4.12 shows the results of the static corrosion test conducted at 1400°C, after soaking for 12 hours and cooled down for measurements. As was expected, the slag-metal interaction resulted in Al_2O_3 pick-up in the slag phase as the slag was not saturated with Al_2O_3. For example, Al_2O_3 content of the slag phase in VS, S1, S2 and S3 increased to around 27wt% from 7wt% in the original slag. However, the impact of Al_2O_3 content, and physicochemical properties such as bulk density and open porosity of formulated castables, is not clear up to S3. S4, with 40% grog addition, higher open porosity, and lower bulk density, experienced higher slag attack as evidenced by the elevated pick up of Al_2O_3 by the slag. Furthermore, it can be inferred that the slag-castable interaction occurred via the slag penetrating through the available pathways (e.g. open pores, cracks, phase boundaries, etc.), with the degree of penetration being controlled by the bulk density and apparent porosity of the castables (Pivinskii 1998; Poirier et al. 2008; Braulio et al. 2011). Thus, the corrosion behaviour reiterates the need to further optimise the bulk density and open porosity properties of the formulated castables.

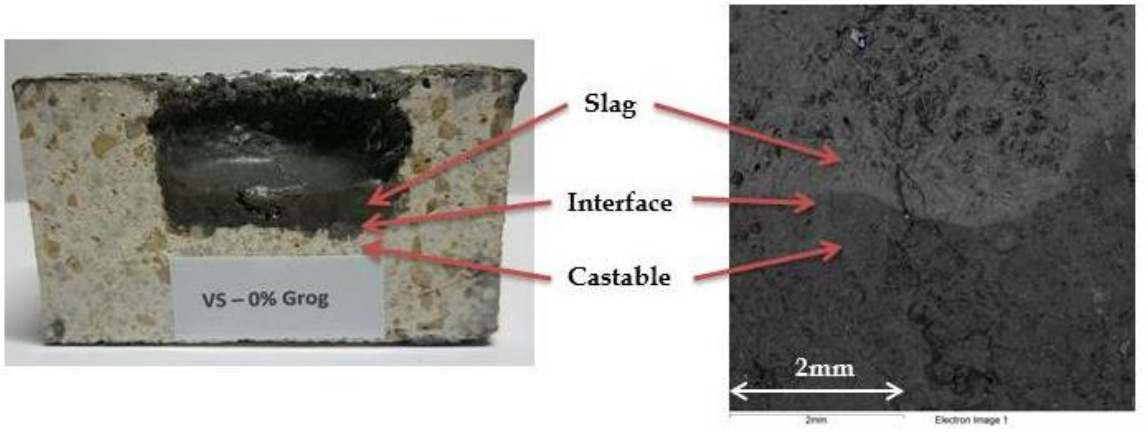

VS EDS	Al_2O_3	SiO_2	CaO	MgO	FeO	MnO	TiO_2	SO_3	Na_2O	K_2O
Slag	27	36	19	5	5	3	0.6	3	0.7	0.7
Interface	45	36	9	3	3	1	0.3	0.7	0.5	0.4
Castable	55	40	2	0	0.9	0	0.3	0.4	0.39	0.4

(a) VS (Reference formulation)

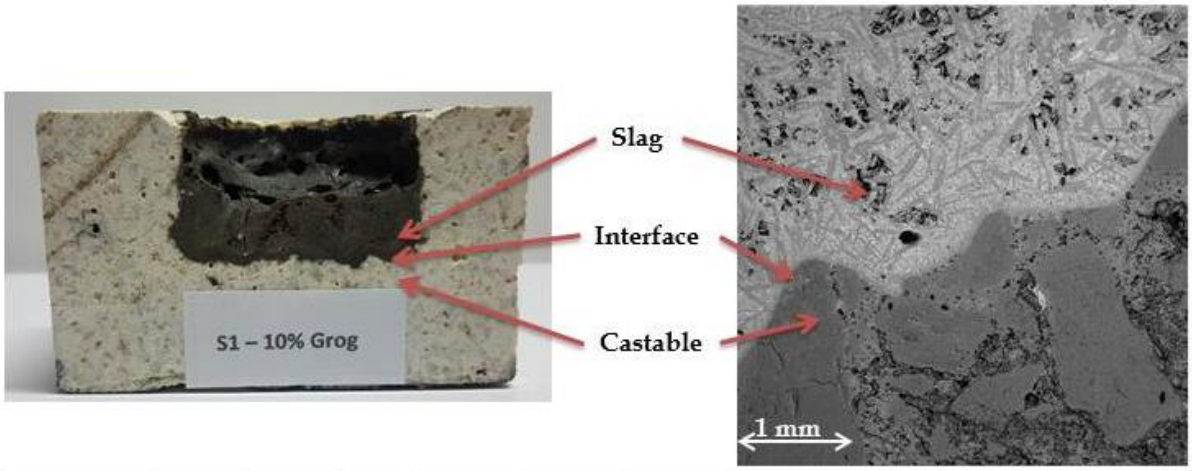

S 1 – EDS	Al_2O_3	SiO_2	CaO	MgO	FeO	MnO	TiO_2	SO_3	Na_2O	K_2O
Slag	28	34	16	9	7	4	0	1	0	0.6
Interface	39	37	12	4	3	2	0.3	2	0.5	1
Castable	55	37	2	0.4	0.7	0	0	2	0.5	0.5

(b) S1 – 10 wt. % recycled grog

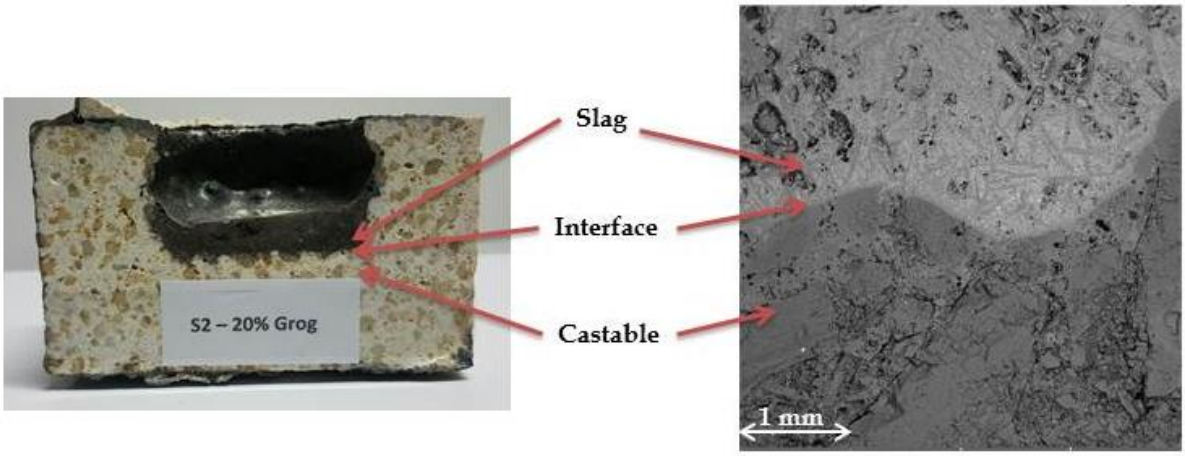

S 2 – EDS	Al_2O_3	SiO_2	CaO	MgO	FeO	MnO	TiO_2	SO_3	Na_2O	K_2O
Slag	28	33.6	16.5	8.9	7.2	3.94	0	0	0	0
Interface	43	36.9	11.3	3.5	3.1	1.7	0.36	0		
Castable	55	39	2.6	0.43	1.2	0	0.49	0	0.29	0.41

(c) S2 – 20 wt. % recycled grog

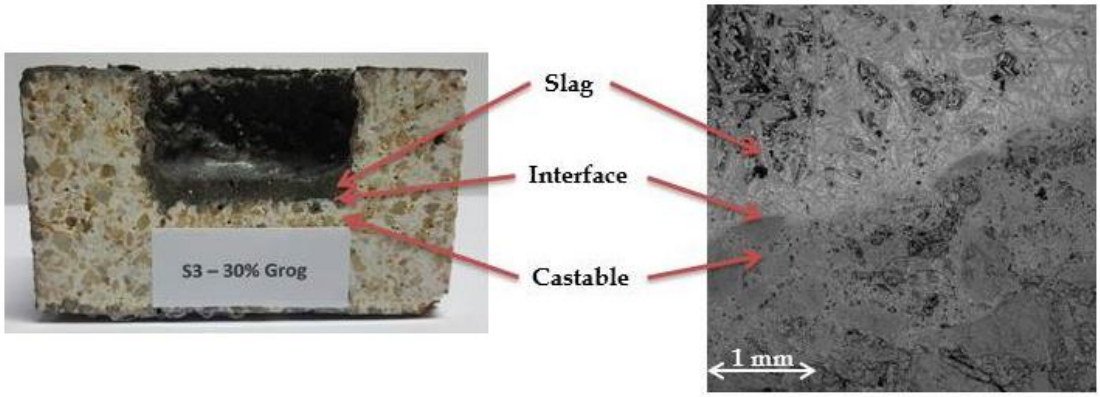

S 3 – EDS	Al_2O_3	SiO_2	CaO	MgO	FeO	MnO	TiO_2	SO_3	Na_2O	K_2O
Slag	27	31	17	6.11	5	2.7	1.82	2.44	0.53	2.12
Interface	47	36.7	8	1.6	1.8	0.82	0.54	1.8	0.52	0.94
Castable	57	36.5	3	0	0.75	0	0.34	0	0.36	0.64

(d) S3 – 30 wt. % recycled grog

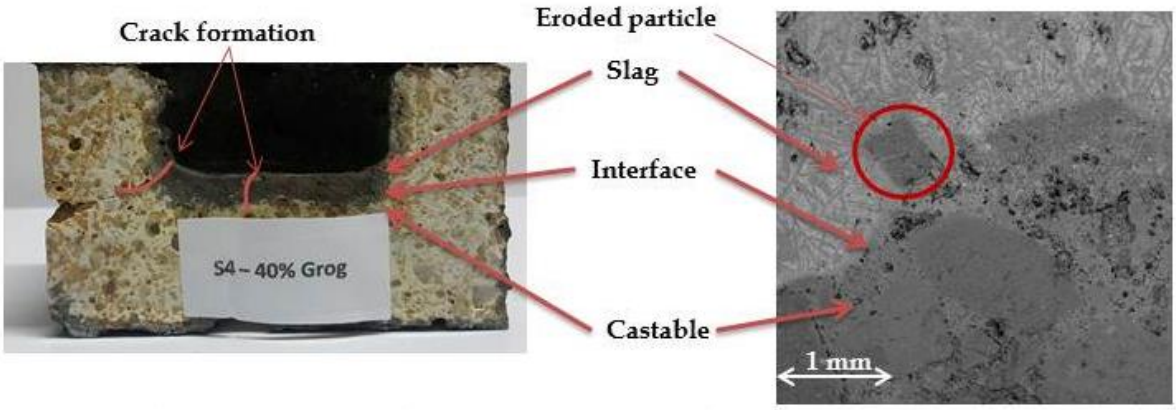

S 4 – EDS	Al_2O_3	SiO_2	CaO	MgO	FeO	MnO	TiO_2	SO_3	Na_2O	K_2O
Slag	33.8	45	14.2	1.23	1.42	0.46	0.27	1.8	0.61	0.71
Interface	33.2	28	17	1.7	2.8	0.9	0.94	7.32	1.7	3.5
Castable	62	37	0.67	0	0.31	0	0	00	0	0

(e) S4 – 40 wt. % recycled grog

Figure 4.12 Results for static corrosion tests, SEM and EDS analysis for the formulated castables

Sako et al. (2011) stated that Al_2O_3 dissolution can be expected between the interaction of CaO-rich slags and Al_2O_3- rich refractory aggregate as indicated in this study. The corrosion mechanism of alumina aggregate by CaO-rich slags is thermodynamically governed by the reactions shown in Equations 4.1 and 4.2:

$$CaO.6Al2O3\ (s) + CaO\ (l) \rightarrow 3CaO.2Al2O3(s);\ \Delta G = -\frac{65kJ}{mol} \qquad [4.1]$$

$$6Al2O3\ (l) + CaO\ (l) \rightarrow CaO.6Al2O3(s);\ \Delta G = -\frac{261kJ}{mol} \qquad [4.2]$$

Braulio et al. (2011) and Sako et al. (2011) proposed that the formation of CA_2($CaO.2Al_2O_3$) is favoured over that of CA_6 ($CaO{\cdot}6Al_2O_3$) due to a much lower Gibbs free energy (ΔG) value of CA_6 and the unidirectional grain growth which result in significant volume expansion and crack formation. Therefore, in this study, it can be deduced that the higher Al_2O_3 rich aggregate in S4 may result in the formation of CA_6, thereby resulting in crack formation (see Figure 4.12e). Moreover, S1 S2 and S3 samples were all visually intact with no noticeable signs of crack formation or dimensional deformation. However, S4 showed sign of macro-cracking and had experienced higher corrosion and slag penetration.

The change in the volume of corroded portions of the castable was used to further interpret the extent of corrosion of the Al_2O_3-castable with tundish slag. Based on the initial castable dimensions (50mm diameter and 35mm depth), the corresponding volume change after reaction was calculated by measuring the changes in the diameter and depth as a result of slag penetration. Table 4.4 shows that lower corrosion volume changes (%) were observed for S1, S2, and S3 when compared against the reference VS. In essence, the lower the % $\Delta V_{Corrosion}$, the higher the resistance to slag attack, and the better the performance of the castable when exposed to slag conditions in the tundish. Likewise, S4 with 40 % grog addition, higher open porosity, and lower bulk density, experienced higher % $\Delta V_{Corrosion}$.

Table 4.4: Static test measurements for the formulated samples

	$Ø_{average}$	Radius	Depth	$V_{initial}$	V_{final}	$\%V_{corrosion}$
VS	53.5	26.75	35.5	68.71	79.79	16.13%
S1	53.2	26.6	35.5	68.71	78.90	14.83%
S2	53.5	26.75	35	68.71	78.67	14.49%
S3	53.2	26.6	35	68.71	77.79	13.21%
S4	54	27	35.5	68.71	81.29	18.31%

Subsequently, the change in corrosion volume (%) was calculated using Equation 3.3 as discussed in section 3.4.3 and the results were then plotted in Figure 4.12.

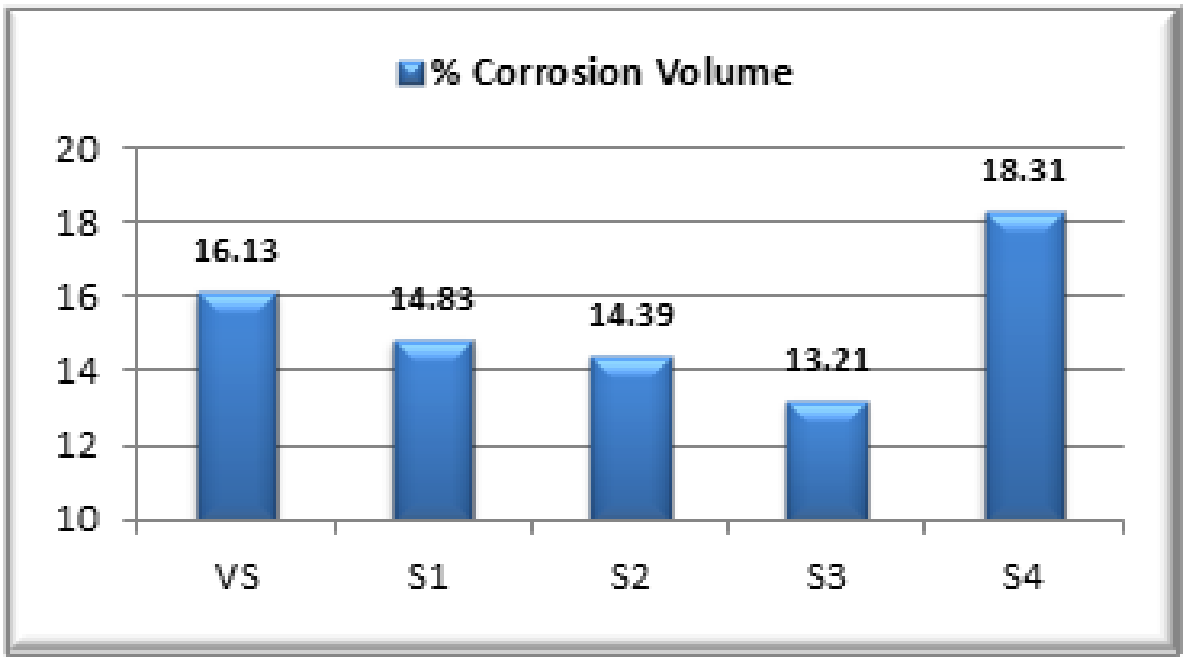

Figure 4.13: Calculated corrosion volume change for the formulated castables

The better corrosion resistance of S1, S2 and S3 may be attributed to the substitution of andalusite aggregate by bauxite which has higher refractoriness. As such, the 80% bauxite aggregate grog which is added to replace 60% andalusite is beneficial in the castable. As much as, Harbison and Walker (2000) noted that the refractoriness of alumina-based refractories is a function of its alumina content, the benefit of higher refractoriness of bauxite was negated in S4 owing to effects of water addition, increased open porosity and lower bulk density, which increased susceptibility to corrosion attack. As discussed in section 2.3.1, Spalling or thermal shock, corrosion and abrasion resistance are three of the key properties to consider in refractories for tundish applications (Frulli 2016; Parr et al. 2003). Therefore, it can be deduced that S1, S2 and S3 corrosion volume result are comparable with VS, however S4 result were rejected due to high corrosion volume and susceptibility to thermal shock.

XRD analyses were further conducted on the unreacted portions of the samples after the static corrosion tests (Table 4.5). Basically, the amounts of mullite and corundum phases increased with increasing the amount of grog. This is due to the higher Al_2O_3 contents of the grog aggregates when compared to the reference andalusite-based castable. The volume and distribution of the mullite and corundum phases is particularly critical to the performance of the formulated castables. Mullite provides chemical stability to corrosion attack, and as such, the better corrosion resistance of S1, S2, and S3 can be attributed to the increased amounts of these phases in the castables. In as much as S4 was expected to have higher resistance to slag attack owing to comparatively higher mullite and corundum phases, the integrity of the formulation was negated by synergistic effects of poor physicochemical properties such as bulk density and open porosity.

Table 4.5: Phase analysis of unreacted portion of the castable after static corrosion test

Phases Present	VS	S1	S2	S3	S4
Corundum	2.7	7.6	11	13	18
Mullite	40	52	49	54	50
Andalusite	38	32	20	18	11
Cristobalite	0.15	0.44	0.06	0.11	0.02
Anorthite	3.7	4.7	4.2	4.8	4.7
Amorphous	15	3.1	16	9	12

Myhre 2008 proposed that the more alumina is available in castable, the more mullite bond is likely to form, as such, the castable will exhibit higher hot strength and thermal shock resistance. Myhre (2008) further proposed that when dealing with mullite bond, it is important that mullite is stable. This implies that the composition of the castable and the bond phases must be in either of the two alkamade triangles corundum, Anorthite and mullite or mullite, Anorthite and cristobalite (Figure 4.14).

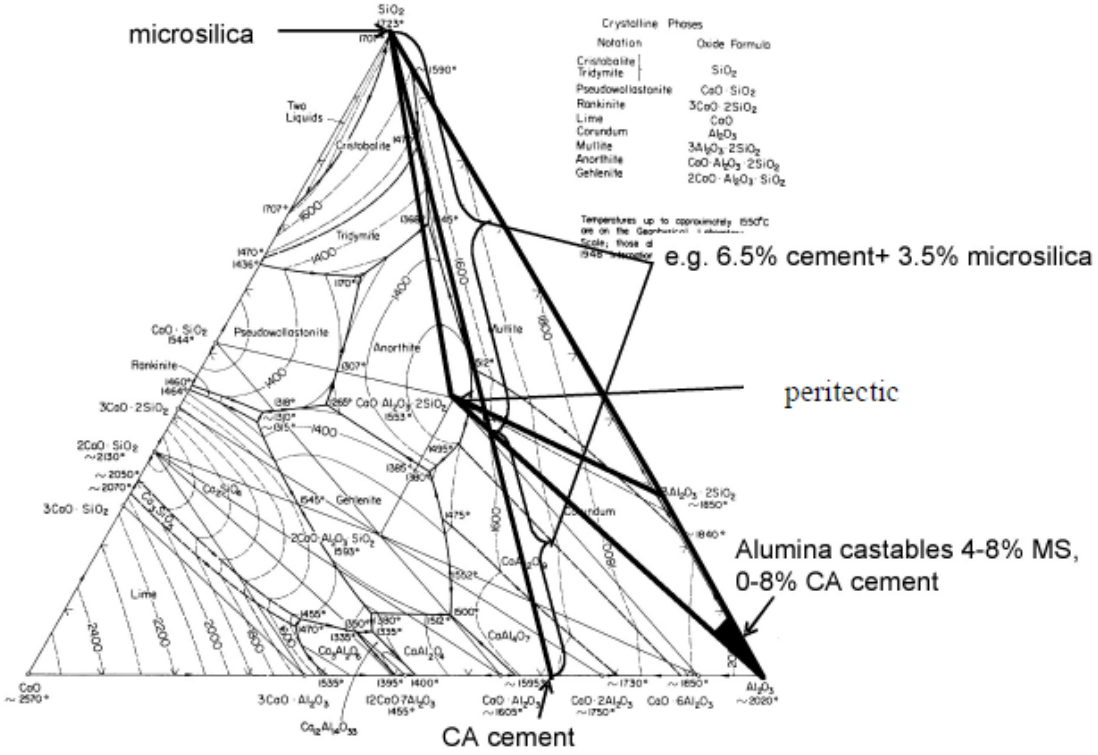

Figure 4.14: CaO-Al_2O_3-SiO_2 phase diagram (Slag atlas 1995)

The above proposition is congruent with the approximation for the formulated castables in Figure 4.11 which indicated that VS, S1 and S2 fall within the alkamade triangle anorthite-mullite-cristobalite, whilst, S3 and S4 fall within the alkamade triangle anorthite-mullite-corundum. Thus, indicating that the mullite bond formation is stable in all the formulations.
The effect and distribution of amorphous phases on the corrosion resistance of the castables is not clear from the findings. However, it can be inferred that the impurities in raw materials (e.g., Fe_2O_3, Na_2O, TiO_2, and K_2O in andalusite VS, and Fe_2O_3 in recycled grog) could have reacted with the Al_2O_3 and SiO_2 to form amorphous glass phases. Nevertheless, apart from S1 and S3, the amount of amorphous phases is congruent with the 10-15% proposed for high alumina refractories (Yuan et al. 2015).

4.2.5 Hot Modulus of Rupture (HMOR), Apparent Porosity and Permanent Change at 1500°C

Hot Modulus of Rupture (HMOR): Figure 4.15 shows that S1 and S3 both have higher HMOR values when compared to the reference sample VS. As proposed in Table 4.5, the high higher HMOR results for S1 and S3 can be attributed to higher mullite formation which significantly increases hot strength in refractory castables. S2 and S4 both have comparable HMOR values to the reference VS.

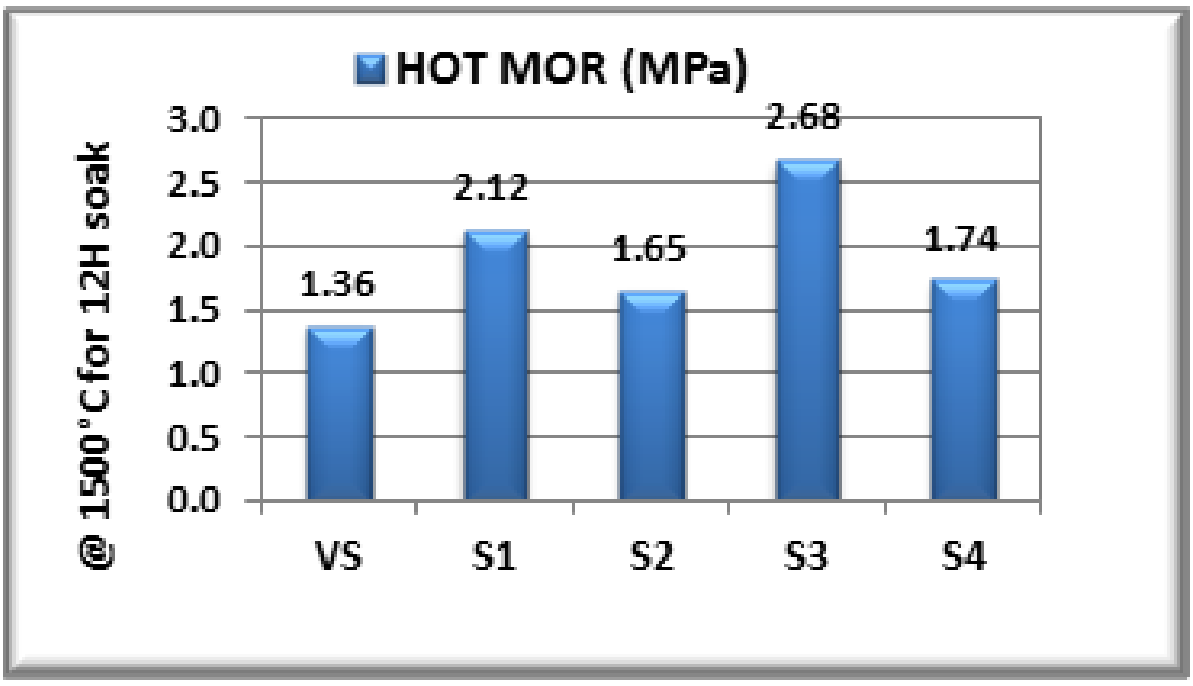

Figure 4.15: Hot Modulus of Rupture (HMOR) results for the formulated castables

Parr et al. (1997) proposed that mullite formation significantly increases the hot strength properties of refractory castables. Frulli (2016) emphasized that both HMOR and corrosion resistance are key properties for tundish applications. Therefore, although there is no clear trend in the hot strength for the formulated castables, overall the HMOR results were acceptable for all formulation at 1500˚C as guided by propositions by Parr et al. (2003).

Apparent Porosity at 1500˚C: Figure 4.16 shows that apparent porosity increases with the increase in grog addition. The observed trend was supported by findings in previous studies by Bradley and Hutton (2014) and Hutton et al. (2009).

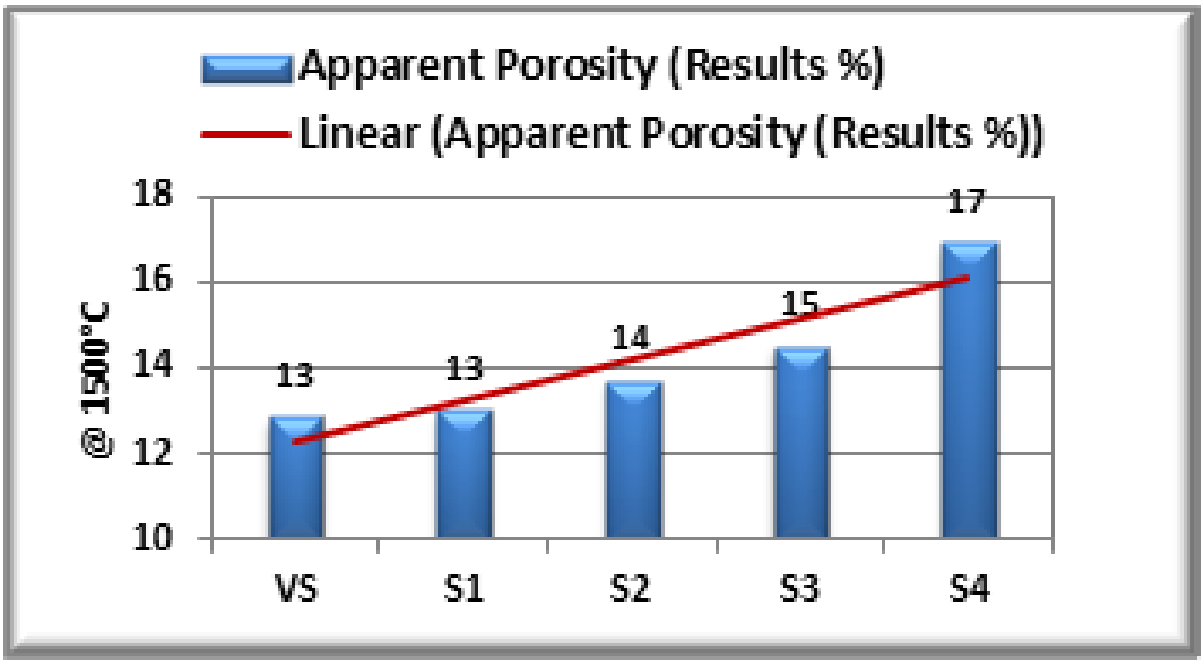

Figure 4.16: Apparent porosity at 1500°C results for the formulated castables

The apparent porosity values for S1, S2 and S3 are also comparable to VS. However, the observed apparent porosity values for S4 were significantly higher than that of VS, and this behaviour may be attributed to the higher water addition required for the castable during mixing. The studies by Hanagiri et al (2008), Bradley and Hutton (2014) stated that grog addition in refractory castable tend to increase water requirements. The studies concluded that water demand, apparent porosity and wear rate generally all increased with the increase in grog addition.

Permanent Change at 1500˚C: The behaviour in permanent linear change (PLC) for S1, S2 and S3 was comparable to VS (Figure 4.17). The PLC values for S4 were significantly higher than VS values and other formulations, as a result, was not considered acceptable for the proposed tundish applications. Dimensional changes in refractories are very important for tundish applications, too much linear change may affect structural integrity of the refractory, and excessive shrinkage may result in joint open of brick or cracking of castables (Hloben 2000). Samanta et al. (2012) attributed the volume expansion to phase changes involved in the conversion of andalusite to mullite. Andalusite transforms into mullite at relatively low temperature, with a minor volume expansion of +4.5%, and this is referred to as the mullitization stage (Frulli 2016).

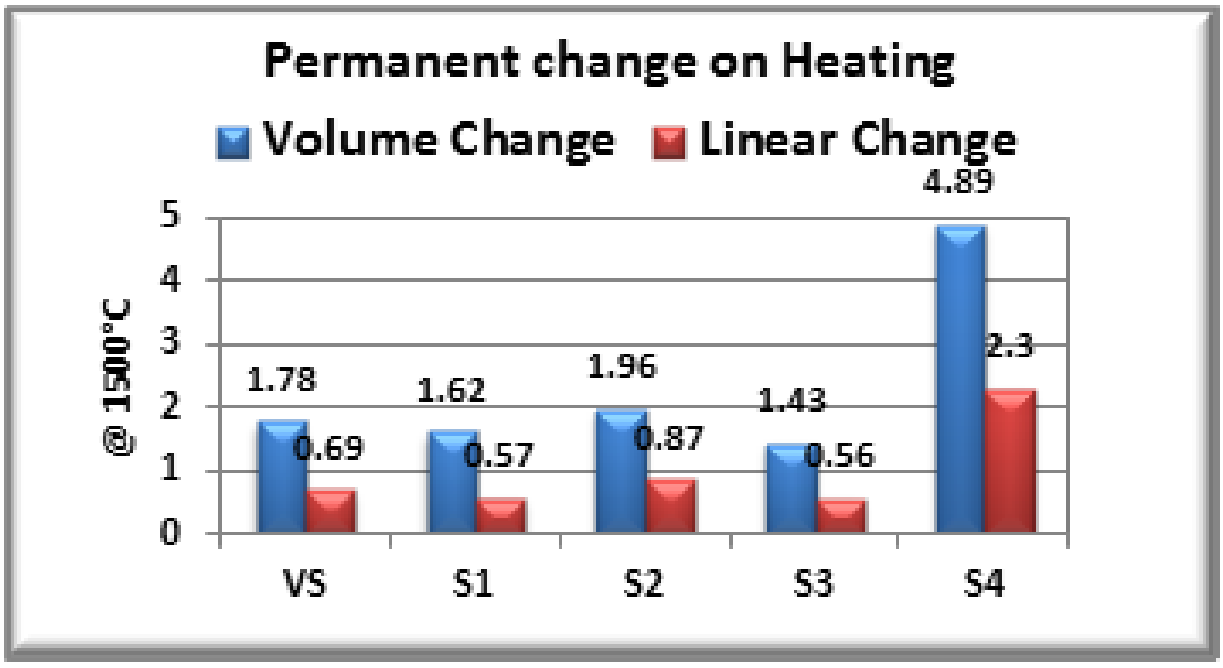

Figure 4.17: Permanent change at 1500°C results for the formulated castables

4.3: Summary of Findings

Physical test results for the grog – fresh castables were all comparable to the reference castable. However, high-temperature test results at 1400˚C and 1500˚C, S4 with 40% grog was rejected for all tests except hot modulus of rupture which was comparable with other formulations as shown in Table 4.6.

Table 4.6: Summary of the formulated castable results

Refractory Properties	**Physical tests comparison of formulated castables**	**Results**
Flow	Average (μ) % flow = 251mm and standard deviation (σ) = 8mm. Trend - Castable flow decreases with increase in grog addition.	Acceptable
Setting Time	Average setting time (μ) = 156 minutes and standard deviation σ = 29minutes. Trend – Setting time decreases with increase in grog addition.	Acceptable
Water Addition	Trend - Increase in the amount of grog added slightly increases the water requirement for the castable.	Acceptable
Apparent Porosity	Trend - Open porosity increases for each individual formulation at different temperatures. However, no clear comparison trend in open porosity for the different formulated castables at different temperatures is evident.	Acceptable
Bulk Density	Trend - Bulk density decreases with the increase in grog addition at 1200˚C. No clear comparison trend in bulk density for the formulated castables at lower temperatures.	Acceptable
Cold Crushing Strength	Although there seem to be a decrease in CCS at 110˚C with the increase in grog content, this decrease is negligible considering that all formulations have comparative CCS at 1200˚C.	Acceptable
	Comparison of high-temperature test results for the formulated products	
Static Test at 1400˚C	S1, S2 & S3 were intact and showed no signs of cracks. However, S4 showed signs of cracks and experience higher corrosion wear and erosion. S1, S2 & S3 corrosion wear and Al_2O_3 dissolution rates are comparable to that of VS, however S4 seem to have experienced the highest dissolution of Al_2O_3	Acceptable for S1 S2 & S3. S4 rejected

% Corrosion volume test at 1400˚C	S1, S2 & S3 showed slightly decrease in corrosion wear when compared to VS. S4 had the highest corrosion volume.	Acceptable for S1 S2 & S3, S4 rejected
Hot Modulus of Rupture (HMOR) at 1500 ˚C	S1 and S3 both had higher HMOR when compared to the VS, this is attributed to mullite formation which significantly increases hot strength properties in castables. S1 and S4 both have comparable HMOR to VS.	Acceptable
Apparent Porosity 1500 ˚C	Trend - Open porosity increases with the increase grog addition.	Acceptable for S1 S2 & S3. S4 rejected
Permanent Linear Change (PLC) at 1500 ˚C	S1, S2 and S3 PLC values are comparable to VS. However, S4 volume and linear change values are significantly higher than VS.	Acceptable for S1 S2 & S3. S4 rejected

4.4 Economic Consideration results

The direct economic benefits from the proposed formulations were calculated based on the replacement ratio of virgin andalusite. Table 4.7 illustrates the hypothetical economic model for the cost reduction of substituting virgin raw material castable with reclaimed bauxite material.

Table 4.7: Cost reduction from substitution of virgin andalusite.

Raw material		**VS**		**S1 (10% grog)**		**S2 (20 % grog)**		**S3 (30% grog)**		**S4 (40 % grog)**	
	Unit costs	**kg**	**Total Cost ($)**	**kg**	**Total Cost ($)**	**kg**	**Total Cost ($)**	**kg**	**Total Cost ($)**	**kg**	**Total Cost ($)**
Binder premix	19.22	75	1 442	75	1 442	75	1 442	75	1 442	75	1 442
Calcined alumina	21.56	20	431	20	431	20	431	20	431	20	431
Bauxite grog 0-1mm	3.43	0	0	20	69	40	137	60	206	80	274
Bauxite grog 1-3mm	3.43	0	0	35.5	122	71	244	107	367	142	487
Bauxite grog 3-6mm	3.43	0	0	15	51	30	103	45	154	60	206
Andalusite 200µm	10.13	200	2 026	200	2 026	200	2 026	200	2 026	200	2 026
Andalusite 0-1mm	8.53	200	1 706	180	1 535	160	1 365	140	1 194	120	1 024
Andalusite 1-3mm	7.85	355	2 787	319.5	2 508	284	2 229	248	1 947	213	1 672
Andalusite 3-6mm	10.6	150	1 590	135	1 431	120	1 272	105	1 113	90	954
Total cost ($)			**10 000**		**9614**		**9287**		**9013**		**8530**
Total savings (%)			**0**		**4**		**7**		**11**		**15**

S1 with 4% cost savings, offers trivial benefit with regards to grog recycling. As such, only substituting 10% grog is not a viable option. On the other hand, S4 offers the highest cost reduction ratio, however, the results from the study showed that higher replacement ratios result in compromised quality of reference castables. Therefore, it can be deduced that S2 and S3 offer the best compromise between cost and quality of the formulated castable product. Furthermore, if dumping costs of refractory waste, such as terms of dumping space, conveying costs, and other salient costs were considered, the direct cost reductions shown in Table 4.7 would be significantly higher.

CHAPTER 5 CONCLUSION AND RECOMMENDATIONS

5.1. Summary and conclusions

The results for physico-chemical characterization of the spent bauxite-based refractory bricks from furnace roof showed that brick A is viable for reclamation while brick B and C were discarded. Brick A refers to a sample taken from the roof periphery while B and C refers to samples taken from the electrode pot and off-gas area respectively. Furthermore, brick A was less contaminated and showed no signs of physical degradation. On the other hand, brick B showed signs of crack formation, slag penetration, and was heavily contaminated, and hence was rejected on grounds of poor recyclability. Brick C, although viable for recycling, was rejected on the grounds of economic viability with the least quantities generated for recycling at the end of campaign to make a difference in terms of the environmental footprint.

After brick A was selected for recycling, its grog was then sorted, cleaned, crushed and screened to the required 0-1 mm, 1–3 mm and 3–5 mm aggregate fractions to be used in the grog fresh formulation castables which were then compared to the reference/virgin andalusite based castable. The percentage andalusite substituted with grog in the formulated samples was S1-10%, S2-20%, S3-30 and S4-40% and compared with the virgin sample VS which had 0% grog.

The physico-chemical characterization and comparative analyses of the formulated products showed comparable product compliance to standard quality tests. In summary:

- Castable flow properties decreased with increase in the amount of grog added from 165 to 140%
- Castable setting time decreased with an increase in the amount of grog added from 180 to 120 minutes
- Increasing the amount of grog added slightly increased the water requirement for the castable from 6% to 8%
- Apparent porosity slightly increased with an increase in grog addition for each individual formulation at different temperatures
- Bulk density decreased with an increase in grog addition at 1200˚C
- Cold crushing strengths at 600, 1000 and 1200˚C was comparable for all formulations

- Static corrosion behaviour, apparent porosity, permanent linear change and hot modulus of rupture HMOR for S1, S2 and S3 castables were all comparable against the standard virgin castable (VS). Except for HMOR behaviour, the castable with higher replacement ratio of 40%-S4 failed to meet the quality requirements for these tests.
- Cost savings increased with an increase in grog addition; for example, 40% grog addition translate to a saving of 15%.

Considering this, it can be concluded that formulations S2 and S3 offer the best compromise between cost and quality of the castables. In addition to the cost savings of 7% and 11% respectively, other salient benefits not quantified in this study may include dumping space, conveying costs, environmental levies, as well as goodwill for environmental stewardship.

5.2. Recommendations for further study

It is recommended to conduct a dynamic slag and molten metal corrosion test in order to simulate the conditions in the tundish should the working lining reduces to unacceptable levels thereby exposing the safety lining to direct attack by slag. Rotor slag test is the ideal test method for such a dynamic slag test, however there was no facility available in South Africa to conduct such a test. Poirier (2015) emphasized that the interaction between working lining, in this case $MgSiO_2$ and the refined steel is important in the design of castables. Therefore, further test work is required on this subject.

Although the study concluded that up to 30% grog can be added to a castable without compromising quality for the tundish application. Further testwork at 35% grog is recommended to ascertain the maximum quantity that can be recycled without compromising castable quality, thus improving the environmental footprint. Furthermore, bauxite grog addition can be extended into castable matrix to determine the effected when substituted into finer particles, thus increasing the scope for recycling.

Further testwork proposed by Scaw entails casting a panel in the tundish with 20% and 30% grog and comparing with the reference castable to determine in-situ corrosion wear, before casting the whole tundish with grog-based castable.

REFERENCES

1) Abou-Sekkina, M.M., Abo-El-Enein, S.A., Khalil, N.M. and Salma, O.A. (2011). Phase composition of bauxite-based refractory castables. *Ceramics International*, 37, 411-418.
2) AGC Ceramics (n.d.). Adjustments to workable time and hardening time for castable refractories. *ASTM International*. Available at http://www.agcc.jp/Portals/0/images/en/core/alumi/about/castable.pdf. Accessed 1 January 2018.
3) Almeida, B., de Farai, R, de Oliveira Vieira, Silva, A. & Vernilli, F. (2016). Recycling of steelworks refractories: processing and properties. *Iron and Steelmaking*, 43 (10), 775-779.
4) ASTM 357-07 (2015). Standard test method for bulk density of granular refractory materials. *ASTM International*. Available at https://www.astm.org/Standards/C357.htm. Accessed 20 November 2017.
5) ASTM 865-02 (2002). Standard practice for firing refractory concrete specimens. ASTM International. Available at https://www.astm.org/DATABASE.CART/HISTORICAL/C865-02.htm. Accessed 20 November 2017.
6) ASTM C20-00 (2010). Standard test methods for apparent porosity, water absorption, apparent specific gravity, and bulk density of burned refractory brick and shapes by boiling water. *ASTM International*. Available at https://edisciplinas.usp.br/pluginfile.php/2701821/ mod_resource/content/1/C20-00.pdf. Accessed 1 January 2018.
7) ASTM International. Available at https://www.astm.org/Standards/C125.htm. Accessed 20 November 2017.
8) ASTM-C125. (2016). Standard terminology relating to concrete and concrete aggregates.
9) ASTM-C133. (2003). Standard test methods for cold crushing strength and modulus of rupture of refractories. *ASTM International*. Available at https://www.astm.org/DATABASE.CART/HISTORICAL/C133-97R03.htm. Accessed 20 November 2017.

10) ASTM-C1446. (2011). Standard test method for measuring consistency of self-flowing castable refractories. *ASTM International.* Available at https://www.astm.org/Standards/C1446.htm. Accessed 20 November 2017.
11) ASTM-C16-03. (2012). Standard test method for load testing refractory shapes at high-temperatures. *ASTM International*. Available at https://www.astm.org/Standards/C16.htm. Accessed 20 November 2017.
12) ASTM-C583-15. (2015). Standard test method for modulus of rupture of refractory materials at elevated temperatures. *ASTM International*. Available at https://www.astm.org/Standards/C583.htm. Accessed 20 November 2017.
13) ASTM-C92-95. (1999). Standard test method for sieve analysis and water content of refractories. *ASTM international*, 1999.
14) Bier, T., & Parr, C. (1996). Admixtures with calcium aluminate cements and CAC based castables. *28th Annual SA Ceramic Society Symposium*, Johannesburg, South Africa.
15) Botha, B. (2010). An overview of andalusite in Southern Africa: *Geology and Mineralogy*. Refractories Conference. South Africa Institute of Mining and Metallurgy.
16) Bradley, M. & Hutton, T. (2014). Recycling of Steel Plant Refractories. *Institute of Refractories Engineer*, September 2014 Issue, 22-25.
17) Braulio, M., Martinez, A., Luz, A., Liebske, C., & Pandolfelli, V. (2011). Basic slag attack of spinel-containing refractory castables. *Ceramics International*. 37, 1935-1945.
18) Brown, J. Foseco ferrous foundrymans handbook. 11th Edition. Butterworth-Heinemman, Oxford, UK.
19) Buhr, A., & Laurich, J. (2000). Synthetic Alumina Raw Materials – Key Elements for Innovative Refractories. *Alcoa Industrial Chemicals Europe*. 62-67.
20) Bul'ko, B. Demeter, P. Havran, J. (2014). The influence of slag on the degradation of tundish working lining, 20(3), 318-325.
21) Buzin, P., Heck, N. & Vilela, A. (2015). EAF dust: An overview on the influence of physical, chemical and mineral features in its recycling and waste incorporation routes. *Journal of Materials Research and Technology*, 2015. 6(2).
22) Carniglia, S., & Barna, G. (1992). Handbook of Industrial Refractories Technology. *National Refractories & Minerals Corporation.*

23) Chabas, E., Ulrich, C., Lafaurie, A., Papin, E. & Dumont, D. (2013). Rheology & Dispersion behaviour of calcined aluminas with deflocculants. *UNITECR*, 843 - 847.

24) Cousin, J., Parr, C., Revais, C., & Bier, T. (1998). Formulation of spinel castables and the impact of additives and alumina on their rheology. *IRECON*, Calcutta, India, 1998.

25) De Kock D.J. (2005). Optimal tundish design methodology in a continuous casting process. PhD Thesis. University of Pretoria. Available at http://repository.up.ac.za/xmlui/bitstream/handle/2263/28496/Complete.pdf , Accessed 16 March 2016.

26) DIN 51069 Blatt 2. Testing of ceramic material: Comparing test of the resistance of refractory bricks to the attack of solid and liquid materials at high-temperature, crucible method.

27) Drofelnik, N., Lamut, J., & Knap, M. (2015). Interaction between steel melt and refractory materials in tundish. *Archives of Metallurgy and Materials*, 60 (1), 269-273.

28) Fang, H., Smith, J., Peaslee, K. (1999). Study of spent refractory waste recycling from metal manufacturers in Missouri. *Resource, conservation and recycling*. Issue 25, 111-124.

29) Feytis, A. (2011). Supply Situation Report – Andalusite Invest in the future. Industrial Minerals, 2011.

30) Fruehan, R.J. (1998). Overview of steelmaking processes and their development. Making, shaping and treating of Steel- Steelmaking and Refining Volume 11th. *AISE Steel Foundation*, Pittsburgh.

31) Fruhstorfer, J. and Aneziris, C.G. (2014). The influence of the coarse fraction on the porosity of refractory castables. *Journal of Ceramic Science and Technology*, 5 (2), 155-166

32) Frulli, D. (2016). Production and properties of refractory raw materials based on the Andalusite and Mullite - Influence of impurities in the refractory behaviour. *Refractories world Forum*. 8 (3), 1-4.

33) Garbers-Craig, A.M. (2008). Presidential Address: How cool are refractory materials. *The Journal of Southern African Institute of Mining and Metallurgy*, 108, 491-506.

34) Ghonaim, S. A., Ghazal, H.B.G., & Abadir, M. (2010). Effects of type of Aggregate on the properties of refractory concrete. *Journal of American Science*. 6(12), 1015-1016.

35) Grobler, F. & Minnitt, R. (1999). The increase role of direct reduced iron in global steelmaking. *South Africa Institute of Mining and Metallurgy*.

36) Guézennec, A., Huber, J., Patisson, F., Sessiecq, P., Birat, J., & Ablitzer, D. (2005). Dust formation in Electric Arc Furnace: Birth of the particles. *Powder Technology*, 157, 2-11.

37) Habashi, F. (1997). Handbook of extractive Metallurgy. Volume 1: *The Metal industry Ferrous Metals*.

38) Hanagiri, S., Shimpo, A., Inuzuka, T., Sakaki, S., Matsui, T., Aso, S., Matsuda, T., Nakagawa, H. (2008). Recent Improvement of Recycling Technology for Refractories. *Nippon Steel Technical Report*, No.98, 96-97.

39) Hancock and Cannon J.D. & Cannon, J.H. (2000). Practical Refractories. Refractories for Industrial users.

40) Harbison and Walker. (2005). Handbook of Refractory Practice. Harbison-Walker Refractories Company.

41) Haufe, J., Gynz-Rekowski, C., & Bier, T. (2011). Characterisation of crack formation in refractory concrete by the use of different methods. *Institute of Ceramics, glass and Construction Materials*, 66-71.

42) Hloben, P. (2000). Refractory Materials, Major Industrial Applications.

43) Hutton, T., Yates, V., Green, J., Coppack, J., & Goff, A. (2009). Reclaimed Raw Material Resources and their use in Modern Monolithics Refractories. *The Refractories Engineer*, September 2009 issue, 20-25.

44) Industrial Minerals. (2010). Sillimanite supply surge. Available at http://www.andalusiteresources.com/wp-content/uploads/2012/07/Sillimanite-supply-surge-_-Industrial-Minerals.pdf. Accessed 21 November 2017

45) Kessellheim, B. (2008). Monolithic refractory technology to metallurgical application. *Refratechnik Steel GmbH*.

46) Kumar, A., Khanna, R., Ikram-ul-Haq, M., Spink, J. and Sahajwalla, V. (2015). Corrosion behaviour of Al_2O_3- C refractories with casting mould meniscus slags at 1550˚C. *Steel Research Int*. 87 (1): 46

47) Lee, W., & Zhang, S. (2004). Direct and Indirect slag corrosion of oxide and oxide-c refractories. VII International Conference on Molten Slag Fluxes and Salts. *South Africa Institute of Mining and Metallurgy*, 309-319.

48) Lee, W., Vieira, W., Zhang, S., Ghanbari Ahari, K., Sarpoolaky, H., & Parr, C. (2001). Castable Refractory Concretes. *International Material Reviews*, 145-159.

49) Lee, W., Vieira, W., Zhang, S., Ghanbari Ahari, K., Sarpoolaky, H., & Parr, C. (2001). Castable Refractory Concretes. *International Material Reviews*.

50) Liu, X., Büchel, G., & Buhr, A. (2002). Upgrading Castable Performance through Matrix Optimization. *Austceram*.

51) Lottermoser, B.G. (2011). Recycling, reuse and rehabilitation of mine wastes. Elements 7, 405-410.

52) Luz, A., Martinez, A., Braulio, M., & Pandolfelli, V. (2011). Thermodynamic evaluation of spinel containing refractory castables corrosion by secondary metallurgy slag. *Ceramic International*, 37, 1191 – 1201.

53) Mangabhai, R. & Glasser, F. (2001). Calcium aluminate cements. Proceedings of the International Conference on Calcium Aluminate Cements (CAC).

54) Mazzanti, F., Brentari, A., Burresi, E., Coglitore, A., Labanti, M., Martelli, S., Mingazzini, C., Ricci, A., Sangiorgi, S., Scafe, M., & Villa, M. (2010). Exploitation of ceramic wastes by recycling in alumina-mullite refractories. *12th Inter. Ceramics Congress*: 9, 10-14.

55) Melcher, F., Reiter, V., & Harmuth, H. (2007). Investigation of corrosion of different alumina spinel castables by ladle slags. *UNITECR*, 230-233.

56) Myhre, B. (1993). The effect of Elkem Microsilica addition on the flow and strength of alumina castables. *95th Annual Meeting and Exposition of the American Ceramic Society*, 1-10.

57) Myhre, B. (1994). Effect of particle size distribution on the flow of refractory castables. *Refractories Application and News*. 2-6.

58) Myhre, B. (2008). Let's make a Mullite Matrix. *Refractories Application and News*.

59) Myhre, B., Sandberg, B. & Hundere, A.M. (1998). Flow and flow decay of refractory castables. *3rd India International Refractories Congress*.

60) Ndlovu, S., Simate, G.S., and Matinde, E. (2017). Waste Production and Utilization in the Metal Extraction Industries. Taylor & Francis CRC Press, Bocca Raton. https://doi.org/10.1201/9781315153896

61) Nyirenda, R. (1991). The processing of steelmaking flue dust: A Review. Mineral Engineering, 4(7–11):1003-1025.

62) Ødegård, C., Myhre, B. Hundere, M., & Sandberg, B. (1998). Mullite bonded castable with andalusite as aggregate. *International Colloquium on Refractories*, 2-5.

63) Overbeek, P. (1989). Andalusite in South Africa. *Journal of the South African Institute of Mining and Metallurgy*, 1989.

64) Parr, C. Bier, T., Bunt, N., & Spreafico, E. (1997). Calcium Aluminate Cement (CAC) based castables for demanding Applications. *1st Monolithic Conference*, 3-11.
65) Parr, C., Fryda, H., and Wöhrmeyer, Ch. (2013). Recent advances in refractories-aluminate binders and calcium aluminate bonded high-performance monolithic castables. *The Journal of Southern African Institute of Mining and Metallurgy*, 113, 619-629.
66) Parr, C., Simonin, F., Touzo, B., Wöhrmeyer C., Valdelièvre B., & Namba, A. (2004). The impact of calcium aluminate cement hydration upon the properties of refractory castables.
67) Parr, C., Wöhrmeyer, C., & Steffes-Tun, W. (2003). The use of calcium aluminate cements in monolithic refractories for steel applications. *Prague International Conference on Refractories*, 2-13.
68) Peng, H., & Myhre, B. (2008). High-temperature properties of bauxite-based castables with microsilica. *Eurogress Aachen*. 99-102.
69) Pivinskii, Yu.E., Dyakin, P.V., & Perepelitsyn, V.A. (2015). Research in the field of preparing molded and unmolded refractories based on high-alumina HCBS. Part 1. High-alumina bauxite as a raw material. *Refractories and Industrial Ceramics*, 56 (4), 344-349.
70) Plunkert, P. (2004). Bauxite and Alumina. *US Geological survey minerals yearbook*.
71) Poirier, J. (2010). Analysis and interpretation of microstructures after liquid oxide corrosion. *12th International Ceramics Congress Part 1*. 114-127.
72) Poirier, J. (2015). A review: Influence of refractories on steel quality. *Metallurgical Research and Technology*, 112 (410), 1-20.
73) Pretorius, E. EAF and Ladle slag Fundamentals. No Date. Available at http://etech.lwbref.com/Downloads/Theory/Fundamentals%20of%20EAF%20and%20ladle%20slags%20and%20ladle%20refining%20principles.pdf
74) Raja, B. (2009). Breakouts in continuous casting of steel. *Steelworld Monthly Journal*.
75) Rebouillat, L. and Rigaud, M. (2002). Andalusite-based high alumina castable. *Journal of American Ceramic Society*, 85 (2), 373-378.
76) Ressler, A. (2009). Deflocculating Additive Effect on the setting time of the Andalusite Based LCC Castables. *Centre for Abrasives and Refractories Research and Development GmbH*, 1-4.
77) Routschka, G. & Wuthnow, H. (2008). Refractory materials: Design, Properties, testing. Refratechnik Pocket Manual.

78) Sadiki, C., El-Amrani, I.E and Albizane, A. (2014). Recent advances in silica-alumina refractory: *A review. Journal of Asian Ceramics Societies*, 2, 83.
79) Sahai, Y., & Emi, T. (2008). Tundish Technology for clean steel production. *World Scientific Publishing Company*.
80) Sako, E., Braulio, M., & Pandolfelli, V. (2011). The corrosion and microstructure relationship for cement-bonded spinel refractory castable. *Ceramic International*. 38, 2177-2185.
81) Samanta, A., Satpathy, S., Ganguli, S., Goswami, J., & Adak, S. (2012). Effect of microsilica and calcium aluminate cement on different thermo-mechanical properties of low-cement castables. *Eurogress*, 33-36.
82) Sandberg, B., & Myhre, B. (1994). Microsilica- A Versatile Refractory Raw Material. Elkem Refractories.
83) Schacht, C.A. (2004). Refractories Handbook.
84) Schnabel, M., Buhr, A. (2013). Castable for industrial applications – still room for improvements. *Eurogress,* Aachen, Germany. 13 – 17.
85) Schnabel, M., Buhr, A., Kockegey-Lorenz, R., Schmidtmeier, D., & Dutton, J. (2014). Benefits of Matrix Alumina and Modern Dispersing Systems in Low-cement Castables. *Inteceram-Refractories Manual*, 284-281.
86) Schutte, M. (2010). Refractory recycling – earning your environmental brownie points. Proceedings of the Refractories 2010 Conference. *South Africa Institute of Mining and Metallurgy*, 75-82.
87) Seetharaman, S. (2014). Treatise on Process Metallurgy. *Industrial Processes, Part A.*
88) Slag Atlas (1995). Slag Atlas, 2nd Edition. *Verein Deutscher Eisenhuttenleute (VDEh)*, 273.
89) Sofilić, T., Radovic, V., Cerjan-Stefanović, Š., & Rastovčan-Mioč, A. (2004). The mineralogical composition of dust from an Electric Arc Furnace.
90) Sutcliffe, N. (2004). Slag/refractory and metal/refractory interactions during the production of stainless steels. 7th International conference on molten slags, fluxes and salts, *South Africa Institute of Mining and Metallurgy*, 423-434.
91) Valdelièvre, B. Wöhrmeyer, C., & Parr, C. (2002). Application of calcium aluminate cement (CAC) to dense low water demand refractory castables. *IREFCON*.
92) Vert, T. (2016). Refractory Material Selection for Steelmaking. *The American Ceramic Society*.

93) Wöhrmeyer, C., Parr, C., & Chassaing, P. (2000). The full range of calcium aluminate cements for conventional and deflocculated castables. *Refractories Conference in Kosice*.

94) Wöhrmeyer, C., Parr, C., & Myhre, B. (2006). The optimisations of deflocculated high cement castables (HCC). *49th International Colloquium on Refractories*.

95) Wöhrmeyer, C., Simonin, F., & Parr, C. (2005). The control and optimisation of low-cement castables. *UNITECR*.

96) World Steel Association (2015). Steel in a circular economy: A life cycle assessment. Available at https://www.worldsteel.org/en/dam/jcr:00892d89-551e-42d9-ae68-abdbd3b507a1/Steel+in+the+circular+economy+- +A+life+cycle+perspective.pdf . Accessed 20 November 2017

97) Yilmaz, S. (2006). Corrosion of high-alumina spinel castables by steel ladle slag. 33 (2), 151-156.

98) Yuan, W., Zhu, Q., Deng, C. and Zhu, H. (2015). The effect of glass phase on the modulus of rupture of high alumina refractories. *Journal of Ceramic Science and Technology*, 6 (3), 215-220.

99) Zawrah, M.F.M. and Khalil, N.M. (2008). Effect of mullite formation on properties of refractory castables. *Ceramics International*, 27, 689-694.

100) Zhang, S. & Lee, E. (2000). Use of Phase diagrams in studies of refractory corrosion. 41-59.